Essays on Dynamic Conditional Score Models and Breaks

A thesis submitted for the degree of

Doctor of Philosophy

by

Willy Arturo Alanya Beltran

B. Sc., Pontificia Universidad Católica del Perú, Peru

M. Sc., The University of Warwick, United Kingdom

MPhil., University of Cambridge, United Kingdom

Department of Econometrics and Business Statistics

Monash Business School

Monash University

Australia

September 2022

Contents

Copyright notice

Abstract

In this dissertation I develop three essays on dynamic conditional score (DCS) models for univariate and multivariate models. In the first essay, I focus on a DCS model with a short memory process with changes in regimes for volatility. I also study volatility dynamics in my second essay using score-based copula models with time-varying dependencies with two components. For my last essay, I propose a score-driven multivariate model with factors for the location or mean of a set of macroeconometric variables. All my essays deal with episodes of atypical observations such as the global financial crisis and the recent pandemic.

In my first essay I propose and study a dynamic conditional score model with random shifts, the RS-Beta-t-EGARCH model, for modelling volatility in financial markets. The addition of random shifts can explain the high volatility persistence typically estimated for these financial series. This setting constitutes an alternative approach to long memory models; moreover, the new model identifies volatility clusters. I apply the model to stock returns in South American emerging markets. The estimates for the random shifts fit the main regime disturbance events in the period of study. Monte Carlo simulations show that the new model replicates the time and spectral domain properties of the original series. Finally, out-sample forecast evidence favours the new specification.

For my second essay, I study score-driven copula models for modelling high persistence dependence between financial volatility series. I model this persistence dependence with two components, one for the long memory and the other for the short-term process. The addition of components offers a parsimonious solution for modelling high persistence while also allowing for a short-term component that captures transient shocks. I apply the model to emerging equities in the Americas. The estimates are robust to the advent of the pandemic, and data resampling delivers similar parameter estimates. The proposed two-component model improves the in-sample diagnostics and generates more accurate out-of-sample forecasts.

Lastly, in my third essay, I develop and study a factor-augmented quasi-vector autoregressive model for economic policy analysis in tumultuous times. An observation-driven framework that exploits the score model information allows maximum likelihood estimation. This multivariate local model approach, which assumes a Student t error distribution, is robust to atypical observations such as the global financial crisis and the recent pandemic. The model outperforms the factor-augmented

VARMA model because of the assumed heavy tails that capture the COVID-19 atypical data and other turbulent episodes. An empirical application to the U.S. economy that assess monetary policy reveals that estimates and impulse responses are stable when considering the sample before and after COVID-19.

Thesis including published works declaration

I hereby declare that this thesis contains no material which has been accepted for the award of any other degree or diploma at any university or equivalent institution and that, to the best of my knowledge and belief, this thesis contains no material previously published or written by another person, except where due reference is made in the text of the thesis.

This thesis includes one original article published and two submitted manuscripts in peer reviewed journals. My first essay was published at *Finance Research Letters* journal, my second essay has received a conditional acceptance from *Studies in Nonlinear Dynamics & Econometrics* journal subject to the submission of source files, codes and data, which have been already sent, and my third essay has been submitted to *Journal of Money, Credit and Banking*. The core theme of the thesis is dynamic conditional score models and breaks. The ideas, development and writing up of all the papers in the thesis were the principal responsibility of myself, the student, working within the PhD in Econometrics and Business Statistics program under the supervision of Heather Anderson and Benjamin Wong.

I have renumbered sections of submitted and published papers in order to generate a consistent presentation within the thesis. In addition, I have included a slightly extensive version of the published article in this thesis, which maintains the main results and conclusions of the journal article.

Student name: Willy Arturo Alanya Beltran

Date: 19/09/2022

I hereby certify that the above declaration correctly reflects the nature and extent of the student's contributions to this work.

Main Supervisor name: Heather Anderson

Date: 19/09/2022

Publications during enrolment

This thesis consists of one article and two academic manuscripts that have been written during my candidature.

Journal article:

1. Alanya-Beltran, Willy (2022a), "Modelling Stock Returns Volatility with Dynamic Conditional Score Models and Random Shifts", *Finance Research Letters* **45**, 102121.

Manuscripts:

2. Alanya-Beltran, Willy (2022b), "Modelling Volatility Dependence with Score Copula Models", conditionally accepted, *Studies in Nonlinear Dynamics & Econometrics.*
3. Alanya-Beltran, Willy (2022c), "Factor-Augmented QVAR Models: An Observation-Driven Approach", Mimeo.

Acknowledgements

Firstly, I dedicate this work to my family for its unconditional support in all stages of this PhD journey. Since I accepted this challenge they were confident I could finish this degree. However, I did not imagine that a small break after my first year of enrolment in 2020, would mean not seeing my family for more than two years as a result of the pandemic and border closures. This was a critical episode in my home country in particular, since Peru, sadly, was terribly impacted by the COVID-19 causing more than 200 000 deaths. Fortunately, my family overcame the virus, and this kept me relatively calm. I give special thanks to the Department of Health and Human Services Victoria for giving me three doses of the vaccine against coronavirus, so that I was able to continue with my research.

I want to acknowledge my supervisors, Professor Heather Anderson and Dr. Benjamin Wong, for their support throughout the PhD program. The circumstances were very special, as we faced many restrictions during these years with several quarantine mandates and even curfews. They were always attentive to my research progress and my well-being since I arrived, with a mix of in-person and virtual regular meetings. In addition, they helped me with the development of every manuscript and milestone with useful suggestions and comments thanks to their expertise in the field.

In addition, I thank my PhD panel: Professor Gael Martin, Professor George Athanasopoulos and Professor Brett Inder, for their useful comments and insights that allowed me to improve the content and quality of my dissertation. Also, I recognize the solid ground in statistics and econometrics from my first year modules run by Professor Mervyn Silvapulle and Professor Donald Poskitt. Deborah Fitton, Andrea Meyer and Marcela Niculescu from the Department of Econometrics and Business Statistics were always keen to help me with any queries and doubts about the logistics within the department. I had the opportunity to submit my essays to academic journals through the peer review process and I learned a lot from this process with the guidance of my supervisors, anonymous referees and Editors.

I would like to acknowledge the Monash Student Association and its Clubs and Societies division for providing me with a necessary platform for a break from my studies. They brought me a space where I could share my culture and learn from others, and also make innumerable new friends from across the world. Furthermore, I had the privilege to live on campus through Monash Residential Services who always cared for all their residents offering many activities for integration and recreation. Although that we only shared most of our time together during my first year of enrolment, I am fortunate to have met brilliant PhD students in this program.

Finally, it would not be possible to complete this degree in Australia without the generous scholarship and living expenses from Monash International Tuition Scholarships. In addition, I want to thank my employer, the Central Bank of Peru, for giving me a leave of absence to pursue my doctoral studies.

Abbreviations

ACF	Autocorrelation function
AIC	Akaike information criterion
BIC	Bayesian information criterion
Beta-t-EGARCH	Beta Student t exponential generalized autoregressive conditional heteroskedasticity
Beta-t-GARCH	Student t exponential generalized autoregressive conditional heteroskedasticity
COLCAP	Colombian capital market index
DCS	Dynamic conditional score
DGP	Data generating process
DSGE	Dynamic stochastic general equilibrium
EGARCH	Exponential generalized autoregressive conditional heteroskedasticity
EM	Expectation maximization
FAQVAR	Factor-Augmented Quasi-vector autoregressive
FAVARMA	Factor-Augmented vector autoregressive moving average
FFR	Federal funds rate
FRED-MD	Federal Reserve economic data - monthly data
GARCH	Generalized autoregressive conditional heteroskedasticity
GAS	Generalized autoregressive score
GJR-GARCH	Glosten-Jagannathan-Runkle generalized autoregressive conditional heteroskedasticity
G20	Group of 20
HQ	Hannan and Quinn information criterion
IBOV	Ibovespa Brasil Sao Paulo stock exchange index
IC	Information criterion
IGBVL	*Índice General de la bolsa de valores de Lima*
IPSA	*Índice de Precios Selectivo de Acciones*
LATAM	Latin America
$\log L$	Logarithm of likelihood

LR	Likelihood ratio
MA	Moving average
MAE	Mean absolute value
MERVAL	*Mercado de valores de Argentina*
MEXBOL	Mexican stock exchange
MILA	*Mercado integrado latinoamericano*
MSCI ACWI	Morgan Stanley Capital International All Country World Index
MSE	Mean square error
QVAR	Quasi-vector autoregressive
RS	Random shifts
RS-Beta-t-EGARCH	Random shifts Beta Student t exponential generalized autoregressive conditional heteroskedasticity
SAAR	Seasonally adjusted annual rate
SIC	Standard Industrial Classification
S&P 500	Standard & Poor's 500
SMV	*Superintendencia del Mercado de Valores*
ST	Multivariate Student t distribution
SV	Stochastic volatility
t-GARCH	Student t generalized autoregressive conditional heteroskedasticity
TSX	Toronto Stock Exchange
VaR	Value at Risk
VAR	Vector autoregressive
WHO	World Health Organization
ZLB	Zero lower bound

List of Tables

List of Figures

1 Introduction

1.1 Motivation

Countries in Latin America are susceptible to multiple shocks, due to internal social and political conflicts, their dependence on larger economies and unstable commodity prices. Given these types of shocks in emerging economies, the modelling of financial volatility, changes in volatility, breaks and their effects on such markets is important. Accordingly, in this dissertation I develop models for volatility in my first two essays with the aim of contributing to the growing literature on modelling financial series using dynamic conditional score models. For my last essay, I propose and analyse a score-based model for the multivariate location of macroeconomic variables with factors and heavy tails, and I use it to analyse monetary policy in the United States.

The proposed models in this thesis are specified and estimated within the dynamic conditional score (DCS) framework because this framework facilitates maximum likelihood estimation and it can handle shocks of large magnitude. Further, all of these models assume a Student t distribution in their structure. This distribution can accommodate abnormal shocks because of its heavy tail features. As time passes the world faces new challenges. The emerging economies in South America have experienced episodes of turmoil such as those associated with the Asian and global financial crises, as well as other more local shocks. They have also experienced the recent health crises, and now there is a conflict in Europe, which could mean another big shock in the short to medium horizon.

Fry-McKibbin, Hsiao and Tang (2014) describe nine episodes of significant stock crashes in the world from 1997 to 2013. Four of them originated in the Americas: the Brazilian sudden devaluation from January to February 1999, the capital control in Argentina at the end of 2001, as well as the Dot-com and the Great Recession U.S. shocks that began in March 2000 and September 2008, respectively. These events suggest a variety of breaks, regimes and periods of co-movements in stock volatility.

The main motivation for studying stock markets in South America comes from their vulnerability to these shocks, but also from their susceptibility to regional and political shocks that the DCS framework is able to handle. For example, Figure 1.1 plots the squared returns from Chilean, Colombian and Peruvian, as a proxy of their conditional volatility.

Figure 1.1: Squared returns

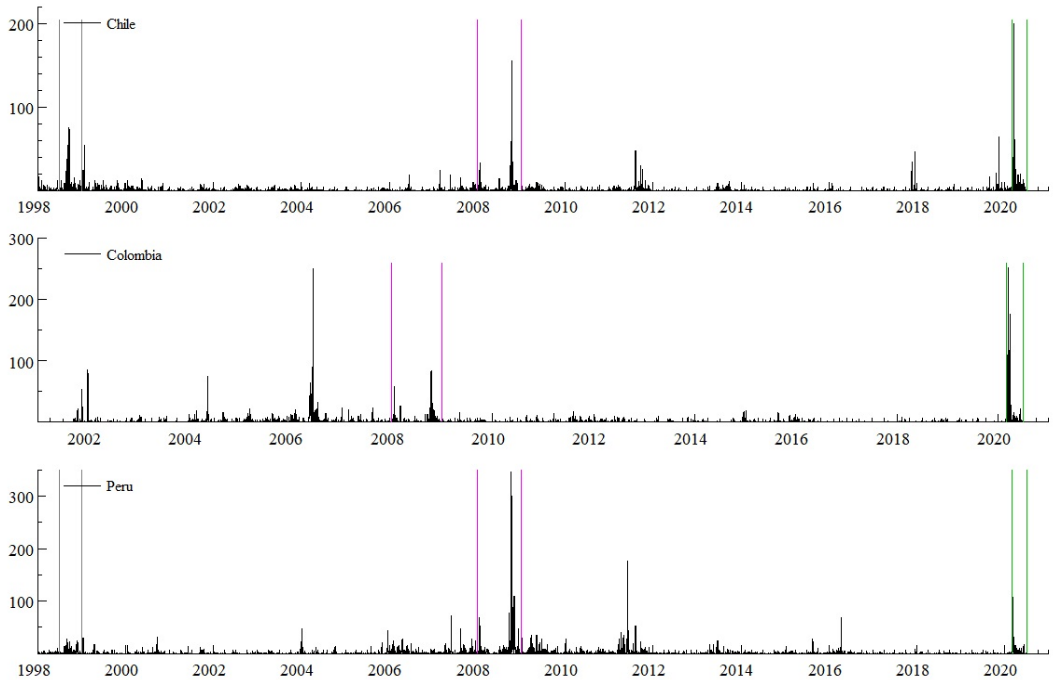

Notes: The grey lines mark the second half of 1998; the purple lines, the 2008; and the green lines, the period March-June 2020, associated with the Asian crisis, U. S. financial crisis, and the pandemic, respectively.

We can identify episodes such as the crisis of 1998 triggered in Asian countries as a result of continuous currency devaluations (Dungey, González-Hermosillo, and Martin, 2011). In addition, the Great Recession in the United States in 2008 exacerbated the stock market's volatility in South America, as did the pandemic that started in 2020. Further, these stock markets reflect sentiment about national elections, which in these developing countries could mean potential structural reforms. For instance, it is clear that the Peruvian market reacted strongly around mid-2006 and mid-2011 when the national elections took place.

Stock market volatility series generally display persistent behaviour as a consequence of these shocks, in addition to their heightened volatility. In my first essay, I formally test if the volatility in South American stock markets fits a model with a long memory pattern, or if instead it follows a structure of a short term process with changes in regime. I propose a model that captures these features so that we can identify volatility regimes in South America.

In my second essay I seek to find common patterns in pairs of American countries that share economic and trade linkages. Figure 1.2 plots overlapping stock return series of Argentina and Brazil (top panel), and Canada and Mexico (bottom panel) from October 1996 to December 2020.

Argentine and Brazilian stock returns seem to have overreacted similarly to the capital flows occasioned during the Brazilian devaluation shock in 1999, the Argentinian capital control distress of 2001, the Asian crisis, and also to the global financial crisis and the pandemic. We can find similar co-movements in the stock markets for both pairs around these crisis episodes, which gives evidence of interdependence in stock market volatility. It is important to distinguish these global shocks from regional shocks, either in South America for Argentina and Brazil, or North America for Canada and Mexico. There are also local shocks in each of these markets. In my second essay, I propose a two-component model to deal with long-lasting shocks, but at the same time the model also identifies more transient shocks in their markets.

The pandemic shock generated a higher cluster of volatility. Recently, Fry-McKibbin, Greenwood-Nimmo, Hsiao and Qi (2022) describe the COVID-19 shock and its impacts on the group of 20 (G20) countries, which includes these four economies. They identify two COVID phases, the first one in China at the early stages of the coronavirus spread, and the second phase originated in the USA, after the official pandemic announcement from the World Health Organization (WHO). They find that Argentina was particularly affected in the first phase as we can see in the top panel of Figure 1.2. Overall, these countries were impacted by the health shock in its second phase.

We should bear in mind that the American continent was strongly affected by the recent pandemic, which rendered numerous life losses estimated to be 2.7 million people[1] according to Our World in Data. Many countries (including Latin American countries), imposed early and drastic restrictions such as quarantines, and closures of borders at the beginning of the pandemic generating a period of huge uncertainty. This unprecedented health shock affected Canada with a similar severity.

[1]Data as of April 2022.

Figure 1.2: Stock market returns for Argentina, Brazil, Canada and Mexico

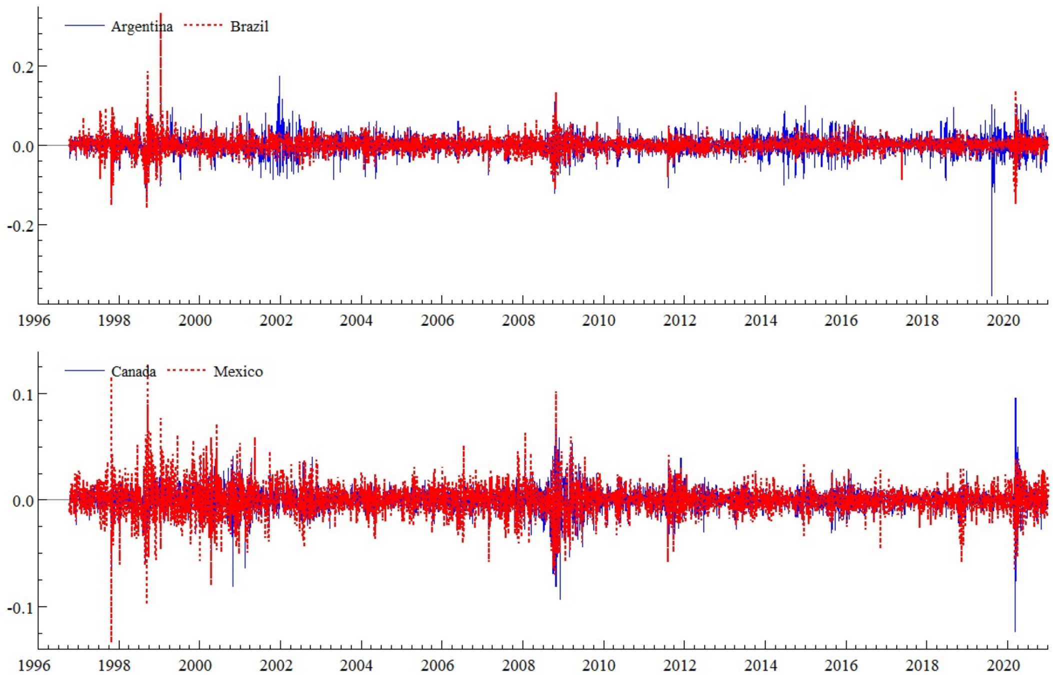

In my final essay I assess monetary policy shocks in the United States. The U.S. is one of the biggest economies in the world and its economic decisions will often have a significant impact on many countries. To give some examples, Latin American countries have high levels of dollarization, and so they experience pressure to devaluate their currencies when they receive exchange rate shocks. Further, a rise in the U.S. Federal funds rate could mean a flow of capital from Latin America, assuming investors seek greater returns. The U.S. economy is subject to many types of shocks. I show the first-differenced real personal income and the evolution of the U.S. Federal funds rate in Figure 1.3.

Figure 1.3: Real personal income and Federal funds rate

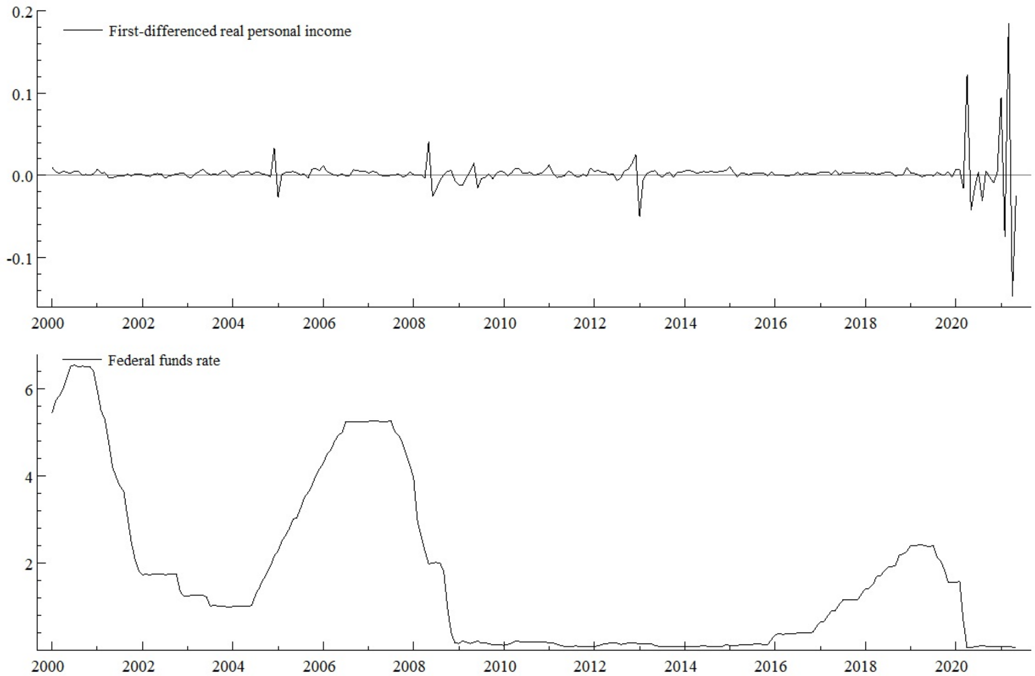

We see how the big pandemic shock hit the U.S. economy. Real personal income has considerable variance at the end of the sample, which is marked by big outliers when the data is transformed into first differences. This shock was unprecedented if we compare it with the financial crisis and other major shocks. Monetary policy during the financial crises and also during the pandemic consisted of a quick decrease in the Federal funds rate to just above the zero lower bound, in order to stimulate the economy. We can identify zero lower bound episodes associated with the Great Recession from December 2008 to December 2015, and a recent second episode that started in March 2020.

Figure 1.4 shows the U.S. unemployment rate and the stock return of the main representative index market in that country, the S&P 500. We can observe a smooth increase in the unemployment rate towards the end of 2009 as a result of the Great Recession. After this shock, unemployment showed a marked trend to its level before the financial crisis. However, the pandemic lead to an outlier episode in 2020. Similarly, monthly S&P 500 stock returns display large losses in market capitalization in 2008 and 2020.

Figure 1.4: U.S. Unemployment rate and stock returns

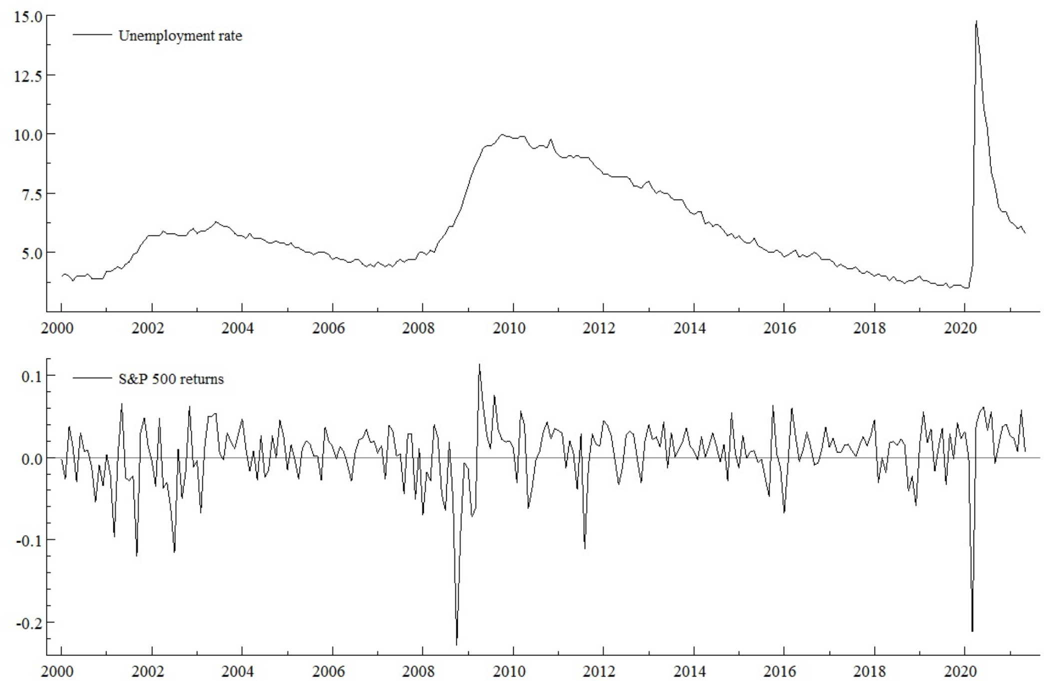

I use principal components and many economic indicators of U.S. output, income, labor, consumption, housing, inventories, interest rates, exchange rates, credit and prices, to capture the main features of U.S. data. These components (factors) capture the variability in the panel data of economic indicators and reflect the most turbulent episodes. I then incorporate these factors into a score-driven macroeconomic model that is capable of dealing with these shocks and evaluate monetary policy in the USA.

1.2 The dynamic conditional score framework

The work of Harvey and Chakravarty (2008), Creal, Koopman and Lucas (2013) and Harvey (2013) emphasized that the scaled score of the likelihood can be exploited to facilitate the estimation of models with time varying parameters. Such score-driven models, often known as dynamic conditional score (DCS) models, or versions of DCS models that use time-varying scaling parameters for the score (known as generalised autoregressive score (GAS) models), have become popular in the literature. By design, the DCS framework can be used to model the location or mean, as well as the scale or volatility. Current applications of DCS methodology includes its use in Markow switching settings (Bazzi, Blasques, Koopman and Lucas, 2017); censoring (Harvey and Ito, 2020); dynamic Tobit models (Harvey and Liao, 2019); and vector autoregressive models, as introduced by Blazsek and Licht (2020).

The DCS framework for modelling volatility provides an alternative approach for estimating the traditional generalized autoregressive conditional heteroskedasticity (GARCH) model of Bollerslev (1986) and the discrete stochastic volatility (SV) model first proposed by Jaquier, Polson, and Rossi (1994). In addition, in the macroeconomic literature, this approach can be used for the estimation of dynamic stochastic general equilibrium models (DSGE) and vector autoregression (VAR) models with heavy tails. Given the recent pandemic and other shocks in the recent decades, this approach provides an alternative way to modelling these episodes of turmoil observations.

The gains from modelling volatility using the DCS framework in comparison to the traditional GARCH models comes from the score term of the model. Let us consider the t-GARCH model for a demeaned return y_t given by

$$y_t = \sigma_t \epsilon_t, \tag{1.1}$$

$$\sigma_{t+1}^2 = \alpha + \beta_0 \sigma_t^2 + \beta_1 y_t^2, \tag{1.2}$$

$$\sigma_{t+1}^2 = \alpha + \phi \sigma_t^2 + \beta_1 \sigma_t^2 u_t^*, \tag{1.3}$$

$$\epsilon_t \sim t_\nu, \tag{1.4}$$

with $\phi = \beta_0 + \beta_1 < 1$ and $u_t^* = y_t^2/\sigma_t^2 - 1$. u_t^* is a martingale difference sequence and can be viewed as a volatility shock. The DCS framework exploits this martingale property by replacing u_t^* with

u_t so that equation (1.3) becomes:

$$\sigma_{t+1}^2 = \alpha + \phi\sigma_t^2 + \beta_1\sigma_t^2 u_t, \tag{1.5}$$

$$u_t = [(\nu+1)y_t^2/\{(\nu-2)\sigma_t^2 + y_t^2\}] - 1, \tag{1.6}$$

$$u_t = (\nu+1)b_t - 1, \tag{1.7}$$

$$b_t = \frac{y_t^2/(\nu-2)\sigma_t^2}{1 + y_t^2/(\nu-2)\sigma_t^2}, \tag{1.8}$$

$$b_t \sim Beta\left(\frac{1}{2}, \frac{\nu-2}{2}\right), \tag{1.9}$$

where u_t is a term proportional to the score of the process. This model is called a Beta-t-GARCH model since the score term follows a Beta distribution. The use of u_t leads to efficient and robust estimates when atypical observations are present relative to the t-GARCH model. This is because the Beta-t-GARCH model takes into account the information of the degrees of freedom through the score of the model, as we can see in equation (1.6).

A disadvantage of standard Stochastic Volatility models is that they require an approximation for the likelihood function because of the assumed latent components. However, in the DCS setting the likelihood function is derived in closed form, given that the model is fully conditioned by its score.

The gains from the DCS model when modelling the location of a model driven by a Student t multivariate error comes from the use of the score, which replaces the error term in state-space models. As discussed in Harvey (2013), we may think of a simple state space model with the following representation for series x_t:

$$x_t = \gamma_t + \varepsilon_t,\ \varepsilon_t \sim N(0, \sigma_\varepsilon^2), \tag{1.10}$$

$$\gamma_{t+1} = \gamma_t + \eta_t,\ \ \eta_t \sim N(0, \sigma_\eta^2), \tag{1.11}$$

where ε_t is an error term, and γ_t follows a random walk process with innovation η_t. Further, the Kalman filter representation depends on the prediction error υ_t and the Kalman gain k_t:

$$\upsilon_t = x_t - \gamma_{t|t-1}, \tag{1.12}$$

$$\gamma_{t+1|t} = \gamma_{t|t-1} + k_t\upsilon_t. \tag{1.13}$$

The DCS framework replaces this prediction error term with a term proportional to the score u_t scaled by a fixed parameter k. One important advantage of this observation-driven representation is that it can be estimated by maximum likelihood. This is an alternative approach in contrast to Bayesian estimation, which might become computationally demanding when considering large non-linear models.

A further advantage of the DCS is its flexibility since it can model directly the main parameters of a distribution. Specifically, I model the univariate scale and multivariate location Student t distribution in my first and third essays, respectively. Meanwhile, in my second manuscript I utilise a Student t copula.

1.3 Overview and outline

My thesis is comprised of three essays: My first two essays focus on the scale or volatility of univariate and multivariate models, whereas the last chapter focuses on a multivariate location model.

In the first essay of my dissertation, I analyse financial univariate series with high persistence in their volatility, using a novel dynamic conditional score (DCS) framework. This approach exploits the information from the score of the model and the benefits of this approach include the modelling of time-varying parameters such as changes in the location or scale of a distribution and its robustness to outliers.

I adapt the DCS model for volatility to include random shifts, and I show that high persistence in volatility can be modelled as a combination of short-memory and random shifts processes. The new model is able to capture short-term persistence and identify the breaks and changes in regimes of volatility in South American stock market volatilities. I use Monte Carlo simulations to show that this process resembles the original time and spectral properties of the data. Compared to the model without shifts, this model presents a better in-sample and density forecast performance. I have published this essay at *Finance Research Letters*.

My second essay also examines high persistence in volatility, but in time-varying dependence parameters arising from score-driven copula models. I model explicitly the high persistence using a specific long-term component, but at the same time account for transient shocks with another component. The empirical application considers three country pairs in the American continent that are linked geographically and economically.

The treatment of the dependence parameter identifies shocks in the long-component with more duration such as the Asian and US. financial crises, and the current pandemic. The short-component accounts for shorter-run local shocks that affect the dynamics of these markets. The model with components outperforms the single-component baseline model according to different criteria.

Finally, in the third essay I develop a factor-augmented multivariate location model using the DCS approach. This model adds component factors to a quasi-vector autoregressive (QVAR) model for the assessment of monetary policy in the United States. My approach assumes a Student t distribution for the shocks, which accommodates events such as the global financial crisis and the COVID-19 shock.

I estimate this model with a two-step estimation procedure. In the first step, I estimate the principal factors from information variables for the U.S economy. Then, in the second step I add these estimated factors into a QVAR model with the monetary policy instrument. I study the monetary policy shocks in the USA and find that the non-linear model outperforms the linear model. Also, the proposed model is robust to big shocks and produces stable estimates, even when considering zero lower bound episodes.

The next chapter presents my article on a dynamic conditional score model with random shifts. In chapter 3, I present the results from my proposed multivariate copula model with components. Chapter 4 develops an augmented-factor multivariate location model for assessing monetary policy. Finally, in chapter 5, I present the conclusions of my dissertation and some proposals for further research.

2 Modelling Stock Returns Volatility with DCS Models and Random Shifts

2.1 Introduction

In this chapter, I develop a dynamic conditional score (DCS) model for volatilities with random shifts (RS) based on the assumption that they follow a Student t distribution. Introducing RS enables the capture of volatility shifts in return data and I explore various ways in which RS improve the DCS specification, especially for South American emerging markets which are subject to many unpredictable shocks.

A recent trend in the volatility literature is to use observation-driven approaches— the dynamic conditional score models of Harvey and Chakravarty (2008), Creal, Koopman, and Lucas (2013), and Harvey (2013)— to model time-varying parameters. Creal et al. (2013) and Harvey (2013) assert that this specification is robust to outliers because this setting directly incorporates the information from the score of the process, which is ignored in the GARCH model of Bollerslev (1986).

Recently, the DCS model has emerged as an alternative approach for modelling volatility, to be used instead of the traditional generalized autoregressive conditional heteroskedasticity (GARCH) model of Bollerslev (1986) or the discrete stochastic volatility (SV) model first proposed by Jaquier, Polson, and Rossi (1994). Creal et al. (2013) and Harvey (2013) assert that this specification is robust to outliers because this setting directly incorporates the information from the score of the process, which is ignored in GARCH models.

A disadvantage of SV models is the need to approximate the likelihood function because of the assumed latent components. Further, due to its unobservable nature, an SV model captures the volatility in an indirect way, and its estimation requires a preliminary transformation (e.g., taking logarithms) of its error terms. This approximation requires a mixture of normal distributions. Nonetheless, in the DCS setting the likelihood function is derived in closed form, and this observation-driven approach models the time-varying volatility directly through the scale of the distribution.

The main contribution of this study is the combination of the DCS model for volatility with random shifts. The addition of RS follows the work of Qu and Perron (2013) and this process is mainly driven by a Bernoulli parameter. My model not only captures the main volatility episodes, including outliers, but also allows for random shifts that are capable of identifying volatility regimes. This is a novel approach because the literature concerning DCS models often assumes that volatility is a long memory process. For example, Lucas and Opschoor (2019) model the fractional integration parameter, and Harvey and Palumbo (2019) establish long and short memory processes for their two-component model for realised volatility.

Perron and Qu (2010) develop a graphical device using the log periodogram of a series. Given an estimated periodogram with M frequencies, they identify three features that mimic a short-term process with random shifts in a sample of T observations: a sharp decay for values less than $T^{1/3}$, a steady shape between $T^{1/3}$ and $T^{1/2}$, and a slow decay starting at $T^{2/3}$. In a long memory process, by contrast, the periodogram will remain steady across the sample. Figure 2.1 plots the periodogram for the proxy of volatilities in South American returns, where the vertical lines mark $T^{1/3}$, $T^{1/2}$ and $T^{2/3}$. These estimated periodograms support the hypothesis of random shifts.

Figure 2.1: Volatility proxy periodogram

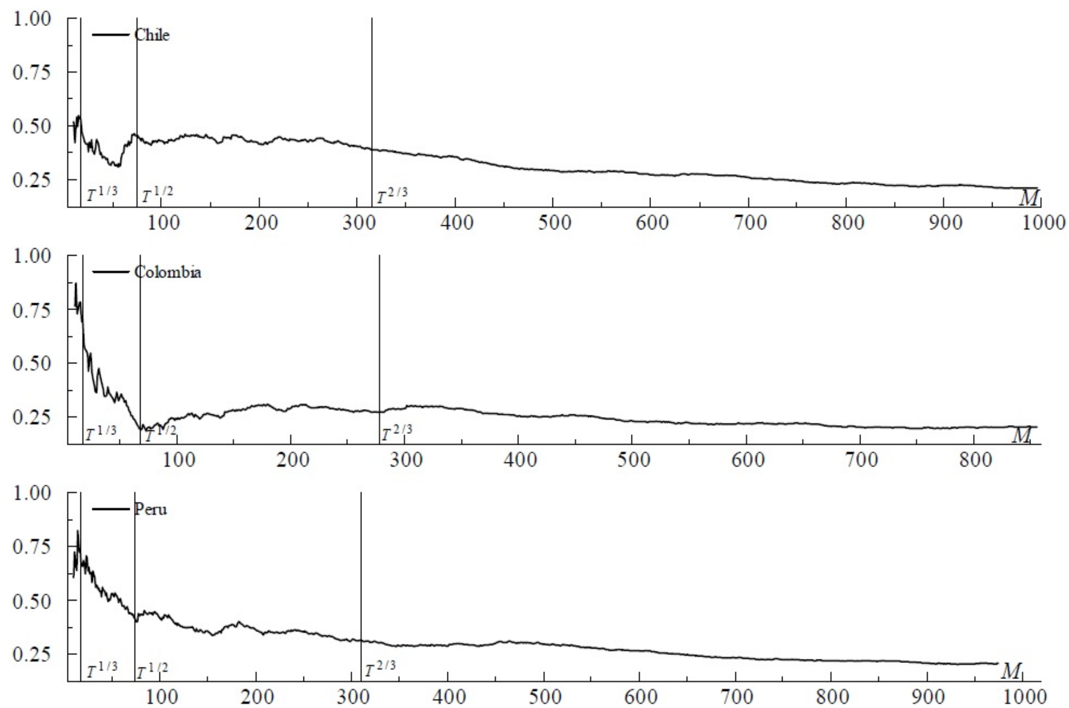

Note: The proxy is computed as $\ln(x_t^2 + 0.001)$, where $x_t$are the demeaned stock returns.

In addition, Qu and Perron (2013) incorporate RS in a stochastic volatility model. Alvaro, Guillén, and Rodríguez (2017) use this stochastic volatility model with random shifts to study the volatility of commodity prices. They find that, in Latin America, the estimated regimes of volatility are highly correlated with business cycles. This underscores the importance of random shifts when modelling volatility in emerging markets. However, a limitation of these studies is that they assume normality or mixed normal distributions.

In this chapter, volatilities follow a Beta-t-EGARCH model with RS. This model not only captures the main volatility episodes, including outliers, but also allows for random shifts that are capable of identifying volatility regimes. This is a novel approach because the literature concerning DCS models often assumes that volatility is a long memory process. For example, Lucas and Opschoor (2019) model the fractional integration parameter, and Harvey and Palumbo (2019) establish long and short memory processes for their two-component model.

The addition of RS follows the work of Qu and Perron (2013) and the process is mainly driven by a Bernoulli parameter. When the Bernoulli parameter takes the value of 1, then a shift occurs in the volatility of returns and is adjusted at the level of the volatility shock, but if there is no such shift, the process maintains the level of the previous period. A scale parameter in the RS process captures the aggregate magnitude of the shifts in the sample.

Monte Carlo simulations show that the proposed model captures the time and frequency properties of the original series. As an empirical application, I use the stock returns of the main emerging market economies in South America: Chile, Colombia and Peru. After the Pacific Alliance trade agreement in 2011, these economies established deeper trade and financial linkages. The Pacific Alliance represents about a third of the gross domestic product of the region.

I find that the persistence of a shock in the Beta-t-EGARCH model without RS for the stock market returns that I analyse is relatively higher than that in a model with RS since the RS component captures part of the persistence. These results highlight the importance of modelling shifts in volatility because this will have a significant effect on the forecast of the duration of shocks, and hence, on the transitory effects of a shock to the volatility. In addition, the model captures the main volatility regimes in these emerging markets as a result of multiple shocks, regardless of whether they arise from internal or external turmoils.

In comparison with the base Beta-t-EGARCH model, the new model shows a better fit to the data. According to the log-likelihood and the information criterion, the RS-Beta-t-EGARCH model improves in-sample fit. Monte Carlo simulations show that the new model replicates the time and spectral domain properties of the original series. In addition, the model with shifts presents more accurate density forecasts which might be employed in applications such as value-at-risk and expected shortfall.

The structure followed in this chapter is as follows: Section 2.2 discusses the Beta-t-EGARCH model with random shifts. Section 2.3 and 2.4 present the main empirical findings in the application of the model to emerging market economies. Section 2.5 shows, through Monte Carlo simulations, the relevance of random shifts, and density forecast comparison. The conclusions are set out in the final section.

2.2 The RS-Beta-t-EGARCH model

The Beta-t-EGARCH model with random shifts (RS-Beta-t-EGARCH) employs an exponential link function to model the volatilities through the scale.[2] The RS-Beta-t-EGARCH model for the demeaned return y_t, for $t = 1, ..., T$, is as follows:

$$y_t = \exp(\tilde{\lambda}_t)\varepsilon_t, \ \varepsilon_t \sim t_\nu, \tag{2.1}$$

$$\tilde{\lambda}_t = \omega + \lambda_t + \mu_t, \tag{2.2}$$

$$\lambda_t = \phi\lambda_{t-1} + \kappa_\lambda u_{t-1}, \tag{2.3}$$

$$\mu_t(s_t) = \mu_{t-1}(s_{t-1}) + \delta_t \kappa_\mu u_{t-1}, \tag{2.4}$$

$$u_t \propto \frac{\partial \ln f_t(y_t|Y_{t-1})}{\partial \tilde{\lambda}_t}. \tag{2.5}$$

This model uses an exponential link function between the logarithm of the scale[3] $\tilde{\lambda}_t$ and the volatility σ_t so that $\sigma_t = [\exp(\tilde{\lambda}_t)/\{(\nu-2)\hat{}(1/2)\}]$, where ν are the degrees of freedom of the zero mean Student t distribution ε_t. The scale $\tilde{\lambda}_t$ has three components: the constant term ω, the short-term component λ_t and the random shifts process given by μ_t.

[2]This model retains and improves the properties of the EGARCH model presented by Nelson (1991).
[3]Hereafter, I use the term scale when referring to the logarithm of the scale.

The short-term component λ_t has persistence ϕ and it captures temporary increments in the scale as a result of a volatility shock. On the other hand, a shock to the random shifts process in equation (17) will be maintained until another shock occurs. Random shifts occur when a Bernoulli variable δ_t takes the value of 1 and an associated indicator s_t is then equal to 1. This occurs with probability α. There is no random shift when $s_t = 0$, and this occurs with probability $1 - \alpha$.

Following Klaassen (2002), the dependence of μ_{t-1} on s_{t-1} is integrated out, so that

$$\mu_{t-1}(s_t) = E[\mu_{t-1}(s_{t-1})|s_t, Y_{t-1}], \tag{2.6}$$

$$\mu_{t-1}(s_t) = (1-\alpha)\mu_{t-1}(s_{t-1} = 0) + \alpha\mu_{t-1}(s_{t-1} = 1). \tag{2.7}$$

Finally, u_t is proportional to the conditional score, κ_λ is a scaling parameter and κ_μ scales the cumulative contribution of u_t to the random shift process μ_t.

The RS-Beta-t-EGARCH model can be estimated by maximizing the likelihood with respect to the parameter set $\psi = (\omega, \phi, \kappa_\lambda, \kappa_\mu, \alpha)$ and the degrees of freedom ν. The model lies between the single component model of Harvey (2013) when $\alpha = 0$, and the two-component model of Harvey and Sucarrat (2014) when $\alpha = 1$ and the persistence of the long-term component is set to one. The identifiability conditions for the latter model are that $0 < \kappa_\lambda < \kappa_\mu$ and the short-component persistence $\phi < 1$, and these conditions will suffice for the RS-Beta-t-EGARCH model for which $0 \leq \alpha \leq 1$, ensuring that estimates will be consistent and asymptotically normally distributed.

2.3 Empirical Application

Densities of financial series (e.g., returns in stock and currency markets) often show heavy tails due to their considerable instability. South American stocks are particularly vulnerable to episodes of volatility, since they are both influenced by global economic shocks as well as their own frequent local political and economic crises. This study focuses on Chile, Colombia and Peru, because these countries have been in the Pacific Alliance trade agreement since 2011 and their stock markets are integrated through the *Mercado Integrado Latinoamericano* (MILA) program.

Table 2.1 presents statistics for daily returns on the S&P 500 for the United States, and the stock returns from the main equity markets of Chile (IPSA), Colombia (COLCAP) and Peru (IGBVL).[4] The sample covers the period between January 1998 and June 2020, but it starts from January 2001 for Colombia, which is when the Colombian equity index was created. The mean returns are close to zero, indicating a lack of arbitrage opportunities. In addition, the statistics indicate departures from a normal distribution, with negative skewness, high kurtosis and a rejection of normal density behaviour from the Jarque-Bera test.

Table 2.1: Stock market returns statistics

Country	United States	Chile	Colombia	Peru
Value/Index	S&P 500	IPSA	COLCAP	IGBVL
Mean	0.028	0.031	0.056	0.048
Maximum	11.580	12.528	15.822	13.673
Minimum	-11.984	-14.115	-15.883	-18.633
Standard Deviation	1.254	1.119	1.301	1.366
Skewness	-0.151	-0.214	-0.266	-0.541
Kurtosis	13.177	18.587	24.503	19.583
Jarque-Bera	24434.750	56689.280	89275.590	62653.410
Number of Observations	5657	5596	4631	5445

Note: Returns are computed as $r_t = [\log(P_t) - \log(P_{t-1})] * 100$,where P_t is the index.

Almost all the South American stock returns exhibit a higher skewness, which is statistically significantly larger, when compared to the S&P 500 returns.[5] The more pronounced negative skewness reflects more downturn episodes than in the United States, which might be explained by its relevance worldwide. These features are common in small open economies because of the multiple shocks (i.e., external shocks from commercial partners, as well as internal, political, and commodity shocks) that they face. These properties might also suggest the modelling of multiple regimes of volatility in emerging market economies. The exception is Peru, but this market shows a greater standard deviation and kurtosis relative to the U.S. stock market.

[4] The returns are computed as $r_t = [\log(P_t) - \log(P_{t-1})] * 100$, where P_t is the index.

[5] The 95 percent confidence intervals for the skewness (kurtosis) from each set of returns do not overlap.

Figure 2.2 displays the South American stock market returns. It is clear that key economic events, such as the Asian crisis shock during the 1990s, the global financial crisis in 2008 and the recent pandemic at the beginning of 2020, are episodes of atypical uncertainty. We can also identify episodes of higher instability for each market such as national general elections involving candidates of radical ideas in Peru in mid-2006 and mid-2011, and in Colombia in the middle of a military conflict in May 2022. Further, in Chile there were a series of economic reforms at the end of 1990s after the established dictatorship of Pinochet. Another event that struck the Chilean and Peruvian markets in 1998 was the Russian crisis due to the trade linkages of these countries with the US market, which was considerably affected from this shock (Fry-McKibbin, Hsiao and Tang, 2014).

Figure 2.2: South American stock returns

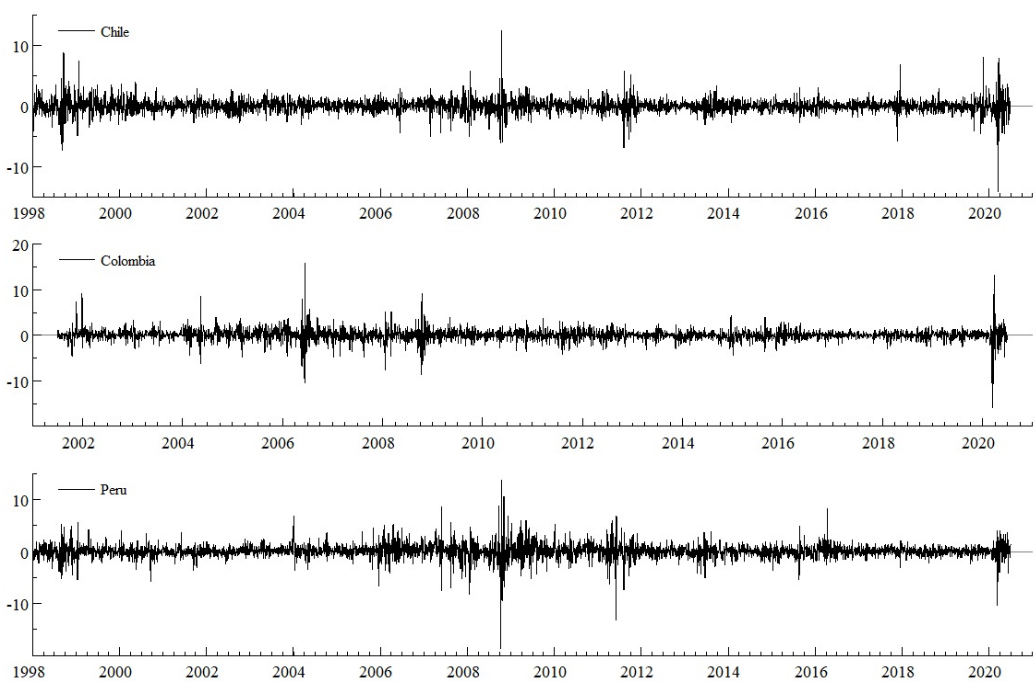

Note: Returns are computed as $r_t = [\log(P_t) - \log(P_{t-1})] * 100$,where P_t is the country index.

Financial markets react quickly to disruptive events such as political upheaval, the global financial crisis, or more recently, global health alarms because of their liquid nature. It is important to develop volatility market models that are useful for financial analysts, including those who evaluate

Value at Risk (VaR). Policymakers in emerging market economies also find volatility models helpful since such economies experience high commodity price volatility.

2.4 Model estimates

Table 2.2 shows estimates for the Beta-t-EGARCH and the RS-Beta-t-EGARCH models[6] using daily demeaned South American stock returns data.[7]

The persistence parameter ϕ decreases significantly[8] in all samples by approximately 0.02-0.05, suggesting that a variance shock has a more transitory effect in the new specification relative to the Beta-t-EGARCH model. This is expected since part of the persistence has now been captured by the random shifts process. Further, the scaling parameter κ_μ and the shift parameter α in the RS process are jointly significant according to the likelihood ratio test.

The random shift parameter has a point estimate of 0.021[9] for Peru, which suggests that approximately 113 shifts occurred in the estimated volatility sample. The shock is permanent until the realization of the next shift; in other words, there are 114 identified regimes of volatility. For Chile and Colombia, the RS parameter estimates are 0.008 and 0.010, which suggest 43 and 48 volatility regimes, respectively. According to the new model, the Peruvian returns volatility presents a relatively high number of shifts; however, the scaling parameter associated with shifts is 0.869 and relatively low, which implies that most of the estimated regimes are not as pronounced. For Colombia, the cumulated magnitude estimate is 1.602, and for Chile 2.060, so these values establish more marked regimes. Based on the likelihood and the Akaike (1974) information criterion (AIC), the new model has a better in-sample fit relative to the Beta-t-EGARCH model.[10]

[6]The optimization procedure corresponds to the interior point algorithm in MATLAB 2020a.

[7]I set $\kappa_\lambda < \kappa_\mu$ and the parameter estimates fulfill these identifiability conditions

[8]The confidence intervals for the parameter estimates from each model do not overlap.

[9]The estimates for the short-memory component are robust to different initial values. However, the initial values for the RS process are sensitive to bigger values in the number of shifts, for instance initial values above 0.1.

[10]Estimates of the Harvey and Sucarrat (2014) two-component model give similar likelihood measures, but this cannot account for volatility shifts (see Figure 2.4 in this essay) generated by a RS-Beta-t-EGARCH model.

Table 2.2: DCS models estimates

	Beta-t-EGARCH			RS-Beta-t-EGARCH		
Parameter	Chile	Colombia	Peru	Chile	Colombia	Peru
ω	-0.210	-0.184	-0.147	0.320	-0.265	0.074
	(0.011)	(0.041)	(0.319)	(0.016)	(0.071)	(0.027)
ϕ	0.970	0.947	0.970	0.951	0.915	0.921
	(0.005)	(0.010)	(0.005)	(0.002)	(0.012)	(0.008)
κ_λ	0.104	0.142	0.104	0.093	0.132	0.100
	(0.010)	(0.046)	(0.025)	(0.006)	(0.108)	(0.016)
κ_μ				2.060	1.601	0.869
				(0.030)	(0.166)	(0.030)
$\log(\nu)$	2.182	1.771	1.677	2.201	1.794	1.701
	(0.020)	(0.070)	(0.238)	(0.013)	(0.305)	(0.037)
α				0.008	0.010	0.021
				(0.003)	(0.004)	(0.008)
$\log L$	-7329.468	-6492.035	-7887.726	-7325.251	-6485.220	-7877.966
AIC	14666.936	12992.069	15783.453	14660.501	12980.440	15765.933
$\phi_{NO}-\phi_{RS}$				0.020***	0.033*	0.049***
$LR\ [H_0 : \kappa_\mu = \alpha = 0]$				8.435***	13.630***	19.520***
Observations	5596	4631	5445	5596	4631	5445

Notes: The standard errors (in parentheses) are computed using the inverse of the Hessian matrix. AIC is the Akaike Information Criterion. ϕ_{NO} and ϕ_{RS} denote the estimated persistence from the Beta-t-EGARCH model and RS-Beta-t-EGARCH model, respectively. LR is the likelihood ratio test statistic and H_0 denotes the null hypothesis. * and *** imply significance at 10% and 1%, respectively.

As evidenced in Figure 2.3, the estimated Beta-t-EGARCH score term periodogram of Geweke and Porter-Hudak (1983) that estimates the fractional integration parameter $\hat{d}$ at frequencies $M = [10, T^{4/5}]$ in a sample of T observations shows a behaviour that Perron and Qu (2010) document as typical of a random shifts process. That is, an abrupt decay in periodogram at frequencies less than $T^{1/3}$. We can see from the gap between both scores at frequencies lower than $T^{1/2}$ that the score for the RS-Beta-t-EGARCH model has removed the shift pattern that is now modelled appropriately in the shift process.

Figure 2.3: Score term periodogram for the Beta-t-EGARCH and RS-Beta-t-EGARCH models

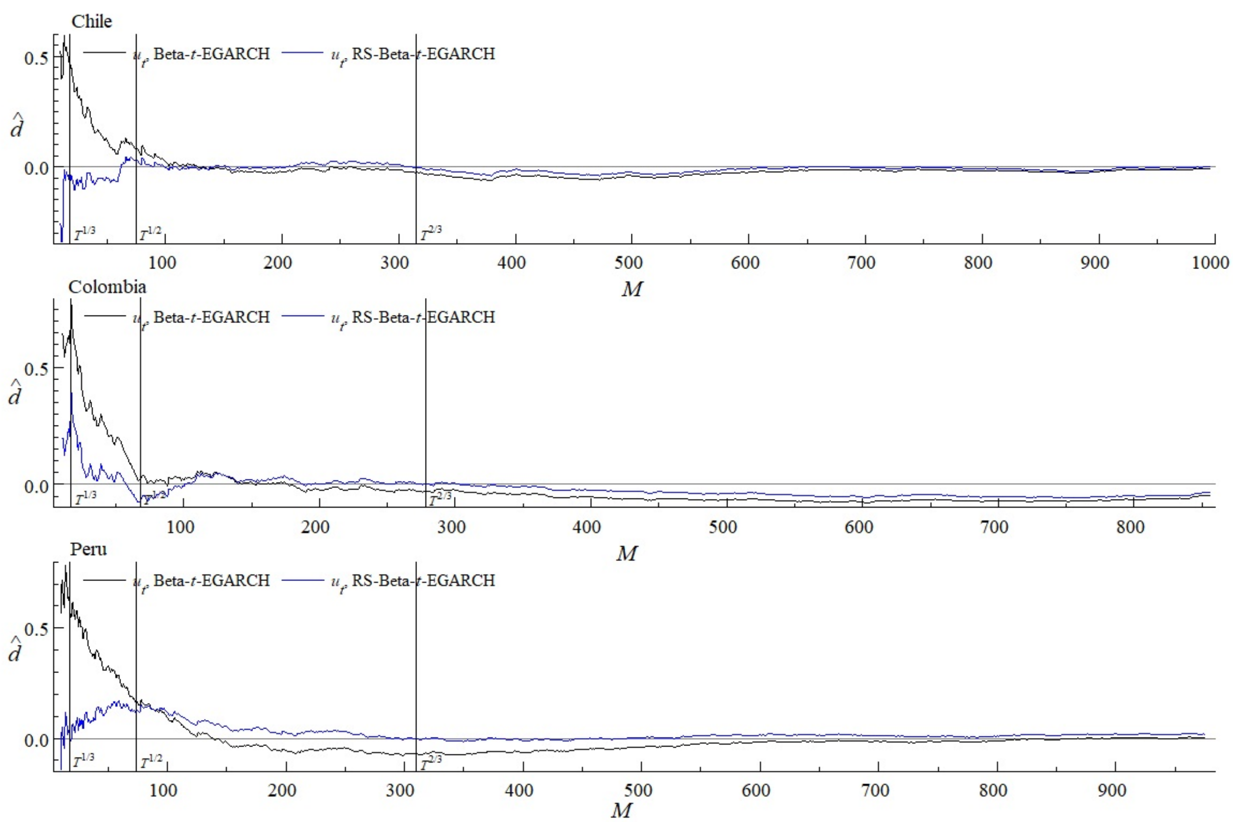

Notes: $\hat{d}$ is the fractional integration parameter at frequencies $M = [10, T^{4/5}]$ in a sample of T observations. The vertical lines represent the frequencies at $T^{1/3}$, $T^{1/2}$, and $T^{2/3}$.

Figure 2.4 plots the smoothed estimates of the random shift processes and the volatility. The gap between these two series corresponds to the short-term process. The RS capture the main regimes of volatility and each regime lasts until the model detects a new shift. These estimates capture the main cycles of uncertainty in each of the South American countries. We can see regimes of high volatility for all the countries because of the currency crisis in Asian countries during the second half of 1998. Also, the U.S. financial crisis, especially in 2008 hit the emerging markets of the region. Last, the pandemic has exacerbated the market with volatility peaks at the end of the sample.

Figure 2.4: Smoothed volatility and random shift process

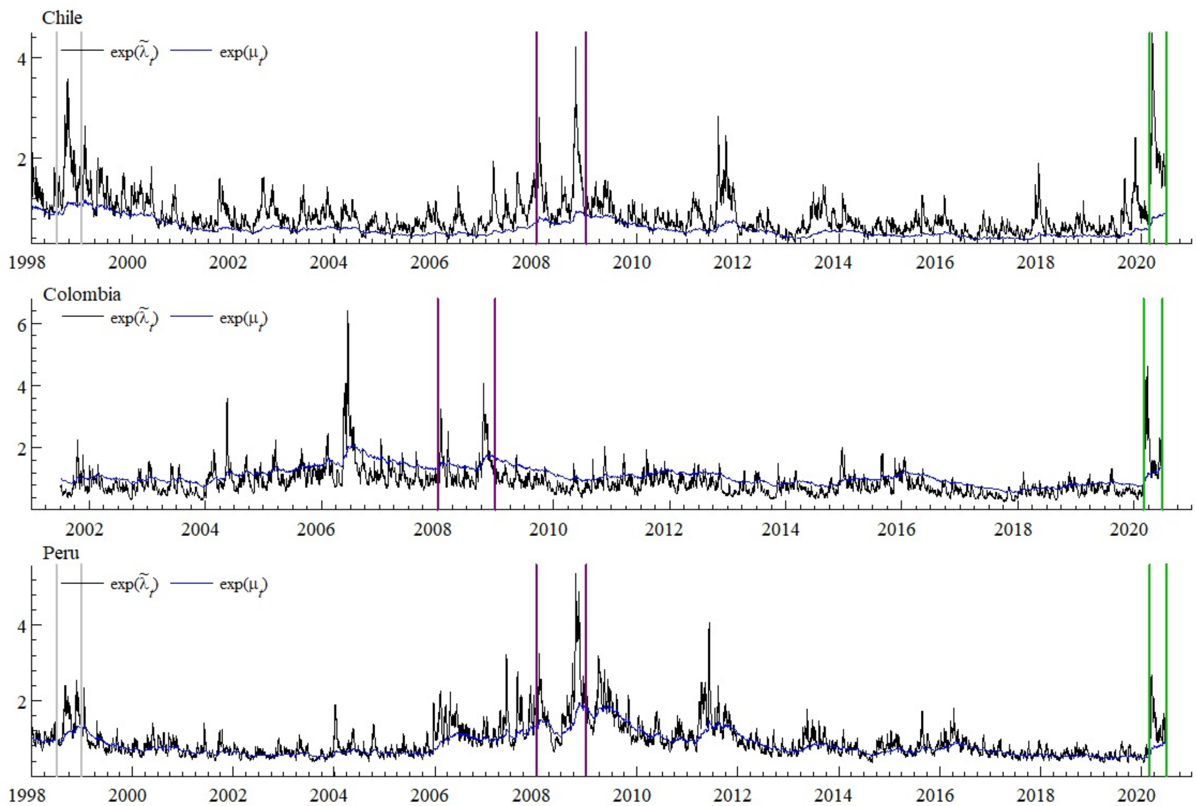

Notes: The grey lines mark the second half of 1998; the purple lines, the 2008; and the green lines, the period March-June 2020, associated with the Asian crisis, U. S. financial crisis, and the pandemic, respectively.

Each one of the countries has specific internal events that make the equity market react when there is good or negative perception about policy decisions. For instance, there were military conflicts between the Revolutionary Armed Forces (FARC) and the police in Colombia during the decade of 2000, which involved the kidnapping of the candidate for the national elections Íngrid Betancourt in February 2002. Mejía-Posada, Restrepo-Ochoa and Isaza (2022) showed that terrorism attacks generated abnormal negative returns in the Colombian stock market, whereas the peace process with the FARC in 2016 produced positive reactions in the COLCAP index.

In addition, the Colombian stock market was particularly vulnerable to the rise in interest rates in the US., after the devaluation of the national currency in June 2006 (Sosa, Ortiz and Cabello, 2017). In Chile, the main economic and labour regulations over issues such as pension funds during the 2000s had negative effects on the market. However, the Chilean stock market showed times of relative calm during the 2010s due to sound performance of the copper industry.

Furthermore, the estimates capture the main cycles of uncertainty confronting the Peruvian economy from 1998-2016: the political and economic reforms of the 2000s; a period of relative stability from 2002-2005; a heightened level of uncertainty in 2006 as a result of general elections when some parties took radical positions against economic openness; and the presidential elections of 2011 and 2016, which again created turmoil in the stock market.

I use the Bai and Perron (2003) global minimizer algorithm to fit the number of regimes estimated by the RS-Beta-t-EGARCH model so that we can determine the average duration per regime and also identify the jumps in volatility. Figure 2.5 shows the smoothed RS process and the fitted regimes for all returns. The average duration regimen is around 130, 96, and 48 days for Chile, Colombia and Peru, respectively. In addition to the Asian and U.S financial crisis, and the pandemic, we can identify relevant volatility regimes for each country. For Chile, there was higher volatility from May 2018 until December 2018, resulting from the election of a new government in March 2018 and the subsequent implementation of new policies. Colombia presents a regime of volatility starting in October 2006 which might originate from the rise in the US policy rate and associated outflows of capitals to that country (Guarín, Moreno and Vargas, 2014). Finally, in the case of Peru there was a regime linked to the tight dispute for presidency that involved radical reforms from February 2006 until after the general elections in April 2006.

2.5 Monte Carlo Evidence

I generate 10000 artificial series for each country assuming a data generating process (DGP) for the Beta-t-EGARCH model (DGP-1) and the RS-Beta-t-EGARCH model (DGP-2) with the estimates of Table 2.2 as the true values, in order to validate the robustness of my results. Since the scaling parameter κ_μ captures the aggregate effect of shifts I assume that each shift is scaled by the same magnitude.[11]

Figure 2.5: Smoothed random shift process and fitted regimes

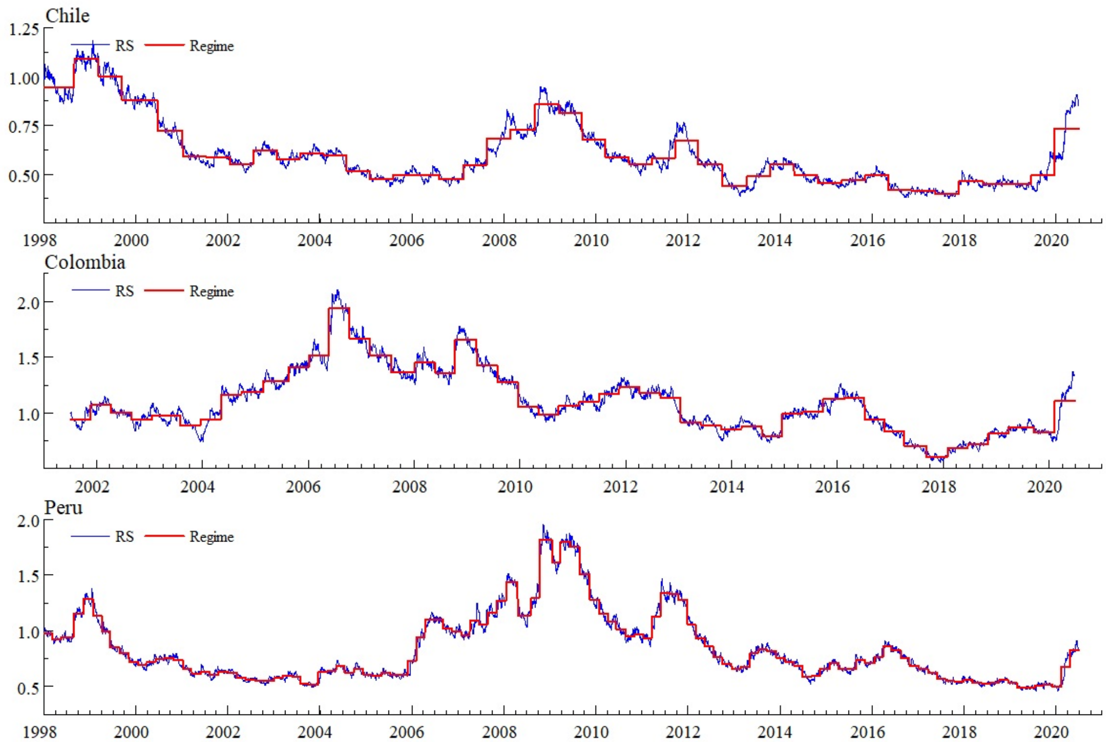

Note: RS denotes the smoothed random shift process from the RS-Beta-t-EGARCH model.

A key time domain characteristic in the analysis of memory persistence is the autocorrelation function (ACF) of the logarithm of squared returns. Figure 2.6 displays similar patterns in the original demeaned data, and the average of each of the simulated series under DGP-1 and DGP-2. The autocorrelations exhibit a quick decline to negative values, and then converge to zero. Also, the ACF for DGP-2 follows the original ACF more closely at longer lags, than does the ACF for DGP-1.

[11]When simulating shifts, the κ_μ parameter aggregates the average shift size each time.

Figure 2.6: Sample autocorrelations for the log-squared returns of demeaned original and simulated series

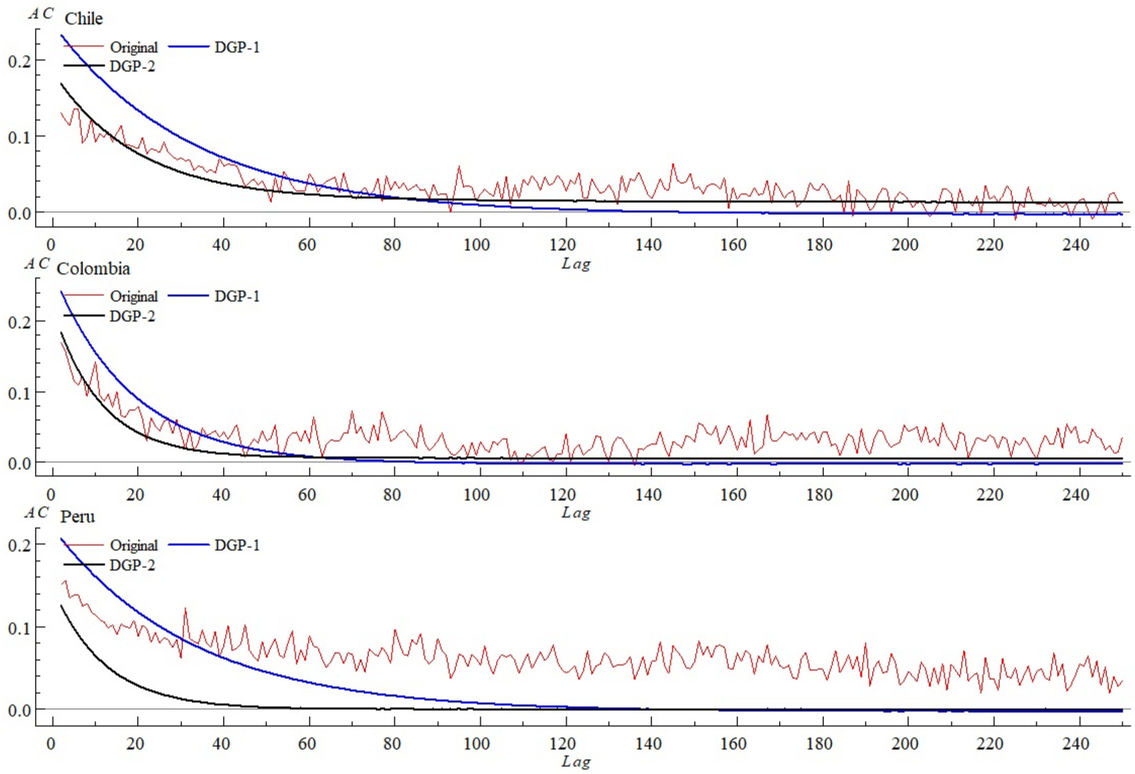

Notes: DGP-1 and DGP-2 are generated under the Beta-t-EGARCH model without shifts and with shifts, respectively. AC denotes the sample autocorrelation.

I also analyse the frequency domain properties to assess memory in the 10000 artificial series for each DGP. We observe the frequency interval for the periodograms of the original data and the average of the simulated data shown in Figure 2.7. When the artificial series comes from DGP-1 or the Beta-t-EGARCH model, the memory parameter generates an inverse pattern from the original series between $T^{1/3}$ and $T^{1/2}$ frequencies. However, if the process follows the DGP-2 from the RS-Beta-t-EGARCH model, a sudden decline appears in the value of the estimate $\hat{d}$ between frequencies $T^{1/3}$ and $T^{1/2}$. This decline in the memory parameter is consistent with the decay in the original series. There is steady behaviour in the memory parameter from $T^{1/2}$ until $T^{2/3}$ for the original and the simulated DGP-2 data. Further, starting from frequency $T^{2/3}$, the original and the simulated series display a slow decrease in $\hat{d}$, indicating that the process starts to be driven by a short memory rather than a long memory process.

Figure 2.7: Periodogram for the log-squared returns of demeaned original and simulated series

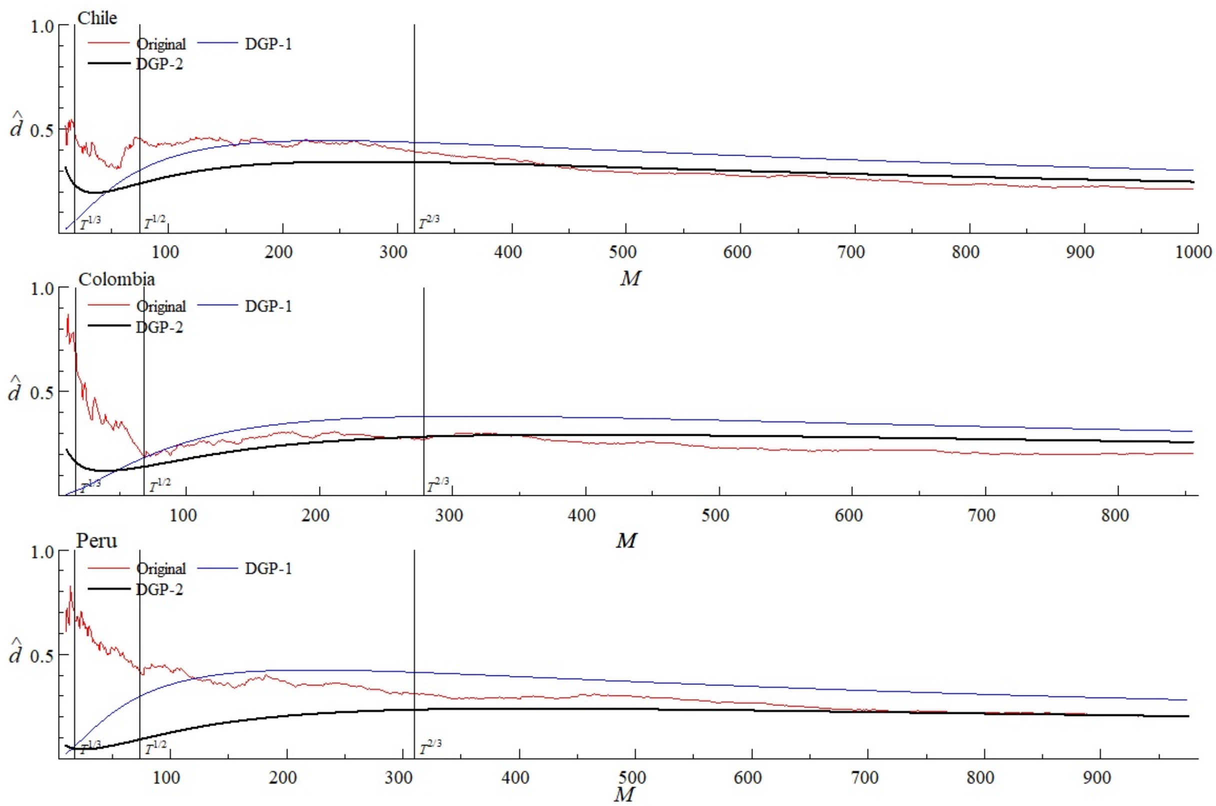

Notes: DGP-1 and DGP-2 are generated under the Beta-t-EGARCH model without shifts and with shifts, respectively. $\hat{d}$ is the fractional integration parameter at frequencies $M = [10, T^{4/5}]$ in a sample of T observations. The vertical lines represent the frequencies at $T^{1/3}$, $T^{1/2}$, and $T^{2/3}$.

Using DGP-1 and DGP-2, I verify the plausibility of the estimates for the new model. Table 2.3 presents the estimates for the South American original data, together with average estimates based on the 10000 simulated DGP-1 and DGP-2 data using the Beta-t-EGARCH and RS-Beta-t-EGARCH models.

We see in the third column of Table 2.3 that when I consider estimates based on DGP-1 the estimates are close to the original values, and when I use the RS-Beta-t-EGARCH model to estimate the shift parameter α, the $\hat{\alpha}$ is almost zero. Under this scenario, the model does not detect many artificial shifts when the true process does not have shifts. To evaluate the alternative hypothesis that DGP-2 is appropriate (in the sixth column), not surprisingly, the shift parameter estimates are closer to the true values for Chile and Colombia.

The estimate for α gives a similar value as in DGP-1 for the Peruvian case because DGP-2 implies that the scale parameter of the cumulative magnitude of shifts is divided equivalently between all the shifts in regimes. In particular, Peru has the lowest estimate (0.869) for κ_μ among the South American countries. Thus, DPG-2 generates less marked regimes and a lower estimate for the shift parameter.

2.5.1 Out-of-sample diagnostic

I employ the density forecast test based on the method of Lopez (2002). He introduces probability scoring-rules for density forecasts that replace the statistical loss functions such as those in Diebold and Mariano (1995). One benefit of this approach is that it considers the model process itself, rather than a proxy for the volatility, which is the case when loss functions take the form of the mean square error (MSE), the mean absolute value (MAE), or other statistical criteria.

Table 2.3: South American original and simulated series estimates

DGP	Original	DGP-1		Original	DGP-2	
			Chile			
Parameter	No RS	No RS	With RS	With RS	No RS	With RS
ω	-0.210	-0.209	-0.209	0.320	0.317	0.317
ϕ	0.970	0.969	0.970	0.951	0.956	0.950
κ_λ	0.104	0.155	0.152	0.093	0.140	0.136
κ_μ			2.660	2.060		1.482
$\log(\nu)$	2.182	2.192	2.192	2.201	2.196	2.203
α			0.001	0.008		0.003
			Colombia			
ω	-0.184	-0.184	-0.183	-0.265	-0.268	-0.266
ϕ	0.947	0.946	0.946	0.915	0.919	0.914
κ_λ	0.142	0.187	0.187	0.132	0.176	0.174
κ_μ			1.393	1.601		0.899
$\log(\nu)$	1.771	1.777	1.777	1.794	1.793	1.796
α			0.000	0.010		0.004
			Peru			
ω	-0.147	-0.147	-0.138	0.074	0.074	0.075
ϕ	0.970	0.969	0.970	0.921	0.921	0.919
κ_λ	0.104	0.133	0.121	0.100	0.129	0.129
κ_μ			1.651	0.869		0.529
$\log(\nu)$	1.677	1.684	1.682	1.701	1.705	1.706
α			0.002	0.021		0.002

Notes: DGP-1 and DGP-2 are generated under the Beta-t-EGARCH model without shifts and with shifts, respectively. No RS and With RS refer to the estimates using the Beta-t-EGARCH model and the RS-Beta-t-EGARCH model, correspondingly.

The weighted likelihood ratio (WLR) test of Amisano and Giacomini (2007) incorporates weights into the Lopez (2002) test that can be arbitrarily chosen. This test is based on rolling window estimates of the one-step ahead density forecasts for the RS-Beta-t-EGARCH model [$\ln \hat{f}_t^*(Y_{t+1})$], and the Beta-t-EGARCH model [$\ln \hat{f}_t(Y_{t+1})$], so that

$$WLR = w_{t+1}[\ln \hat{f}_t^*(Y_{t+1}) - \ln \hat{f}_t(Y_{t+1})], \tag{2.8}$$

where $w_{t+1} = 1/T_f$ are weights for the window sample $t = 1, ..., T_f$. The null and alternative hypotheses are

$$H_0 : E[WLR] = 0. \tag{2.9}$$

$$H_1 : E[WLR] > 0. \tag{2.10}$$

The density forecast test follows the procedure of Diebold and Mariano (1995) by defining the differences

$$d_t = \ln \hat{f}_t^*(Y_{t+1}) - \ln \hat{f}_t(Y_{t+1}), \tag{2.11}$$

and then assessing whether c is significantly greater from zero in the regression

$$d_t = c + \varepsilon_t. \tag{2.12}$$

If the test finds evidence of such a difference, then the RS-Beta-t-EGARCH model outperforms the base model. I set the rolling window to be one third of the total number of observations. The estimates $\hat{c}$ are 0.430, 1.015, and 2.650, for Chile, Colombia and Peru, correspondingly, and their Newey and West (1987) robust standard errors (0.060, 0.063 and 0.122) imply that these estimates are significant at 1 percent. Thus, the out-sample diagnostic favours the new model with random shifts.

2.6 Conclusions

This essay provides a new approach to deal with series of high persistence that are commonly treated in the literature as series with long memory. I analyse a dynamic conditional score model for modelling time-varying volatilities with random shifts. In contrast to long memory models, this model assumes that RS play a significant role in the dynamics of the volatility, affecting its persistence in particular.

The application of this model to South American equity markets shows that multiple regime shifts are linked to major events that disrupted these economies, such as the U.S. financial crisis in 2007 and the current pandemic. The estimated effect on the estimate of the persistence in volatilities when random shifts are included in the model is noticeable, and reduces the impact of a volatility shock. A comparison between the RS-Beta-t-EGARCH model with respect to the base Beta-t-EGARCH model exhibits better in-sample and out-sample performances.

This chapter opens up interesting avenues for further research. The estimated volatilities and shifts seem to be correlated as they react jointly when they face an external shock. Thus, it would be worthwhile to develop an extension for a multivariate setting and to identify common features and co-movements in times of high uncertainty. In addition, the model could be extended to model the skewness and the location of the Student t distribution.

3 Modelling Volatility Dependence with Score Copula Models

3.1 Introduction

Latin American countries are vulnerable to external shocks from bigger economies (e.g., the Asian and U.S. financial crises), and regional shocks (i.e., political and migration-related shocks) in this geographic area can spread quickly from one country to others. Dungey et al. (2011) explain that the 1998 Long-Term Capital Management collapse and the debt crisis in Russia had a very strong spillover effect on Argentina and Brazil across equity and debt instruments, which rendered the region particularly vulnerable. Forbes and Rigobon (2002) study the existence of interdependence episodes in Latin America from the Mexican currency crisis in 1994. Hence, multivariate models offer an important perspective for the analysis of interdependencies or spillovers in these markets.

Spillovers and other dependencies between financial markets can be modelled in many ways. The principal contribution of this paper is the modelling of these interdependencies using score-driven copula models. The score-driven setting emerges as an alternative approach for modelling volatilities, relative to the traditional generalized autoregressive conditional heteroskedasticity (GARCH) model of Bollerslev (1986) and the discrete stochastic volatility (SV) model first proposed by Jaquier et al. (1994). Creal et al. (2013) and Harvey (2013) suggest that this specification is robust to outliers, since this setting incorporates the information from the score of the process in a direct way.

The score-driven models proposed in this paper model the time-varying lower tail dependence with the Clayton and rotated Gumbel copulas. I also consider modelling the lower and upper tails using the Student t copula. In all cases dependence incorporates two components. Doing so, we not only capture the main dependence episodes, but also differentiate between longer and shorter components. First, the long-component process captures relatively long-lasting shocks to dependence, such as global pandemic shocks that affect all stock markets in the Americas similarly. Second, the short-component process identifies transient or local shocks in the dependence across equity indexes.

As a preliminary step, I estimate the marginal models using the GJR-GARCH model of Glosten, Jagannathan, and Runkle (1993) adjusted for skewness and fat tails. The estimated conditional variances show historical peaks during the pandemic for most of the countries in the region. Then, for the analysis of two-component score-driven copula models, I focus on bivariate settings following the work on risky assets by Ayala and Blazsek (2018). Recent studies, such as Niţoi and Pochea (2020), apply the score-driven copula methodology to European equities. In addition, Manguzvane et al. (2020) estimate mixture score-driven copula models for the main equities in South Africa. Nonetheless, no such studies exist for emerging countries in the American continent. I apply the models to Argentina-Brazil, Canada-Mexico and Chile-Peru pairs that are associated naturally by their geographic proximity and trade linkages, and all of these markets are affected by shocks from the U.S.

The study of dynamic copulas begins with the work of Patton (2006). He applies Sklar's (1959) theorem, which incorporates univariate marginal distribution estimates into a multivariate model through a copula. Further, Creal et al. (2011) and Harvey (2013) propose multivariate score-driven copula models. However, their models only consider a unique component for the dependence structure which generally presents a persistence close to one. Bernardi and Catania (2019) extend the copula specification of Creal et al. (2011), allowing a Markovian process to capture the time varying dependence. In their analysis of European equities, they find a high persistence either in the higher or lower regimes. Similarly, Opschoor, Lucas, Barra and van Dijk (2020) report a persistence close to one in their multi-factor copula models. This high persistence suggests long memory in the dependence parameter.

One way to deal with this high persistence is the addition of components. Engle and Lee (1999) introduce two components for long and short memory dynamics as additive processes in GARCH models. Similarly, Alizadeh, Brandt, and Diebold (2002) add components into SV models and use range-based estimation to study U.S. exchange rates markets. Further, Engle and Rangel (2008) develop a spline-GARCH model where the components for the volatility dynamics are multiplicative. In the same line, Engle, Ghysels, and Sohn (2013) establish a GARCH mixed data sampling model. Harvey (2013) includes a two-component structure into a dynamic conditional score model. Later, Ito (2016) uses multiplicative long and short components in her spline dynamic conditional score model. In addition, Harvey and Lange (2018) add two-component into a exponential GARCH in mean model, whereas Harvey and Palumbo (2019) and Ayala, Blazsek and Licht (2022) utilise different component specifications for the error term in score based models of realised volatility and exchange rates, respectively. Opschoor and Lucas (2021) and Linton and Wu (2022) model time-varying volatility ratios with components under the score-driven framework. However, there are no works that deal with high persistence in the dependence term of score-driven copula models and this chapter aims to cover this gap.

The score-driven framework provides robustness to outliers that are common for countries in the Americas, and hence the dynamic dependence between these countries is better characterized. The estimates of the long-component series reveal a high persistence for all copulas, and the short-memory persistence estimate characterises shocks of shorter life. The two-component model improves the fit to the data in comparison to the single component specification. Specifically, the two-component score-driven Student t copula model has the best performance among the models analyzed and it also improves the one-step density forecasts in comparison to the single component specification.

The long-component process highlights major crisis episodes such as the Asian crisis, the US financial crisis, and the recent pandemic. The estimates are robust to the COVID-19 crisis when comparing the subsample October 1996 - December 2019 and the full sample October 1996 - December 2020. An additional robustness check that re-estimates the model with bootstrapped data confirms the stability of estimates.

The structure followed in this chapter is as follows: Section 2 discusses the univariate and bivariate copula models. Section 3 presents the estimates in the application of the model to equity markets in the Americas. Section 4 describes the volatility dynamics across the marginal and score-driven copula models. Sections 5 and 6 validate the robustness of the estimates. Section 7 shows the out-of-sample density forecast from both models. Section 8 concludes.

3.2 Methodology

The approach I follow for the modelling of copulas is the generalized autoregressive model of Creal et al. (2013) and Harvey (2013). This approach exploits the information from the score derived from models. Let us consider the local level model example of Harvey (2013) for series x_t so that

$$x_t = \gamma_t + \varepsilon_t,\ \varepsilon_t \sim N(0, \sigma^2_\varepsilon), \tag{3.1}$$

$$\gamma_{t+1} = \gamma_t + \eta_t,\ \eta_t \sim N(0, \sigma^2_\eta), \tag{3.2}$$

where ε_t is the process error term, and γ_t is a random walk process with innovation η_t. The associated Kalman filter equations are

$$\upsilon_t = x_t - \gamma_{t|t-1}, \tag{3.3}$$

$$\gamma_{t+1|t} = \gamma_{t|t-1} + k_t \upsilon_t, \tag{3.4}$$

where υ_t is the one-step ahead prediction error and k_t is the Kalman gain. In the non-varying version with $\gamma_t = \gamma$ and $\sigma_\eta^2 = 0$, the maximum likelihood estimator of γ satisfies the score condition

$$\sum_{t=1}^{T} (x_t - \hat{\gamma}) = 0. \tag{3.5}$$

This condition suggests that the prediction error υ_t in (3.3) with zero mean may be replaced by a term u_t, where

$$u_t \propto \sum_{t=1}^{T} (x_t - \hat{\gamma}). \tag{3.6}$$

Hence, under the score-driven framework the equation in (3.4) is replaced by

$$\gamma_{t+1|t} = \gamma_{t|t-1} + k u_t. \tag{3.7}$$

Note that u_t is proportional to the score of the process with k being a scale parameter to estimate. The score driven setting is also valid for scale (volatility) models. Moreover, Harvey (2013) shows that this approach is robust to outliers since the score mitigates the impact from those observations.

In this chapter I employ this approach in a variety of copula models for modelling time-varying dependence. For the univariate or marginal models, I estimate the GJR-GARCH model assuming a skewed Student t for its error term.[12] The skewed Student t of the GJR-GARCH model characterises the fat tails and asymmetry typically present in return series. Then, using probability integral transformations of their residuals, I employ time-varying copula models that allow two-components in their dependence structure.

[12] This model for conditional volatility extends the GARCH model to allow asymmetries originating from overreactions in the market due to bad news for instance.

3.2.1 GJR-GARCH Marginal Model

For marginal univariate models, I consider the skewed extension for GARCH type models proposed by Hansen (1994). In particular, I model each univariate series y_{it} for the $i = 1, 2$ demeaned returns with the asymmetric GJR-GARCH(1,1) model assuming the errors follow a skewed Student t distribution as follows[13]

$$y_{i,t} = \sigma_{i,t}\epsilon_{i,t}, \tag{3.8}$$

$$\sigma^2_{i,t+1} = \alpha_i + \beta_{0,i}\sigma^2_{i,t} + \beta_{1,i}y^2_{it} + \beta_{2,i}1_{(-\infty<y_{it}\leq 0)}y^2_{it}, \tag{3.9}$$

$$\epsilon_{i,t} \sim ST(0, 1, \nu_i, \eta_i), \tag{3.10}$$

where α_i represents the constant term for the conditional variance dynamics $\sigma_{i,t}$, $\beta_{0,i}$ the persistence, $\beta_{1,i}$ the impact from the current variance shock and $\beta_{2,i}$ the leverage effect, with $\beta_{0,i} + \beta_{1,i} + (\beta_{2,i}/2) \leq 1$. Finally, the error term is a standardized skewed t distribution with $\nu_{i,}$ degrees of freedom and an asymmetry parameter $\eta_i > 0$ when it is right-skewed.

3.2.2 Two-components

I incorporate two components into score-driven copula models in order to assess long memory patterns such as persistent shocks, and shocks with shorter duration. In particular, I add this extension to Clayton, rotated Gumbel and Student t copulas. The first two copulas measure negative interdependencies, which capture shocks associated with bad news in equity markets. These types of shocks rather than positive shocks are the most recurrent in stock markets. In addition, I assess two-components in Student t copulas that capture positive and negative interdependencies. The time-varying dependence parameter λ_t for all these copulas are score-driven:

$$\lambda_t = \omega + \lambda_{1,t} + \lambda_{2,t}, \tag{3.11}$$

$$\lambda_{1,t} = \phi_1\lambda_{1,t-1} + \kappa_1 u_{t-1}, , \tag{3.12}$$

$$\lambda_{2,t} = \phi_2\lambda_{2,t-1} + \kappa_2 u_{t-1}, \tag{3.13}$$

[13] I employ GARCH models as marginal models because they have been extensively used in the finance literature by researchers and practitioners, but I do not use a score-driven framework for this. The two-step estimation procedure that I use is simpler and places focus on the score-driven copulas.

where ϕ_1 and ϕ_2 represents the persistence for the long and short memory parameter, respectively. The u_t process is a term proportional to the score of the model. Further, the scaling parameters for the score term are κ_1 and κ_2 for each process. To ensure that the equation in (3.12) identifies the long component I impose that $0 < \phi_2 < \phi_1 < 1$ and that $0 < \kappa_1 < \kappa_2$, following the identifiability conditions of Harvey (2013). In contrast, the one-component filters of association only consider the term $\lambda_{1,t}$.

I focus on models that incorporate negative interdependencies first, since these have been popular in the literature. I allow for interdependencies using the time-varying copula models of Harvey (2013), Creal et al. (2013) and Oh and Patton (2018). In bivariate settings, negative interdependencies that are present when there are negative shocks in the market are well captured by a Clayton copula:

$$C_C(\tau_{1t}, \tau_{2t}, \gamma_t) = (\tau_{1t}^{-\gamma_t} + \tau_{2t}^{-\gamma_t} - 1)^{-1/\gamma_t}, \ \gamma_t > 0, \tag{3.14}$$

where $\tau_{it} = F(y_{it})$ is the probability integral transformation of the residuals for $i = 1, 2$ series obtained from the estimation of the GJR-GARCH model for each series, and γ_t is the lower time varying tail dependence parameter. I use an exponential link function so that γ_t is always greater than zero:

$$\gamma_t = \exp(\lambda_t). \tag{3.15}$$

The term proportional to the score for the Clayton copula is given by

$$\begin{aligned} u_t \propto \frac{\partial \log C_C(\tau_{1t}, \tau_{2t}, \gamma_t)}{\partial \gamma_t} &= -\log(\tau_{1t}\tau_{2t}) + \frac{1}{1+\gamma_t} + \frac{\log(\tau_{1t}^{-\gamma_t} + \tau_{2t}^{-\gamma_t} - 1)}{\gamma_t^2} \\ &+ \left(\frac{1+2\gamma_t}{\gamma_t}\right)\left(\frac{\tau_{1t}^{-\gamma_t}\log\tau_{1t} + \tau_{2t}^{-\gamma_t}\log\tau_{2t}}{\tau_{1t}^{-\gamma_t} + \tau_{2t}^{-\gamma_t} - 1}\right). \end{aligned} \tag{3.16}$$

Likewise, I consider the rotated Gumbel copula[14] that also models lower tail dependence. Patton (2013) introduces the time-varying rotated Gumbel copula within the score-driven framework:

$$C_G(\tau_{1t}, \tau_{2t}, \theta_t) = \tau_{1t} + \tau_{2t} + e^{(-[\{-\log(1-\tau_{1t})\}^{\theta_t} + \{-\log(1-\tau_{2t})\}^{\theta_t}])^{1/\theta_t}}, \ \theta_t > 1, \tag{3.17}$$

[14]The Gumbel copula models the upper tail dependence, whereas the rotated Gumbel copula models the lower tail dependence.

which has a lower tail dependence of $2-[2\hat{}(1/\theta_t)]$, and the parameter θ_t is modelled using the link function transformation of λ_t so that

$$\theta_t = 1 + \exp(\lambda_t), \tag{3.18}$$

$$\begin{aligned} u_t \propto \frac{\partial \log C_G(\tau_{1t}, \tau_{2t}, \theta_t)}{\partial \gamma_t} &= -\log([1-\tau_{1t}][1-\tau_{2t}]) + \frac{1}{1+\theta_t} + \frac{\log([1-\tau_{1t}]^{-\theta_t} + [1-\tau_{2t}]^{-\theta_t} - 1)}{\theta_t^2} \\ &+ \frac{(1+2\theta_t)([1-\tau_{1t}]^{-\theta_t}\log[1-\tau_{1t}] + [1-\tau_{2t}]^{-\theta_t}\log[1-\tau_{2t}])}{\theta_t([1-\tau_{1t}]^{-\theta_t} + [1-\tau_{2t}]^{-\theta_t} - 1)}. \end{aligned} \tag{3.19}$$

I also study the symmetric time-varying Student t copula model. This dynamic Student t copula is given by

$$C_S(\tau_{1t}, \tau_{2t}) = F_\rho(\Phi^{-1}\{\tau_{1t}\}, \Phi^{-1}\{\tau_{2t}\}, \rho_t, \bar{\nu}), \tag{3.20}$$

where $\Phi^{-1}\{.\}$ is the inverse of the cumulative Student t distribution, and $F_\rho(.)$ is the bivariate Student t distribution with correlations ρ_t and $\bar{\nu}$ degrees of freedom.

The correlation process ρ_t is driven by the time-varying parameter λ_t such that

$$\rho_t = \frac{1-\exp(-\lambda_t)}{1+\exp(-\lambda_t)}, \tag{3.21}$$

$$u_t \propto \frac{\partial \log C_S(\tau_{1t}, \tau_{2t})}{\partial \gamma_t} = \frac{[(1+\rho_t^2)(z_t\Phi^{-1}\{\tau_{1t}\} - \rho_t) - \rho_t(z_t\Phi^{-1}\{\tau_{2t}\} - 2)]\sqrt{[(\bar{\nu}+4)(1-\rho_t^2)^2]}}{(1-\rho_t^2)^2\sqrt{(\bar{\nu}+2+\bar{\nu}\rho_t^2)}}, \tag{3.22}$$

with $z_t = [(\bar{\nu}+2)(1-\rho_t^2)]/[\bar{\nu}(1-\rho_t^2) + \Phi^{-1}\{\tau_{2t}\} - 2\rho_t^2\Phi^{-1}\{\tau_{1t}\}]$. We should bear in mind that the model assumes that a shock to the correlation process affects the dependence structure for both series at the same time and with the same magnitude.

3.2.3 Estimation

Given the demeaned return process, y_t, the GJR-GARCH model is estimated by maximizing the likelihood with respect to the parameter set $\psi = (\alpha, \beta_0, \beta_1, \beta_2)$. The likelihood for this model is given by

$$\log L(\psi) = \sum_{t=1}^{T} \log f(y_t|Y_{t-1}), \tag{3.23}$$

$$\log f(y_t|Y_{t-1}) = -\frac{1}{2}\left[\log 2\pi + \log \sigma_t^2(\psi) + \frac{y_t^2}{\sigma_t^2(\psi)}\right], \tag{3.24}$$

where $\sigma_t^2(\psi)$ is the conditional volatility dynamics as described in (3.9).

Note, that the GJR-GARCH model assumes a Gaussian error term, and the following step models the residual term $\hat{\epsilon}_t$ using the Skewed Student t distribution of Hansen (1994) with likelihood

$$\log L(\nu,\eta) = \sum_{t=1}^{T} \log(\hat{\epsilon}_t), \tag{3.25}$$

$$g(\hat{\epsilon}_t) = \left\{ \begin{array}{ll} bc\left(1 + \frac{1}{\nu-2}\left[\frac{b\hat{\epsilon}_t+a}{1-\eta}\right]^2\right)^{-(\nu+1)/2} & , \ \hat{\epsilon}_t < -a/b \\ bc\left(1 + \frac{1}{\nu-2}\left[\frac{b\hat{\epsilon}_t+a}{1+\eta}\right]^2\right)^{-(\nu+1)/2} & , \ \hat{\epsilon}_t \geq -a/b \end{array} \right\}, \tag{3.26}$$

$$a = 4\eta c\left(\frac{\nu-2}{\nu-1}\right), \tag{3.27}$$

$$b = \sqrt{1 + 3\eta^2 - a^2}, \tag{3.28}$$

$$c = \frac{\Gamma(\frac{\nu+1}{2})}{\sqrt{\pi(\nu-2)\Gamma\left(\frac{\nu}{2}\right)}}, \tag{3.29}$$

where $\nu > 2$ and $1 > \eta > -1$. Given these estimates, I apply the probability integral transformation to the residuals $\hat{\epsilon}_t$ using the skewed Student t cumulative distribution. The resulting uniform distributed series are denoted by τ_{1t} and τ_{2t}.

Finally, the dependence estimates are obtained by maximizing the log-likelihood of the copula models. For instance, the two-component score-driven t-copula model log-likelihood is

$$\log f_t(\tau_{1t}, \tau_{2t}, \theta_t) = \sum_{t=1}^{T} \log F_\rho(\Phi^{-1}\{\tau_{1t}\}, \Phi^{-1}\{\tau_{2t}\}, \rho_t, \bar{\nu}), \tag{3.30}$$

where $\varphi = (\omega, \phi_1, \kappa_1, \phi_2, \kappa_2, \bar{\nu})$ contains the parameters of the copula model, $\Phi^{-1}\{\tau_{1t}\}$ is the inverse of the cumulative distributive distribution of the Student t distribution, and $F_\rho(.)$ the bivariate Student t distribution with time-varying correlations ρ_t in equation (3.21) and $\bar{\nu}$ degrees of freedom.

3.3 Empirical Application

Table 3.1 presents a description of countries in the American region categorized as developed or emerging according to the world MSCI ACWI Index[15] as of June 2020.

Table 3.1: Sample description

Country	Category	Index	Sample	Source
Canada	Developed	TSX	09/10/1996 - 31/12/2020	Yahoo Finance
United States	Developed	S&P 500	09/10/1996 - 31/12/2020	Yahoo Finance
Argentina	Emerging	MERVAL	09/10/1996 - 30/12/2020	Yahoo Finance
Brazil	Emerging	IBOV	09/10/1996 - 30/12/2020	Yahoo Finance
Chile	Emerging	IPSA	09/10/1996 - 30/12/2020	investing.com
Mexico	Emerging	MEXBOL	09/10/1996 - 31/12/2020	Yahoo Finance
Peru	Emerging	IGBVL	09/10/1996 - 31/12/2020	SMV, Yahoo Finance

Notes: The Peruvian data until December 2016 is obtained from the Stock Market Superintendence (SMV). The country category is classified according to the MSCI ACWI Index.

I filter out dates for which data in at least one country is missing (e.g. national holidays) so that the sample retains the same set of daily observations.[16] Table 3.2 presents statistics for daily returns[17] on the S&P 500 (United States), the TSX (Canada), and the stock returns from the main equity markets of Argentina, Brazil, Chile, Mexico and Peru. The statistics indicate a departure from a normal distribution, positive or negative skewness, high kurtosis and a rejection of normal density behaviour from the Jarque-Bera test.

[15] The full classification description can be found in MSCI Global Market Accessibility Review (June 2020) of MSCI Inc.

[16] Doing so, I removed 877, 941, 1017, 983, 1024, 817, and 1043 observations for Argentina, Brazil, Canada, Chile, Mexico, Peru and the USA, respectively.

[17] The returns are computed as $r_t = [\log(P_t) - \log(P_{t-1})] * 100$, where P_t is the General Index.

Table 3.2: Stock market returns statistics

Values	Argentina	Brazil	Canada	Chile	Mexico	Peru	USA
Mean	0.066	0.051	0.014	0.035	0.042	0.055	0.031
Maximum	17.488	33.419	9.656	8.722	12.923	10.529	10.789
Minimum	-37.931	-15.809	-12.345	-12.086	-13.337	-13.291	-9.511
Standard Deviation	2.326	2.037	1.092	1.091	1.390	1.326	1.220
Skewness	-1.000	0.636	-0.930	-0.140	0.077	-0.306	-0.257
Kurtosis	21.018	23.603	15.704	11.964	11.079	12.683	11.042
Jarque-Bera	69182.612	89696.376	34701.569	16929.404	13744.230	19815.663	13667.979
ACF 1st Lag	0.011	-0.014	-0.026	0.152	0.064	0.134	-0.095
ACF 2nd Lag	-0.025	-0.057	-0.024	0.011	-0.021	0.040	-0.010
ACF 3rd Lag	0.020	-0.006	0.020	0.013	-0.005	0.068	-0.002
ACF 4th Lag	0.037	0.012	-0.022	0.027	0.003	0.032	0.004
ACF 5th Lag	-0.004	-0.026	-0.049	-0.005	-0.044	0.002	-0.032
Observations				5052			
Sample				10/10/1996 - 30/12/2020			

Note: ACF is the autocorrelation function.

Almost all the Latin American stock returns exhibit a higher standard deviation than the U.S. and Canadian markets. This suggests more unstable episodes associated with external shocks from trade country partners, global factors such as financial and health crises, as well as internal or political shocks which are a feature in the LATAM region. Further, from the kurtosis values, in general there are more big shocks or outliers in the developing countries than in the developed markets. These atypical episodes could be explained by shocks originating in border countries, from an economy with which there are more trade linkages, or more overreaction to shocks from bigger markets. Since the mean and first autocorrelation lags are near zero for each series, I work with demeaned returns focusing only on the volatility dynamics.

3.3.1 Model Estimates

I show the marginal univariate skewed Student t GJR-GARCH model estimates in Table 3.3, which are the main inputs for the two-component score-driven t-copula models. The persistence in all conditional volatilities is close to one, meaning that a shock to the volatility will have a long-lasting effect. In addition, the leverage coefficient is significant for all series. Negative news has a greater effect on the conditional volatility given the combined effect from β_0, β_1 and β_2. Meanwhile the effect that prevails when there are positive shocks comes from the coefficients β_0 and β_1. In all cases, the skewness parameter η is negative which means that more observations are above the mean and median, which coincides with the descriptive statistics. We can see low values for the estimates of the degrees of freedom ν revealing heavy tails.

Table 3.3: Skewed GJR-t-GARCH model estimates

Parameter	Argentina	Brazil	Canada	Chile	Mexico	Peru
α	0.267	0.117	0.015	0.033	0.030	0.074
	(0.035)	(0.017)	(0.002)	(0.005)	(0.005)	(0.011)
β_0	0.771	0.876	0.878	0.833	0.874	0.767
	(0.017)	(0.011)	(0.009)	(0.014)	(0.012)	(0.021)
β_1	0.151	0.023	0.042	0.089	0.044	0.164
	(0.014)	(0.007)	(0.009)	(0.012)	(0.008)	(0.018)
β_2	0.080	0.130	0.130	0.105	0.139	0.068
	(0.020)	(0.015)	(0.015)	(0.015)	(0.016)	(0.019)
ν	5.281	9.485	9.102	8.890	8.395	5.125
	(0.303)	(1.061)	(0.944)	(0.932)	(0.822)	(0.284)
η	-0.047	-0.048	-0.177	-0.010	-0.034	-0.003
	(0.017)	(0.020)	(0.019)	(0.019)	(0.019)	(0.018)
$\log L$	-6960.995	-7091.038	-7042.212	-7101.625	-7096.345	-6966.469
AIC	13925.991	14186.076	14088.423	14207.251	14196.691	13936.937

Note: The standard errors (in parenthesis) are computed using the inverse of the Hessian matrix. The $\log L$ and AIC corresponds to the skewed t generalization of Hansen (1994).

These univariate estimates are the main inputs for the multivariate copula models. I analyse three pairwise countries, Argentina vs Brazil, Canada vs Mexico[18], and Chile vs Peru, grouped given their geographic proximity, their trade linkages and because they might face common factor shocks. Table 3.4 reports the estimates for the Clayton and rotated Gumbel copula models described in equations (3.14) and (3.17), respectively.

The estimates for both copulas reveal a persistence close to one, as shown by the estimates of ϕ_C and ϕ_G which suggest a long memory dynamic for the time-varying lower tail dependence. When I consider two components for the dependence structure, the persistence for the long memory maintains similar values as the one-component model, but the estimates for the short-term persistence ϕ_2 are considerably lower.

The short-term persistence estimate ($\hat{\phi}_2$) for the Canada-Mexico pair is around 0.8 in both models, and for Chile-Peru this estimate is approximately 0.3. The values for the pair Argentina-Brazil differ between models; it is 0.216 for the Clayton model and 0.940 for the rotated Gumbel copula. In particular, one may think that the gap between the long-memory (0.997) and short-memory (0.940) persistence estimates for the rotated Gumbel model is not big enough. Nonetheless, the half-life[19] shock to the long component process for this country pair lasts approximately 227 days more than a half-life shock to the short-memory component implying a similar duration to the Clayton specification (187 days). For Canada-Mexico the long persistence half-life shock prevails for 75 to 87 more days in comparison to the single-component specification, meanwhile that for the pair Chile-Peru a further 61 or 42 days, estimating the Clayton and rotated Gumbel models, respectively.

[18]The selection of this pair for the North American region is to assess the impacts from the U.S. economy.
[19]The half-life is defined as $\log(0.5)/\log(\phi)$.

Table 3.4: Score-driven Clayton and rotated Gumbel copula models

Model/ Parameter	Argentina vs Brazil	Canada vs Mexico	Chile vs Peru	Argentina vs Brazil	Canada vs Mexico	Chile vs Peru
Clayton	Single-component			Two-component		
ω	-0.002	-0.005	-0.015	-0.475	-0.328	-0.985
	(0.000)	(0.000)	(0.001)	(0.160)	(0.151)	(0.031)
ϕ_C	0.996	0.983	0.984	0.996	0.991	0.989
	(0.003)	(0.002)	(0.001)	(0.001)	(0.013)	(0.003)
κ_1	0.039	0.049	0.059	0.037	0.030	0.049
	(0.000)	(0.004)	(0.006)	(0.007)	(0.017)	(0.001)
ϕ_2				0.216	0.780	0.322
				(0.034)	(0.373)	(0.011)
κ_2				0.048	0.071	0.171
				(0.022)	(0.017)	(0.023)
logL	728.152	729.681	301.922	729.224	734.792	308.627
AIC	-1450.304	-1453.362	-597.844	-1448.448	-1459.583	-607.254
LR p-value				0.342	0.006	0.001
Rotated Gumbel	Single-component			Two-component		
ω	-0.006	-0.020	-0.031	-0.956	-0.802	-1.499
	(0.000)	(0.003)	(0.003)	(0.189)	(0.130)	(0.130)
ϕ_G	0.994	0.973	0.979	0.997	0.992	0.984
	(0.003)	(0.003)	(0.001)	(0.001)	(0.009)	(0.006)
κ_1	0.077	0.087	0.086	0.044	0.042	0.072
	(0.001)	(0.015)	(0.015)	(0.013)	(0.026)	(0.020)
ϕ_2				0.940	0.784	0.284
				(0.072)	(0.149)	(0.136)
κ_2				0.058	0.110	0.173
				(0.028)	(0.038)	(0.056)
$\log L$	838.035	828.396	343.639	840.617	832.886	348.022
AIC	-1670.070	-1650.791	-681.278	-1671.233	-1655.772	-686.045
LR p-value				0.069	0.012	0.012

Notes: The parameters with subscripts C and G refer to the Clayton and Rotated Gumbel copula models, respectively. The standard errors (in parentheses) are computed using the Huber (1967) sandwich estimator. LR is the likelihood ratio test statistic with null hypothesis $H_0 : \phi_2 = \kappa_2 = 0$.

The two-component model for either the Clayton or rotated Gumbel copula models has a higher likelihood for Argentina-Brazil than the single component approach. However, under the Akaike (1974) information criterion (AIC) which penalizes for a larger number of parameters, the more parsimonious one component seems more suitable for that pair in the case of the Clayton copula model. For the other two pairs, the likelihood, AIC and likelihood ratio test select the two-component extension.

Table 3.5 reports the estimates from the score-driven t-copula and the two-component score-driven t-copula models given in (3.20). Similarly to the rotated Gumbel case, the long-component sequence captures longer lasting shocks to the correlation parameter with persistence near unity. The short-term process exhibits estimates similar to those in the previous case. This means that the persistence of a shock to this process is robust to the dependence specification, regardless of whether the copula is symmetric or asymmetric.

However, under the score-driven t-copula the difference in the half-life between the short and long term components are 242 days, 43 days, and 34 days for the three country pairs. This might be due to the fact that this copula is symmetric and models atypical observations in both tails. The degrees of freedom range from 9 to 17, favouring a Student t specification rather than a Gaussian specification for the correlations in volatility.

The likelihood increases with respect to the base model with a unique component for every pair. In addition, when I use the AIC criterion to account for the additional parameters involved in the component structure, the model with two-components presents a better fit to the data in all cases. Moreover, the short-component parameters ϕ_2 and κ_2 are jointly significant according to the likelihood ratio test. Overall, the two-component score-driven t-copula is the best model since this model takes into account symmetrically lower and upper tails, and the degrees of freedom parameter for heavy tails.

Table 3.5: Score-driven t-copula models estimates

	Single-component			Two-component		
Parameter	Argentina vs Brazil	Canada vs Mexico	Chile vs Peru	Argentina vs Brazil	Canada vs Mexico	Chile vs Peru
ω	0.007	0.032	0.018	1.051	1.132	0.653
	(0.001)	(0.000)	(0.003)	(0.999)	(0.000)	(0.097)
ϕ_1	0.994	0.972	0.973	0.997	0.985	0.980
	(0.000)	(0.000)	(0.003)	(0.000)	(0.000)	(0.000)
κ_1	0.058	0.072	0.059	0.040	0.045	0.049
	(0.009)	(0.016)	(0.008)	(0.024)	(0.005)	(0.007)
ϕ_2				0.798	0.761	0.249
				(0.000)	(0.087)	(0.088)
κ_2				0.068	0.060	0.066
				(0.002)	(0.000)	(0.014)
$\bar{\nu}$	17.049	11.296	9.665	15.000	11.351	9.570
	(3.119)	(2.745)	(0.000)	(0.000)	(0.000)	(1.969)
$\log L$	873.496	865.154	362.846	877.327	868.005	365.625
AIC	-1738.991	-1722.309	-717.691	-1742.654	-1724.010	-719.250
LR *p-value*				0.022	0.058	0.062

Notes: The standard errors (in parentheses) are computed using the Huber (1967) sandwich estimator. LR is the likelihood ratio test statistic with null hypothesis $H_0 : \phi_2 = \kappa_2 = 0$.

3.4 Volatility Dynamics

Figure 3.1 plots the univariate conditional variance from the GJR-GARCH model for Canada, Mexico, and the four countries in South America. The Asian crisis event during 1998 prompted considerable turmoil in Mexican and South American equities. We can identify a rise in the levels of volatility during the second half of 2008 in all markets from the U.S. financial crisis. There are peaks in the end of the sample because of the uncertainty associated with the recent pandemic.

Figure 3.1: GJR-GARCH conditional volatilities estimates

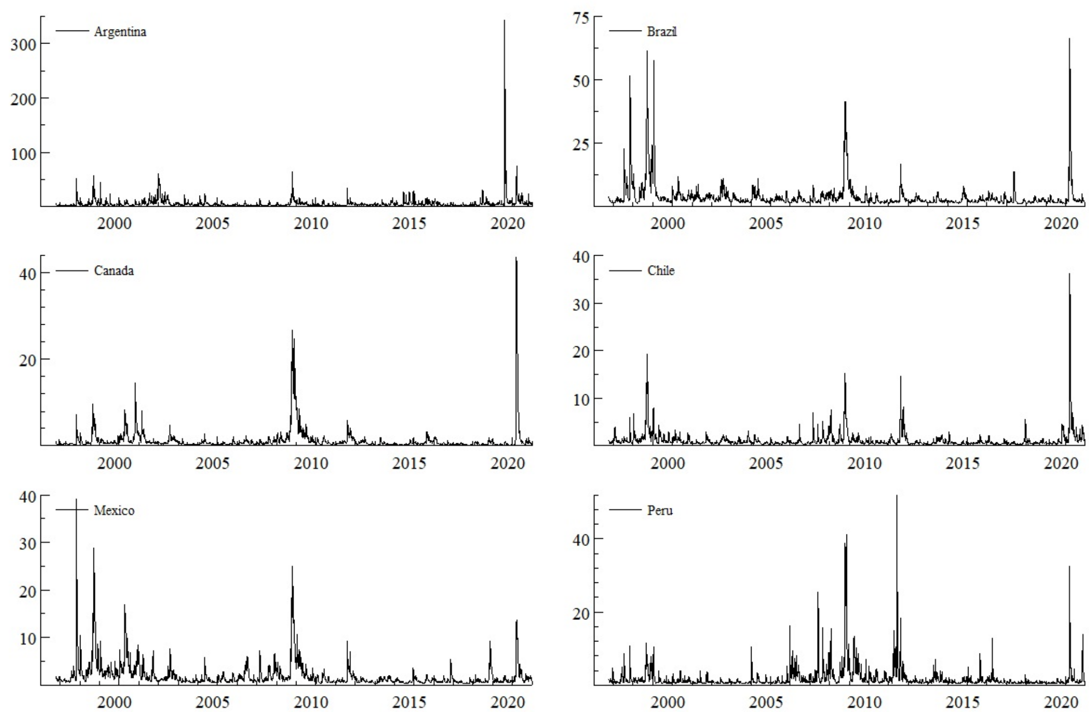

Following Ayala and Blazsek (2018), I transform the dependence parameter from each copula model into its Blomqvist (1950) β^* measure, which lies between -1 and 1. This transformation allows a more comparable picture of the time-varying dependence using different copulas. In Figure 3.2 we can see the time-varying β^* of the score-driven Clayton and rotated Gumbel copulas lower tail parameter.[20] During 1998, the correlations between Brazil and Argentina show a rise given the impacts arising from the Asian crisis. Also, the three pairwise correlations indicate an increase in correlations from July 2008 due to the financial crisis. Comovements in all countries have increased during the recent pandemic, in comparison to comovements observed at the beginning of 2018.

[20]The β^* for the Clayton copula is $4(2^{1+\gamma_t} - 1)^{-1/\gamma_t} - 1$, and for the rotated Gumbel is $\beta^* = 2^{2-2^{1/\theta_t}} - 1$.

Figure 3.2: Two-component score-driven Clayton and rotated Gumbel copula β^* of the lower tail parameter

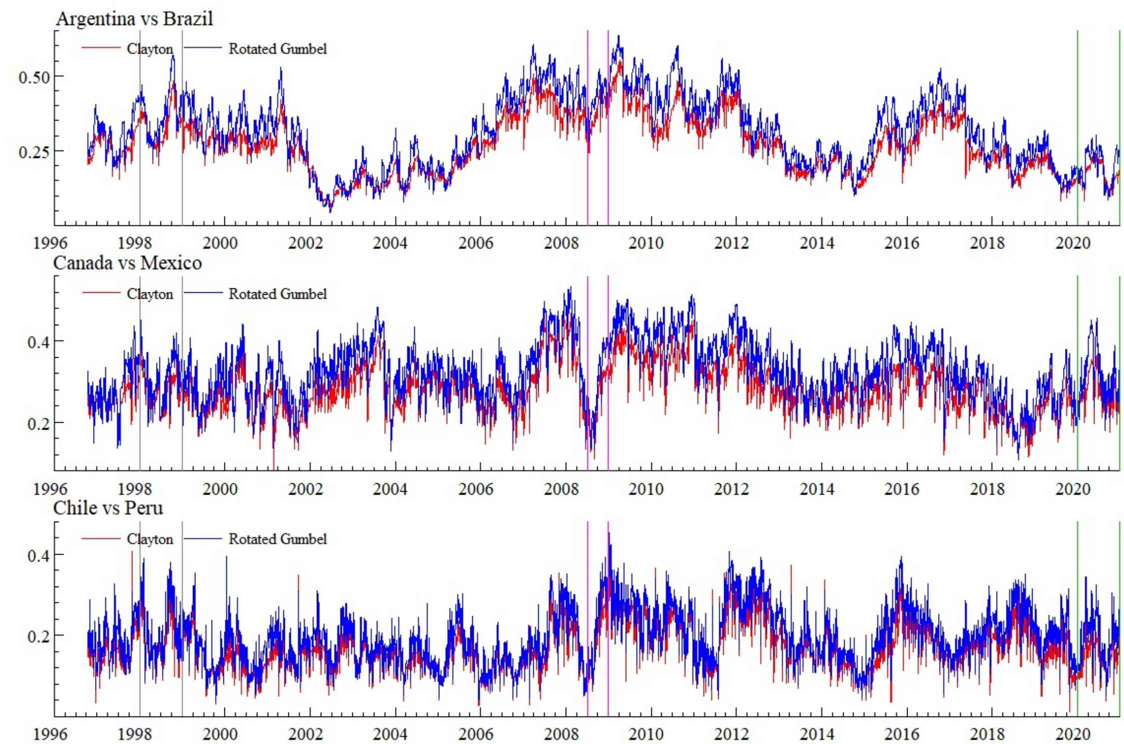

Note: The grey lines mark the year 1998; the purple lines mark the second half of 2008; and the green lines mark the period March to December 2020, associated with the Asian crisis, the U. S. financial crisis, and the pandemic, respectively.

Figure 3.3 shows the dynamics of the two-component score-driven t-copula dependence. The Blomqvist's β^* of correlations[21] generate similar patterns with respect to the lower tail dependence, but the peaks and troughs are more pronounced because the modelling now accounts for both tails.

[21] $\beta^* = 2\arcsin(\rho_t)/\pi$ in this case.

Figure 3.3: Two-component score-driven t-copula β^* of correlations

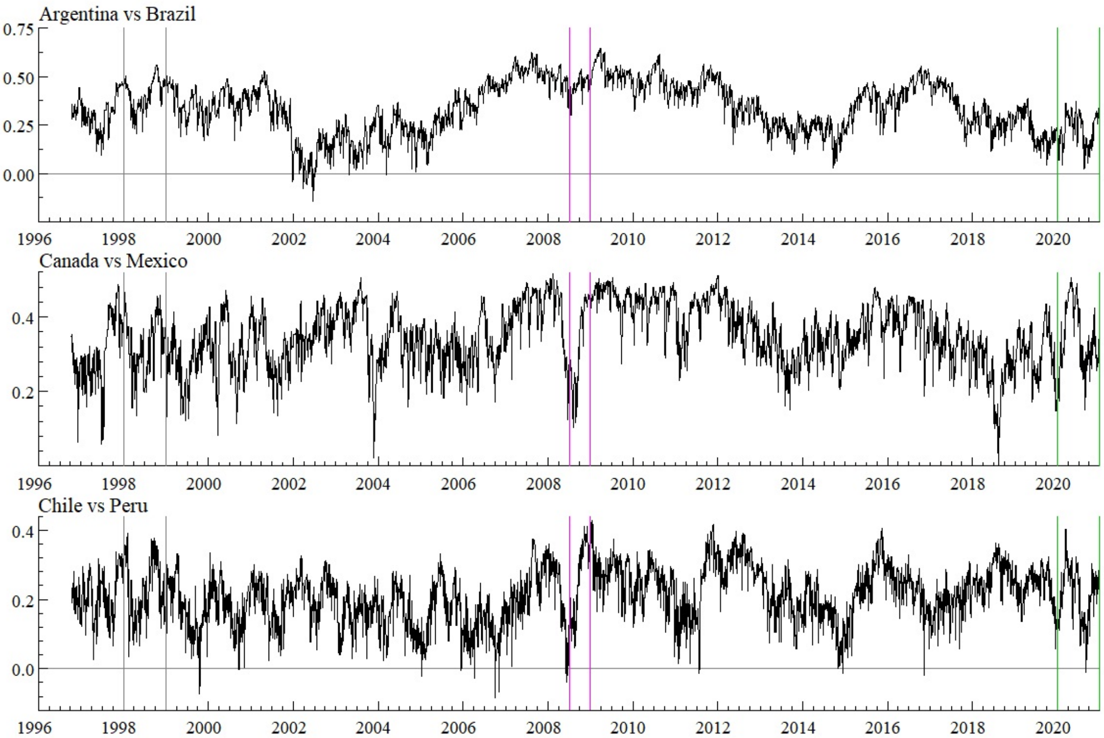

Note: The grey lines mark the year 1998; the purple lines mark the second half of 2008; and the green lines mark the period March to December 2020, associated with the Asian crisis, the U. S. financial crisis, and the pandemic, respectively.

The use of the score-driven t-copula allows us to identify episodes that lower tail dependence copulas cannot identify. As Santa-Cruz (2012) states, by the end of 2003 Canada and Mexico were discussing their positions regarding the US invasion over Iraq, and this meant a sharp decay in market volatility dependence. However, in 2004 both countries signed the Canada–Mexico Partnership which strengthened trade agreements and market integration between both countries. This positive shock was not captured by the Clayton copula whereas the score-driven t-copula model revealed this very clearly.

In a similar downside and upside time, Chile and Peru increased their dependence after the strong and political reforms in Peru that finished in 1999. After this episode, these countries recovered their commercial relationships and stability, but the Clayton specification suggests a peak rather than the sustained regimen suggested by the score-driven t-copula.

Hence after, I will consider only the results from the two-component score-driven t-copula model which takes into account the positive and negative shocks to the dependence and exhibits, in general, a better fit to the data among the models examined. Figure 3.4 depicts the longer and shorter components of the correlation dynamics. The longer process captures common shocks of longer duration, which might be attributable to external and global shocks, whereas the short-component process identifies shocks of shorter duration that affect both markets at the same time.

The rise in the long-term component is clear for the pair Argentina-Brazil over the Asian and the US. financial crisis, but this correlation only increases slightly during the pandemic. On the other hand, the long-term volatility dynamics for Canada and Mexico have increased considerably since the onset of COVID-19, probably in reaction in both stock markets to the growth in cases in the USA. The dynamics between Chile and Peru have peaks for the main events of the sample.

Figure 3.4: Long and short components

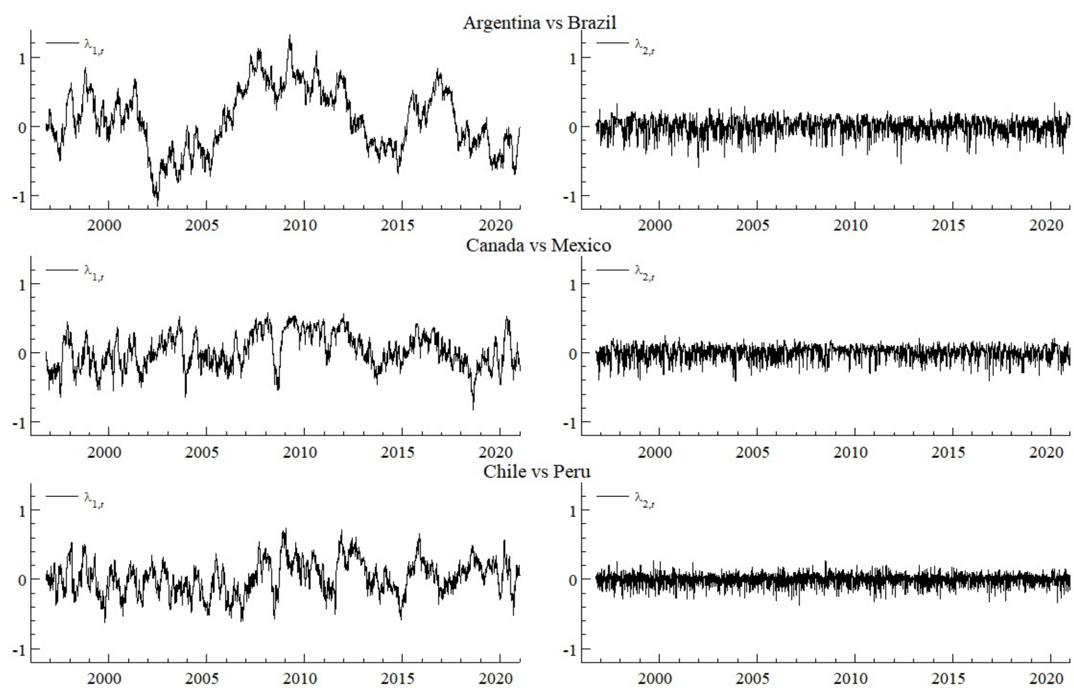

Note: $\lambda_{1,t}$ and $\lambda_{2,t}$ denote the long-term and short-term components, respectively.

Despite the significant and positive autocorrelation in the short-term process, much of the correlation dynamics are attributable to the longer component. Note that both processes are score-driven and modelled assuming a heavy tail distribution. This allows the long-term component to capture tumultuous episodes as described above, and the short term process can capture shocks of short duration that in some cases might be simply noise terms. In fact, Pong, Shackleton and Taylor (2008) assert that the autocorrelation function (ACF) of a short-memory series is geometrically bounded, whereas the ACF of a long-term process exhibits a hyperbolic decay, and Figure 3.5 shows that both components display such behaviour.

Figure 3.5: Long and short component autocorrelation functions

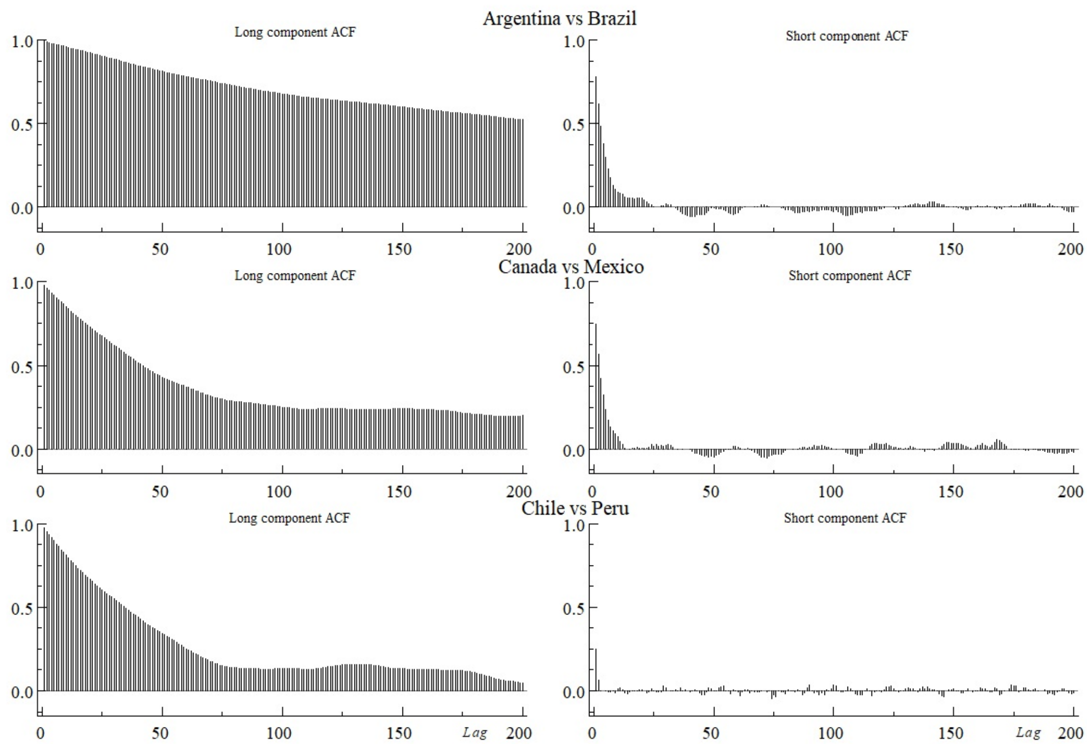

Note: ACF is the autocorrelation function.

3.5 Pre and Post COVID-19

This section provides a robustness check by considering the subsample up to the end of 2019 before the declaration of the COVID-19 pandemic. Table 3.6 compares estimates using the two-component score-driven t-copula model. The long-component persistence (ϕ_1) is fairly similar for Argentina-

Brazil and Chile-Peru pairs, and the difference between the subsample and the full sample for Canada-Mexico is only 0.007. The persistence values for the short-component using the entire sample are slightly higher for Argentina-Brazil and Chile-Peru. We note that the Canada-Mexico set has for the full sample a lower short-term persistence (ϕ_2) in comparison to the subsample.

The changes in the estimates for Canada-Mexico could be explained by the unprecedented uncertainty generated in the Canadian stock market, when the pandemic arrived there, whereas the Mexican market response was not as strong as that during the Asian exchange rate crisis of 1998 or during the 2008 U.S economic downturn. Mexico did not impose radical lockdown until the end of April 2020.

Table 3.6: Two-component score-driven t-copula model: Samples ending in 2019 and 2020

	2019			2020		
Parameter	Argentina vs Brazil	Canada vs Mexico	Chile vs Peru	Argentina vs Brazil	Canada vs Mexico	Chile vs Peru
ω	1.111	1.105	0.668	1.051	1.132	0.653
	(0.103)	(0.101)	(0.003)	(0.999)	(0.000)	(0.097)
ϕ_1	0.997	0.992	0.982	0.997	0.985	0.980
	(0.000)	(0.000)	(0.005)	(0.000)	(0.000)	(0.000)
κ_1	0.043	0.036	0.047	0.040	0.045	0.049
	(0.000)	(0.009)	(0.000)	(0.024)	(0.005)	(0.007)
ϕ_2	0.736	0.792	0.135	0.798	0.761	0.249
	(0.187)	(0.000)	(0.037)	(0.000)	(0.087)	(0.088)
κ_2	0.059	0.064	0.078	0.068	0.060	0.066
	(0.018)	(0.013)	(0.011)	(0.002)	(0.000)	(0.014)
$\bar{\nu}$	15.887	11.908	10.062	15.000	11.351	9.570
	(2.939)	(0.000)	(1.427)	(0.000)	(0.000)	(1.969)
logL	858.810	829.393	342.288	877.327	868.005	365.625
AIC	-1705.621	-1646.785	-672.576	-1742.654	-1724.010	-719.250
Obs	4831			5052		
Sample	10/10/1996 - 30/12/2019			10/10/1996 - 30/12/2020		

Note: The standard errors (in parenthesis) are computed using the Huber (1967) sandwich estimator.

Figure 3.6 shows the differences in dynamics between the subsample until December 2019 and the full sample up to December 2020. The evolution paths for the Argentina-Brazil and Chile-Peru pairs are identical for both samples. As noted earlier, when considering the impact of COVID-19, the Canada-Mexico pair exhibits lower persistence in each component. Overall, the estimated parameters and the implied evolution of components show that the score-driven approach can capture bigger shocks like the recent pandemic.

Figure 3.6: Longer and shorter components

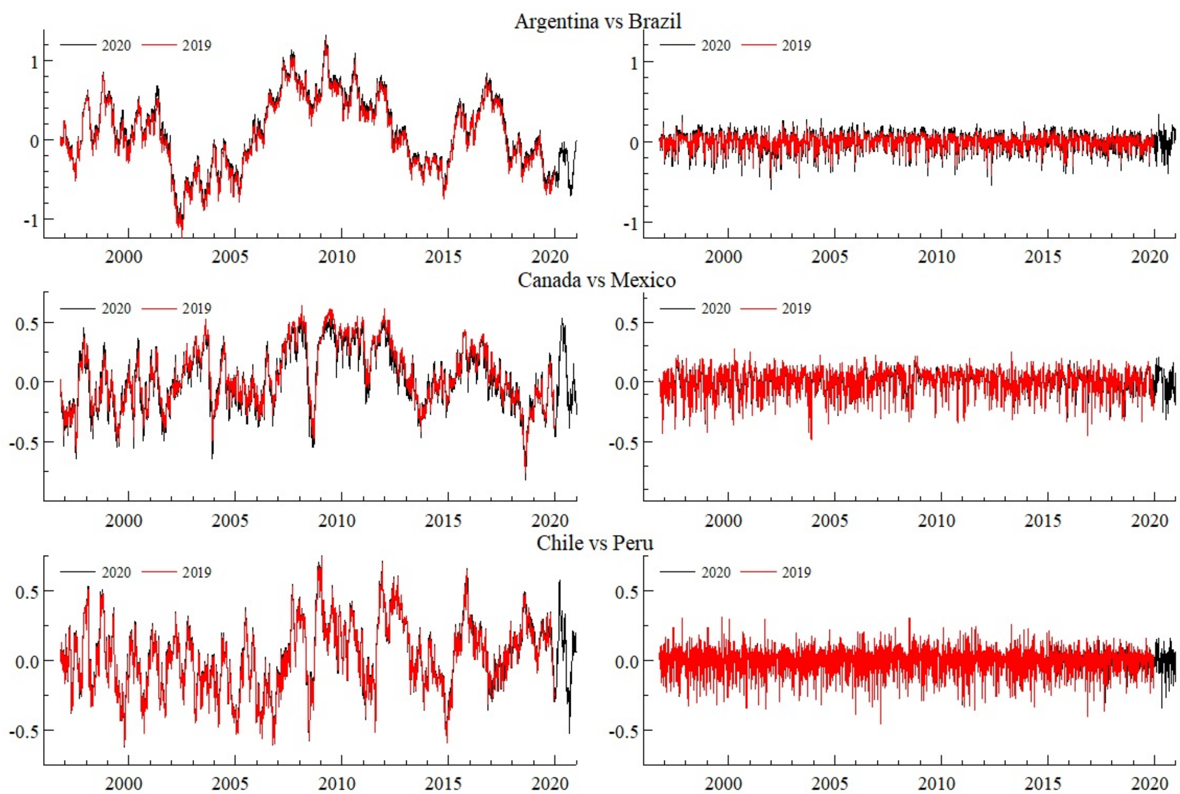

3.6 Bootstrap simulation

I generate 500 artificial series by resampling each pair of countries' datasets. This non-parametric approach assumes that the univariate residuals from the GJR-GARCH Skewed Student t are representative of the truth. I follow the approach of Politis and Romano (1994) generating 60 blocks for each sampling partition given the length of the series and the high persistence of the single component model.

Using the resampled data, I verify the robustness of the score-driven t-copula model estimates for the new model. Table 3.7 presents the estimates from the original data together with average estimates based on simulations.

Table 3.7: South American original and simulated series estimates

	Original			Simulated		
Parameter	Argentina vs Brazil	Canada vs Mexico	Chile vs Peru	Argentina vs Brazil	Canada vs Mexico	Chile vs Peru
ω	1.051	1.132	0.653	1.119	1.156	0.685
ϕ_1	0.997	0.985	0.980	0.983	0.972	0.966
κ_1	0.040	0.045	0.049	0.056	0.044	0.047
ϕ_2	0.798	0.761	0.249	0.802	0.703	0.268
κ_2	0.068	0.060	0.066	0.076	0.074	0.085
$\bar{\nu}$	15.000	11.351	9.570	13.376	11.063	9.439

We see that the averages of the estimates based on resampling draws are similar to the original estimates. The simulated data preserves high persistence close to unity; meanwhile the simulated short-term component estimates have averages of around 0.8, 0.7, and 0.3 for the pairs Argentina-Brazil, Mexico-Canada, and Chile-Peru pairs, respectively. Further, the simulated series maintains the order of the difference in half-lives between the long and short components of the original values.

The average of the estimates for the scale terms for both components are close when compared to the original estimates, and the estimates for degrees for freedom are also close.

3.7 Out-of-sample Density Forecasts

I follow the density scoring-based test of Amisano and Giacomini (2007). An advantage of this approach is the comparison between models that use densities of forecasts rather for the mean square error (MSE), for instance. In addition, Giacomini and White (2006) state that this density approach is applicable to nested models as in this paper, given the non-singularity of the asymptotic variance of this test class.

The density test of Amisano and Giacomini (2007) has as main inputs the one-step ahead density forecasts. Let $\log \hat{f}_t^*[Y_{t+1}]$ be the density forecast for the single-component score-driven t-copula model and $\log \hat{f}_t[Y_{t+1}]$ be the density forecast for the two-component score-driven t-copula model. Then, the likelihood ratio test is

$$WRL = w_{t+1}[\log \hat{f}_t^*[Y_{t+1}] - \log \hat{f}_t[Y_{t+1}]], \tag{3.31}$$

$$w_{t+1} = \frac{1}{T_f}, \tag{3.32}$$

where w_{t+1} are constant weights for the window sample $t = 1, ..., T_f$ with null hypothesis H_0 and alternative hypothesis H_1 given by

$$H_0 : E[WLR] = 0,$$
$$H_1 : E[WLR] > 0.$$

Following the work of Diebold and Mariano (1995), the significance and the positive sign of the c estimate in the regression

$$d_t = c + \varepsilon_t, \tag{3.33}$$

$$d_t = \log \hat{f}_t^*[Y_{t+1}] - \log \hat{f}_t[Y_{t+1}], \tag{3.34}$$

shows that the two-component model generates better one-step ahead forecasts instead of the single-component counterpart model.

The rolling window consists of 60 percent of the full sample[22] which aims to retain the persistence noted in the empirical application. Moving the rolling window one month ahead each time, I project the last day of every month.

[22]The first rolling window starts from 10/10/1996 until 30/03/2011. An increase in the number of observations for the rolling window does not alter the test outcome.

It seems evident that the addition of one more component improves the modelling of shocks especially during the global financial crisis for all groups of countries, and during the first months of the pandemic for the last two-pairs.

The estimates for $\hat{c}$ are 3.241, 1.772, and 2.082, for Argentina-Brazil, Canada-Mexico and Chile-Peru, respectively, and their Huber (1967) robust standard errors (0.418, 0.188 and 0.165) indicate statistically significant gains in the out-sample forecast using the two-component score-driven t-copula model.

3.8 Conclusions

This work studies the benefits of specifying long and short components, when modelling high persistence in the dependence parameter of score-driven copula models. Unlike models for high persistence such as long-memory models or models that employ fractional dynamics, the two components allow for a shorter persistence dynamic that captures transitory shocks. The addition of a second component for modelling dependence characterises common volatility shocks of shorter duration.

In comparison to the base score-driven Clayton, the score-driven rotated Gumbel copula, or the score-driven t-copula models, the two-component models exhibit better in-sample fit according to the likelihood ratio tests. The two-component score-driven t-copula model, which accounts for positive and negative shocks, generates the best fit to the data and out-of-sample density forecast comparison tests. An empirical application of the two components model to bivariate series in American equity markets reveals that the co-movements are high in times such as the Great Financial Crisis in 2008 and the recent pandemic, when external shocks had impact on these economies. Further, the symmetric two-component score-driven t-copula specification is robust to the COVID-19 crisis.

The long-memory process can be modelled as a process of occasional random shifts and a short-term component. Thus, it would be worthwhile to develop an extension from this setting to copula models and identify common regimes of volatilities. In addition, the two-component score-driven copula models could allow for skewness in the dependence parameter, or might be modelled with short, medium and long-term shocks, or more components.

4 Factor-Augmented QVAR Models: An Observation-Driven Approach

4.1 Introduction

Given the recent pandemic and similar global shocks such as the U.S. financial crisis, it is important to account for this information in a model that can identify unusual observations in variables with robust estimates. Harvey (2013) discusses multivariate location models using the dynamic conditional score (DCS) framework where shocks are modelled using a Student t distribution. This approach emerges from the work of Harvey (2013) and Creal, Koopman and Lucas (2013), where they employ an observation-driven approach exploiting the information from the score of the model. In addition, Blasques, Gorgi, Koopman and Wintenberger (2018) derive the invertibility conditions for the consistency of maximum likelihood estimators in these type of models.

Blazsek, Escribano, and Licht (2017) named the Harvey's (2013) multivariate location model as a quasi vector autoregressive (QVAR) model since it allows a similar reduced form in comparison to vector autoregressive (VAR) models. They extend the first-order QVAR model as specified in Harvey (2013) to allow a more general structure with more than one lag. VAR models introduced by Sims (1980) are useful for macroeconomists who assess impulse response functions from monetary and fiscal policy shocks. However, high dimensional VARs imply a large number of parameters to estimate, and adding factors to their structure emerges as a practical solution.

The main contribution of this chapter is the addition of factors into QVAR score-driven models where the multivariate error term follows a Student t distribution. Factor components can capture relevant information from a large dataset of variables from several sectors of the economy. In this way, factor-augmented QVAR (FAQVAR) models do not incorporate many variables explicitly, and at the same time can deal with episodes of great disturbances. The FAQVAR model given its score-driven dynamics can be estimated using frequentist methods rather than Bayesian techniques.

The study of factors using macroeconomic variables starts with the work of Stock and Watson (2002). They show an improvement in forecasts for macroeconomic U.S. series using principal component methods. Bernanke, Boivin and Eliasz (2005) incorporate factors following Stock and Watson's (2002) principal component procedure in VAR dynamics when analysing the effects of monetary policy, and also they jointly estimate factors and VAR models using Bayesian techniques. This model is used extensively in the literature given its flexibility. For instance, Abbate, Eickmeier, Lemke and Marcellino (2016) estimate factor models considering the financial crisis episode and its effects on greater economies, and Laine (2020) assesses the effectiveness of monetary policy with a zero lower bound in the European Union.

I estimate factor-augmented QVAR models using the two-step procedure of Bernanke, Boivin and Eliasz (2005), where in the first step the unobservable factors are obtained using principal component analysis, and then in the second step the estimated factors are added to the QVAR system. Another alternative, is maximum likelihood estimation with two-steps undertaken by Bai, Li and Lu (2016) where they analyse inference properties of estimates and impulse responses for FAVAR models. However, I follow the two-step procedure of Bernanke et al. (2005), and use the bootstrap strategy of Yamamoto (2019) to deal with the uncertainty generated in the first-step from the factors estimation.

Defour and Stevanović (2013) utilise a bootstrap approach for their factor-augmented vector autoregressive moving average (FAVARMA) model, and argue that the VARMA structure is able to capture the information from VAR models with long lags, so parsimonious VARMA models allow similar impulse response estimates with considerably less parameters to estimate. The QVAR model collapses to a VARMA model with Gaussian errors when the degrees of freedom of the Student t distribution errors goes to infinity (Blazsek et al. 2017), and therefore, a limiting case for the FAQVAR model is the FAVARMA model, which is the benchmark model in this study.

My model is related to the work of Angelini and Gorgi (2018) where they apply the score-driven approach to dynamic stochastic general equilibrium (DSGE) models with time-varying parameters and volatility, whereas Blazsek, Escribano and Licht (2020) establish score-driven representations with fat tails and heteroskedastic errors for DSGE models. In addition, Blazsek, Escribano and Licht (2022) develop a multivariate location plus scale model and derive its maximum likelihood conditions. These works constitute the first applications of the DCS approach in macroeconomic systems that consider just a few variables in their composition. I extend this analysis to include factor-augmented variables that have not yet been studied in the literature and that this work aims to cover.

Recent literature dealing with observations from the pandemic include the work of Lenza and

Primiceri (2021), who model the specific change in volatility during the pandemic within a VAR framework. Carriero, Clark, Marcellino and Mertens (2021) treat the pandemic episode as outliers in their VAR model with stochastic volatility errors instead, following the approach of Stock and Watson (2016). Antolín-Díaz, Drechsel and Petrella (2021) make a nowcasting analysis of the U.S economic activity with a dynamic factor model that also includes outliers.

Schorfheide and Song (2021) analyse the forecasts of a mixed-frequency VAR model and conclude that the model without the pandemic data generates more accurate long-term forecasts. However, Hartwig (2021) and Bobeica and Hartwig (2022) highlight the importance of modelling errors with a Student t distribution when the COVID-19 shock is considered in a VAR model, since the parameter estimates and density forecasts from a Gaussian version are sensitive to the pandemic data. All these works employ a Bayesian approximation for the estimation of their VAR models, whereas this essay utilises an observation-driven approach, which can be estimated using frequentist methods.

In addition, Guerron-Quintana (2021) covers non-linearities and asymmetries in state and measurement equations in VAR models using Bayesian estimation. The factor-augmented QVAR model proposed in this study is observation-driven with a closed form likelihood which is estimated by maximum likelihood. Further, the FAQVAR model is robust to recently experienced extreme episodes such as the pandemic, given the modelling of errors as a Student t distribution. To the best of my knowledge this is the first work considering the pandemic sample using a score-driven factor-augmented QVAR model.

I analyse the U.S. economy estimating the factor components using McCracken and Ng (2016)'s macroeconomic monthly variables from January 1959 to May 2021, which cover tumultuous times for this market. Then, in the second step I estimate the model using the previously estimated factors and the federal funds rate to evaluate monetary policy shocks. The factor-augmented QVAR model proposed in this study is robust to extreme episodes recently experienced such as the pandemic, and outperforms the FAVARMA model producing a better fit to the data. The FAQVAR impulse response forecasts from a monetary shock follow the expected reactions from the economic theory. Additional robustness checks using different numbers of factors, a subsample before COVID-19, and the zero lower bound episodes, indicate the stability of the estimates.

The structure followed in this chapter is as follows: Sections 4.2 and 4.3 discuss the structure of the FAQVAR model and its estimation. Section 4.4 presents the estimates in the application of the model to assess monetary policy in the US. economy. Section 4.5 checks the robustness of the estimates through the estimation of models with different numbers of factors, samples, and the unbounded shadow rate. The conclusions are presented in the last section.

4.2 Methodology

I incorporate factor components into the first-order QVAR model of Harvey (2013) and Blazsek et al. (2017). The model for a $y_t = (f_t, x_t)$ vector of $K = k + r$ variables contains the k factors, f_t, and the vector of r observed macroeconomic variables, x_t, as follows:

$$y_t = c + \mu_t + \varepsilon_t, \tag{4.1}$$

$$\mu_t = \Phi\mu_{t-1} + \Psi u_{t-1}, \tag{4.2}$$

$$\varepsilon_t \sim t_\nu(0, \Sigma), \tag{4.3}$$

$$u_t \propto \frac{\partial \ln f(y_t|Y_{t-1})}{\partial \mu_t}, \tag{4.4}$$

where c is a vector of constants, μ_t is a location component with persistence Φ, Ψ is the updating scale matrix from the score term component u_t, and the error term ε_t follows a centered multivariate Student t distribution with scale Σ and $\nu > 2$ degrees of freedom. The multivariate scale matrix is positive definite so that $\Sigma = \Omega^{-1}\Omega^{-1\prime}$ can have a Cholesky decomposition which allows the identification of the model. The likelihood conditional on past information $Y_{t-1} = (y_1, ..., y_t)$ is given by

$$\begin{aligned}\log f(y_t|Y_{t-1}) = \log\Gamma\left(\frac{\nu+K}{2}\right) - \frac{K}{2}\log(\nu\pi) - \log\Gamma\left(\frac{\nu}{2}\right) - \frac{\log|\Sigma|}{2} \\ - \frac{\nu+K}{2}\log\left(1 + \frac{\varepsilon_t'\Sigma^{-1}\varepsilon_t}{\nu}\right).\end{aligned} \tag{4.5}$$

Further, the score term u_t is proportional to

$$\frac{\partial \ln f(y_t|Y_{t-1})}{\partial \mu_t} = \frac{\nu+K}{\nu}\Sigma^{-1} \times \left(1 + \frac{\varepsilon_t'\Sigma^{-1}\varepsilon_t}{\nu}\right)^{-1} \varepsilon_t, \tag{4.6}$$

$$= \frac{\nu+K}{\nu}\Sigma^{-1} \times u_t. \tag{4.7}$$

Finally, following Bernanke et al. (2005), I consider a set of informational variables z_t for the estimation of factors, and these variables are linked to the main observed variables with the linear representation:

$$z_t = \Lambda_f f_t + \Lambda_x x_t + e_t, \tag{4.8}$$

where Λ_f are the factor loadings, Λ_x is the effect of the observed economic variables on the informational data set, and e_t is an error term.

4.3 Estimation

Factors are not observable and I first estimate these factors using the strategy of Bernanke et al. (2005). The first step involves the estimation of factors that capture the main features from the informational variables z_t. When evaluating monetary policy we may consider indicators such as economic activity, stock markets, and inventories.

I divide the group of informational variables as contemporaneously affected or not by the monetary policy instrument i_t.[23] Stock and Watson (2002) remark that the principal components from the informational data set, $\hat{C}_k(f_t, z_t)$, may generate linear combinations of the policy instrument i_t when forecasted. In order to remove this effect, Bernanke et al. (2005) consider the following regression:

$$\hat{C}_k(f_t, z_t) = \omega_k + a_k \hat{C}_k(f_t) + b_k i_t + \xi_{kt}, \tag{4.9}$$

where $\hat{C}_k(f_t)$ are the components from all non-contemporaneous variables, ω_k is an intercept, a_k and b_k are elasticities, and ξ_{kt} an error term. The estimate for the factor components is given by

$$\hat{f}_{kt} = \hat{\omega}_k + \hat{a}_k \hat{C}_k(f_t, z_t) + \hat{\xi}_{kt}. \tag{4.10}$$

The second estimation step consists of augmenting the QVAR system with the factors so that $y_t = (\hat{f}_t, x_t)$. The FAQVAR model is estimated by maximizing the logarithm of the likelihood with respect to the parameter set $\psi = (\Phi, \Psi, \Sigma, \nu)$:

$$\log L(\psi) = \sum_{t=1}^{T} \log f(y_t | Y_{t-1}). \tag{4.11}$$

[23]I estimate the model with one observed variable x_t, which is the monetary policy instrument i_t.

Following Proposition 39 of Harvey (2013), the maximum likelihood estimates are consistent since the score and the errors model are assumed to be identically and independently distributed. In addition, Harvey (2013) and Blazsek and Licht (2020) establish conditions for the explicit derivation of the information matrix for the QVAR model standard error estimates. Instead I apply the non-parametric approach of Yamamoto (2019) for the estimation of standard errors and impulse response functions of the FAQVAR model, which also capture the error estimation uncertainty from the first-step.

4.3.1 Impulse Response Function

Blazsek et al. (2017) establish the moving average representation of the stationary process μ_t, provided its persistence Φ has a modulus λ less than one in equation (4.2). The MA form is

$$\mu_t = \sum_{h=1}^{\infty} \Phi^h \Psi[(\nu-2)\nu]^{1/2}\Omega^{-1} \frac{\epsilon_{t-1-h}}{\nu - 2 + \epsilon'_{t-1-h}\epsilon_{t-1-h}}, \tag{4.12}$$

with ϵ_t being the error term for the moving-average representation of the FAQVAR model,

$$\epsilon_t = \left[\frac{\nu}{\nu-2}\right]^{-1/2} \Omega \times \varepsilon_t. \tag{4.13}$$

The impulse responses for the shock ϵ_t at the horizon $j = 1, ..., \infty$ to the variable y_t are given by

$$\hat{\Theta}_j = E\left[\frac{\partial y_{t+j}}{\partial \epsilon_t}\right], \tag{4.14}$$

$$= \Phi^j \Psi[(\nu-2)\nu]^{1/2}\Omega^{-1} E[D_{t-1-j}], \tag{4.15}$$

where

$$D_t = \begin{bmatrix} \frac{\nu-2+\epsilon'_t\epsilon_t-2\epsilon^2_{1t}}{(\nu-2+\epsilon'_t\epsilon_t)^2} & \frac{-2\epsilon_{1t}\epsilon_{2t}}{(\nu-2+\epsilon'_t\epsilon_t)^2} & ... & \frac{-2\epsilon_{1t}\epsilon_{Kt}}{(\nu-2+\epsilon'_t\epsilon_t)^2} \\ \frac{-2\epsilon_{2t}\epsilon_{1t}}{(\nu-2+\epsilon'_t\epsilon_t)^2} & \frac{\nu-2+\epsilon'_t\epsilon_t-2\epsilon^2_{2t}}{(\nu-2+\epsilon'_t\epsilon_t)^2} & ... & ... \\ ... & ... & ... & ... \\ \frac{-2\epsilon_{Kt}\epsilon_{1t}}{(\nu-2+\epsilon'_t\epsilon_t)^2} & ... & ... & \frac{\nu-2+\epsilon'_t\epsilon_t-2\epsilon^2_{Kt}}{(\nu-2+\epsilon'_t\epsilon_t)^2} \end{bmatrix}. \tag{4.16}$$

The expectation in (4.15) can be obtained considering the time average of D_t. The impulse responses to the full description of informational variables comes from the regression in (4.8) since

$$\hat{z}_t = \hat{\Lambda}_f \hat{f}_t + \hat{\Lambda}_x x_t, \tag{4.17}$$

$$= \begin{bmatrix} \hat{\Lambda}_f & \hat{\Lambda}_x \end{bmatrix} \begin{bmatrix} \hat{f}_t \\ x_t \end{bmatrix}, \tag{4.18}$$

$$= \hat{\Lambda} y_t'. \tag{4.19}$$

For the estimation of standard errors and impulse responses, I follow the residual approach of Yamamoto (2019). This bootstrap method deals with the 2-step estimation errors from the pre-estimation of factors of Bernanke et al. (2005). Defour and Stevanović (2013) adapts the Yamamoto (2019)'s algorithm for a FAVARMA model, which is the limiting case of the first order FAQVAR model. The score-driven framework assumes that the second moments for the score and errors are finite and normally distributed as in Yamamoto (2019) bootstrap method, then we can modify the linear algorithm to the FAQVAR model with the following steps:

1. Obtain the parameter estimates $\hat{c}$, $\hat{\Phi}$, $\hat{\Psi}$, $\hat{\Sigma}$, $\hat{\nu}$, $\hat{\Lambda}_f$, $\hat{\Lambda}_y$ from the model in (4.1), and their respective residuals $\hat{\varepsilon}_t$ and $\hat{e}_t$. We also estimate the impulse responses $\hat{\Theta}_{i,j}$.

2. Proceed with sampling residuals with replacement to generate ε_t^* and e_t^* for the bootstrapped samples y_t^* so that

$$y_t^* = \hat{c} + \mu_t^* + \varepsilon_t^*, \tag{4.20}$$

$$\mu_t^* = \hat{\Phi}\mu_{t-1}^* + \hat{\Psi}u_{t-1}^*, \tag{4.21}$$

$$z_t^* = \hat{\Lambda}_f f_t^* + \hat{\Lambda}_y x_t^* + e_t^*. \tag{4.22}$$

3. Estimate the two-step system with y_t^* and get the bootstrapped parameter estimates $\hat{c}^*$, $\hat{\Phi}^*$, $\hat{\Psi}^*$, $\hat{\Sigma}^*$, $\hat{\nu}^*$, $\hat{\Lambda}_f^*$, $\hat{\Lambda}_y^*$, and the bootstrapped impulse responses $\hat{\Theta}_{i,j}^*$.

4. Repeat steps 2-3 R times.

5. Compute the bootstrapped standard errors for model parameters.

6. Sort the bootstrapped impulse responses from the centered statistic $s_{i,j} = \hat{\Theta}_{i,j}^* - \hat{\Theta}_{i,j}$, select the significance level α to obtain the confidence interval $[\hat{\Theta}_{i,j} - s^{1-\alpha/2}, \hat{\Theta}_{i,j} - s^{\alpha/2}]$, where $s^{1-\alpha/2}$ and $s^{\alpha/2}$ are $1-\alpha/2$ and $\alpha/2$ percentiles, respectively.

4.4 Empirical Results

I use 128 variables from the McCracken and Ng (2016) dataset that spans 1959:01 to 2021:05. I screened the data for observations associated with input errors and events such as labor strikes as noted by Stock and Watson (2002) assuming these observations are greater than 10 times their interquartile range.[24] In addition, I use their expectation maximization (EM) algorithm to replace the missing and the screened values in the standardised panel data. The panel contains the Federal funds rate (FFR) and a group of informational variables z_t with indicators for output and income, the labor market, consumption, housing starts and sales, inventories and orders, the stock market, exchange rates, interest rates, money and credit, prices, as well as average hourly earnings and the consumer index. Further details for all variables are given in the Appendix.

I estimate the first ten factors using principal components as in Bernanke et al. (2005), and a preliminary scree plot provides evidence of the contribution of each component to the total variance. Figure 4.1 shows this decomposition.

Figure 4.1: Scree plot

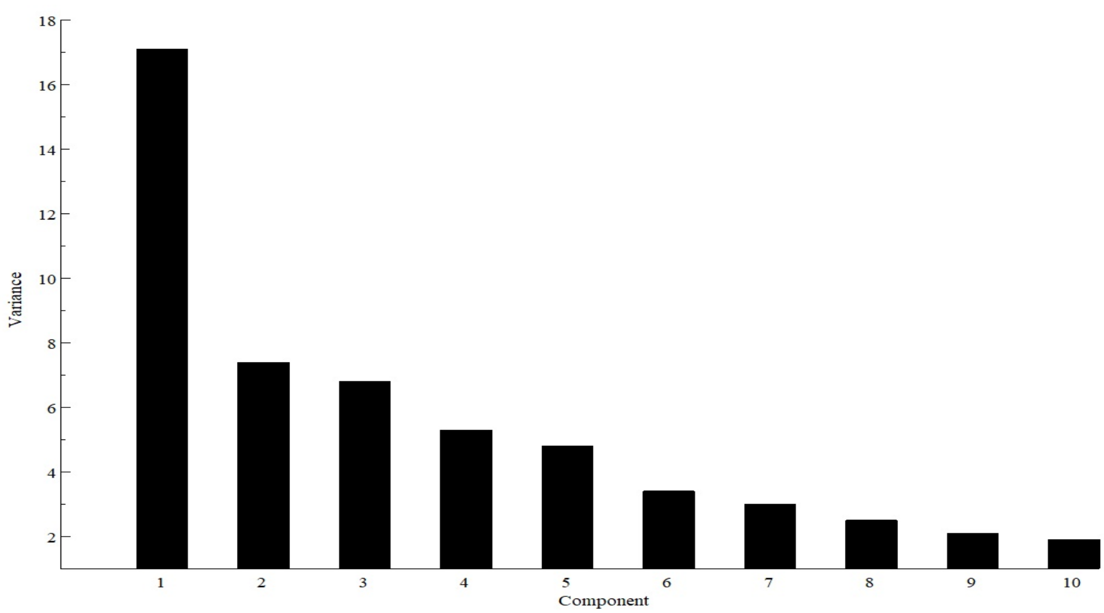

[24]Antolín-Diaz et al. (2021) carry out a similar data treatment for their factor model. This treatment does not impact the estimation of principal components and the outliers generated around the financial crisis and the pandemic.

Jointly these ten components contribute 54.4 percent of the explained variance of the data. The first, second, third and fourth components explain 17.1, 7.4, 6.8 and 5.3 percent of the total variance, respectively, and the other factors contribute smaller amounts of less than five percent each. Bai and Ng (2002) propose information criteria[25] for the optimal selection of factors in a dynamic factor model and I consider the following three criteria:

$$IC_{p1}(k) = \log\left(\frac{1}{N}\sum_{i=1}^{N}\frac{\hat{e}'_{ki}\hat{e}_{ki}}{T}\right) + k\left(\frac{N+T}{NT}\right)\log\left(\frac{NT}{N+T}\right), \tag{4.23}$$

$$IC_{p2}(k) = \log\left(\frac{1}{N}\sum_{i=1}^{N}\frac{\hat{e}'_{ki}\hat{e}_{ki}}{T}\right) + k\left(\frac{N+T}{NT}\right)\log\left(\min[N,T]\right), \tag{4.24}$$

$$IC_{p3}(k) = \log\left(\frac{1}{N}\sum_{i=1}^{N}\frac{\hat{e}'_{ki}\hat{e}_{ki}}{T}\right) + k\frac{\log\left(\min[N,T]\right)}{\min[N,T]}, \tag{4.25}$$

where k is the number of factors, $N = K - 1$ since the Federal funds rate is not considered directly for the estimation of factors, and $\hat{e}_{ki}$ are the residuals from the estimate of a dynamic factor model assuming k factors. I evaluate the criteria using the first 10 components, and Table 4.1 presents their values.

Table 4.1: Bai and Ng (2002) number of factors criteria

	Factors									
Criteria	1	2	3	4	5	6	7	8	9	10
IC_{p1}	-0.145	-0.195	-0.246	-0.283	-0.319	-0.335	-0.349	-0.355	-0.355	-0.353
IC_{p2}	-0.143	-0.192	-0.242	-0.278	-0.312	-0.327	-0.338	-0.344	-0.342	-0.339
IC_{p3}	-0.150	-0.205	-0.261	-0.304	-0.344	-0.366	-0.384	-0.396	-0.401	-0.404

The first two criteria suggest eight factors, while the last criterion indicates 10 factors.[26] I chose the model with 8 factors as the main model. I estimate these eight factors using principal components following Bernanke et al. (2005). In addition, I compare the factor estimation with the updated sample until May 2021 and the factor estimates of Bernanke et al. (2005) in Figure 4.2.[27]

[25] Bernanke at al. (2005) asserts that this criteria may not suffice to determine the added number of factors. I check the robustness of Bai and Ng (2002)' selection in the next section.

[26] The results for criteria IC_{p1} and IC_{p2} are the same using 30 factors, meanwhile that IC_{p2} chooses 18 factors.

[27] Both panels slightly differ, as McCracken and Ng (2016) take into account 8 more series. I also adjust the sign of the third, fourth and fifth factors from the Bernanke et al. (2005) sample, which arises because of identifiability of the principal components.

Figure 4.2: Factor estimates

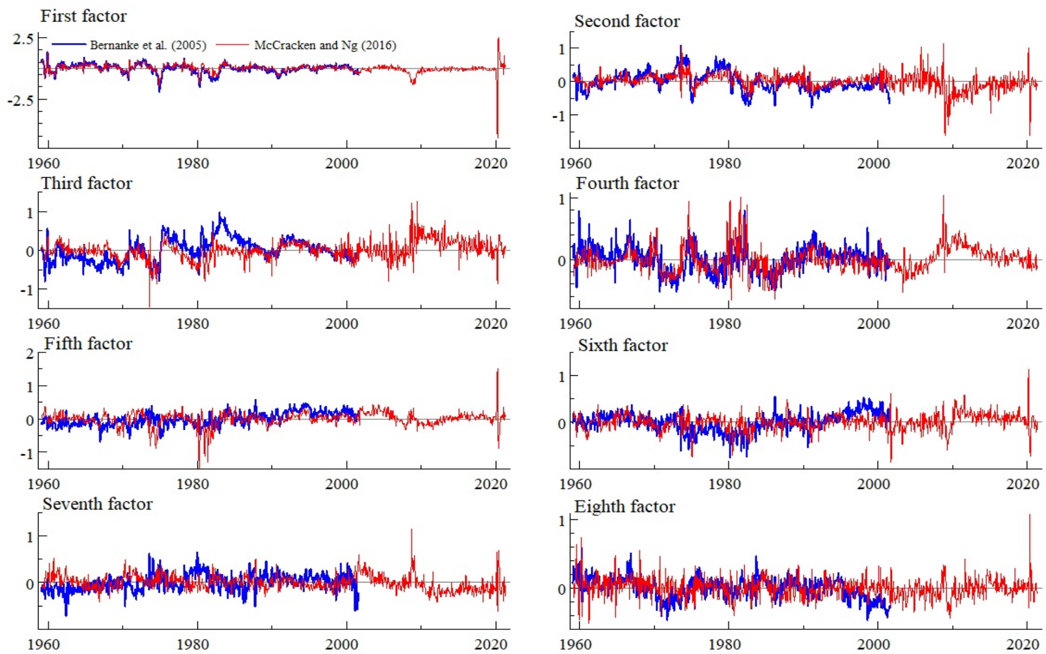

The first two factors show similar peaks and troughs across the sample for both panels. These factors capture most of the variance according to the principal components methodology. We can see the atypical observations and outliers generated after 2005 associated mainly to the U.S. financial crisis and the pandemic. Moreover, this different behaviour can be due to the fact that these factors assign relatively less weight for the total variance and so they are sensitive to the new observations.

I analyse a FAQVAR model using eight factors chosen according to Bai and Ng (2002)'s criteria, and these factors are able to capture the large variability of the data, especially during the U.S. financial crisis and the pandemic. Hence, the dependent variables are composed of nine variables ordered from the first to the eight factors, and the federal funds rate. I also estimate the limiting FAVARMA Gaussian model of Dufour and Stevanović (2013) when $\nu \to \infty$. Table 4.2 reports the FAVARMA and FAQVAR model estimates, with each column containing estimates for one of the nine dependent variables.

Table 4.2: FAVARMA and FAQVAR models estimates

Parameter	FAVARMA									FAQVAR								
	$1^{st}F$	$2^{nd}F$	$3^{rd}F$	$4^{th}F$	$5^{th}F$	$6^{th}F$	$7^{th}F$	$8^{th}F$	FFR	$1^{st}F$	$2^{nd}F$	$3^{rd}F$	$4^{th}F$	$5^{th}F$	$6^{th}F$	$7^{th}F$	$8^{th}F$	FFR
c'	0.09^b	0.06	-0.02	-0.10^a	0.10^a	-0.01	0.04	0.02	0.00	0.07^a	0.04^c	0.01	-0.13^a	0.14^a	-0.01	0.05^a	0.01	-0.09^a
	0.76^a	-0.10	-0.02	-0.47^a	-0.13	0.13	-0.06	-0.09	-0.02	1.07^a	-0.11^a	0.14^a	-0.30^a	-0.31^a	-0.15^a	0.01	0.07^c	-0.02^b
	0.42^a	0.49^a	-0.18^a	-0.04	-0.19^c	-0.18	-0.03	-0.12	-0.02	0.13^a	0.66^a	-0.29^a	0.10^b	0.19^a	-0.06	-0.10^a	0.05	0.01
	-0.07	-0.15^b	0.65^a	0.20^b	0.49^a	-0.23	-0.49^a	-0.16	-0.02	0.07^b	-0.18^a	0.73^a	0.23^a	0.26^a	0.03	-0.03	-0.03	-0.04^a
	0.17	-0.45^a	0.04	0.18	-0.81^a	-0.31	-0.20	0.12	0.02	-0.04	-0.08^b	0.04	0.59^a	-0.33^a	0.10^b	-0.02	-0.03	-0.01
$\hat{\Phi}$	0.02	-0.12	0.14^b	-0.35^a	0.66^a	-0.97^b	-0.67^b	0.80^b	0.04	0.03^b	0.03	0.10^a	-0.14^a	0.82^a	-0.04^c	-0.01	0.00	-0.04^a
	0.16^b	0.06	0.11^a	0.21^a	0.06	0.66^a	-0.12	0.10	0.00	0.01	0.10^a	0.14^a	0.07^b	0.03	0.78^a	-0.04	0.00	0.02^a
	0.00	-0.05	-0.06^c	-0.14^a	-0.03	-0.04	0.78^a	-0.08	-0.03^a	0.01	0.02	-0.01	0.00	-0.01	0.05^b	0.97^a	0.00	-0.03^a
	0.19^a	-0.02	0.05	0.08	-0.10	0.10	0.17	0.70^a	-0.03	0.05^a	0.01	0.01	0.01	-0.01	0.05^c	0.01	0.88^a	-0.02^a
	1.33^a	-0.69^b	0.79^a	-1.40^a	-2.15^a	-0.16	0.60	0.09	0.56^a	0.35^a	-0.23^a	0.94^a	-1.93^a	-1.98^a	-0.33^a	-0.06^b	-0.02	0.79^a
	-0.30^a	0.00	0.00	0.00	0.00	0.00	0.00	0.00	0.00	-0.18^a	0.00	0.00	0.00	0.00	0.00	0.00	0.00	0.00
	0.07^a	-0.17^a	0.00	0.00	0.00	0.00	0.00	0.00	0.00	0.03^b	-0.15^a	0.00	0.00	0.00	0.00	0.00	0.00	0.00
	-0.03^a	-0.13^a	-0.09^a	0.00	0.00	0.00	0.00	0.00	0.00	-0.01^b	-0.11^a	-0.08^a	0.00	0.00	0.00	0.00	0.00	0.00
	-0.01	-0.02^a	0.05^a	-0.14^a	0.00	0.00	0.00	0.00	0.00	-0.01^c	-0.01^b	0.03^b	-0.12^a	0.00	0.00	0.00	0.00	0.00
$\hat{\Omega}^{-1}$	0.05^a	0.02^a	0.05^a	-0.08^a	-0.10^a	0.00	0.00	0.00	0.00	0.02^b	0.02^b	0.03^a	-0.06^a	-0.08^a	0.00	0.00	0.00	0.00
	0.01	0.00	0.05^a	0.02^a	0.02^a	-0.13^a	0.00	0.00	0.00	0.00	0.01	0.05^a	0.01^b	0.02^b	-0.11^a	0.00	0.00	0.00
	-0.01^a	-0.01^b	0.02^a	-0.04^a	0.06^a	-0.06^a	-0.09^a	0.00	0.00	0.00	0.00	0.01^b	-0.04^a	0.05^a	-0.04^a	-0.08^a	0.00	0.00
	0.00	-0.01^b	0.01^c	-0.02^a	0.02^a	0.03^a	0.00	-0.14^a	0.00	0.02^b	-0.02^b	0.02^b	-0.02^b	0.02^b	0.03^b	0.01^b	-0.12^a	0.00
	-0.07^b	0.13^a	-0.17^a	-0.05^c	0.14^a	-0.09^a	0.17^a	-0.06^b	0.76^a	-0.03	0.06^b	-0.13^b	-0.03	0.07^b	-0.10^b	0.06^b	-0.02	0.62^a
	0.43^a	0.23^a	-0.22^a	-0.47^a	0.56^a	-0.19^a	-0.11^b	0.00	0.03^a	0.82^a	0.44^a	-0.32^a	-0.43^a	0.72^a	-0.66^a	0.03	0.01	0.05^b
	0.06^a	-0.07^b	-0.39^a	0.14^a	-0.08^c	0.09^b	0.14^a	0.10^a	0.01	0.32^a	-0.11^b	-0.97^a	-0.13^a	-0.31^a	0.03	0.14^a	0.08	0.02
	-0.01	-0.40^a	0.12^a	0.13^a	0.29^a	0.16^a	0.04	0.12^a	-0.04^a	-0.05	-0.92^a	0.33^a	0.27^a	0.42^a	0.17^a	-0.08	-0.01	-0.11^a
	0.05^b	0.06^c	-0.14^a	0.38^a	-0.08^b	0.15^a	-0.25^a	-0.01	0.05^a	-0.03	-0.20^a	-0.13^a	0.81^a	-0.44^a	0.21^a	-0.46^a	-0.01	0.11^a
Ψ	0.14^a	0.23^a	-0.04	-0.21^a	0.38^a	-0.14^a	0.13^a	0.01	-0.01^b	0.26^a	0.44^a	-0.11^b	-0.09^c	0.60^a	-0.23^a	0.04	-0.03	-0.03^b
	-0.02	-0.09^a	0.30^a	0.03	0.05	0.06^b	0.02	-0.03	0.00	0.15^a	0.12^a	0.21^a	0.31^a	-0.27^a	0.21^a	-0.16^a	-0.03	0.03^c
	-0.03^b	-0.02	0.08^a	-0.03	0.24^a	0.06^b	0.11^a	0.05^b	0.01^c	-0.20^a	0.04	0.01	0.03	0.24^a	0.05	0.09^b	0.01	0.03^c
	-0.08^a	0.01	0.16^a	0.18^a	-0.13^a	0.12^a	0.01	0.02	-0.01^b	0.01	0.06	0.06	0.07	0.07	0.03	0.00	0.07	0.01
	0.52^a	-0.70^a	1.23^a	-0.18	2.54^a	0.09	-0.27^b	-0.44^a	0.32^a	1.39^a	-0.83^a	1.76^a	0.42^a	4.91^a	-0.40^a	0.07^a	-0.01	0.97^a
ν					∞									5.86^a				

Notes: [a], [b], and [c] denote residual bootstrapping significance at 1%, 5%, and 10%, respectively. The model is $y_t = c + \mu_t + \varepsilon_t$, where $\mu_t = \Phi\mu_{t-1} + \Psi u_{t-1}$ and $\varepsilon_t \sim t_\nu(0, \Omega^{-1}\Omega^{-1\prime})$. F and FFR denote factor and federal funds rate, respectively.

The persistence estimates,[28] $\hat{\Phi}$, for the FAQVAR model are generally higher than the FAVARMA values, the estimates for the impact matrix $\hat{\Omega}^{-1}$ are lower for the FAQVAR model. This might be explained because the degrees of freedom capture (to some extent) the impact from shocks. In addition, the entries for the updating matrix $\hat{\Psi}$ are more pronounced relative to those of the FAVARMA specification.

Table 4.3 presents the model diagnostics that allow assessment of stationary conditions and fit to the data. Both systems are stable given that for both models the maximum eigenvalues of $\hat{\Phi}$ are 0.958 and 0.994 in absolute value. There are important gains in the in-sample fit to the data from the likelihood values and the Akaike (1974) information, Bayesian information (Schwarz, 1978), and Hannan and Quinn (1979) criteria when I consider the DCS approach. The estimate of the degrees of freedom is small and the addition of this parameter to the model is statistically significant, this means that the FAQVAR model is able to capture the atypical observations in the panel data.

Table 4.3: FAVARMA and FAQVAR model diagnostics

	Diagnostic				
Model	λ	$\log L$	AIC	BIC	HQ
FAVARMA	0.985	2623.881	-4815.762	-3818.692	-4839.630
FAQVAR	0.994	3250.469	-6066.939	-5065.253	-6090.917

Notes: λ is the maximum eigenvalue for the persistence matrix $\hat{\Phi}$. AIC, BIC and HQ are the Akaike, Bayesian and Hannan and Quinn information criteria, respectively.

After the estimation of parameters and factor loadings, I produce and plot the impulse responses[29] to a one standard-deviation contractionary monetary shock, or equivalently to a 116 basis point rise in the Federal funds rate, as shown in Figure 4.3. I evaluate the impacts over some relevant variables in the economy after scaling them in levels, although all impulse responses can be reproduced from the informational set z_t. As in Yamamoto (2019), the variables considered for analysis are: Industrial production index, consumer price index, the exchange rate of Yen to US. dollar, the civilian unemployment rate and new orders for durable goods. The dotted 95 percent confidence bands are obtained using 1000 residual bootstrap iterations.

[28] The initial conditions are set by using the previous estimates from a model with one less factor. I start the loop with a model with one-augmented factor whose estimates are robust to general initial conditions.

[29] I use $R = 1000$ bootstrap iterations from the algorithm described in Section 3.1.

Figure 4.3: Impulses responses from a negative monetary policy shock

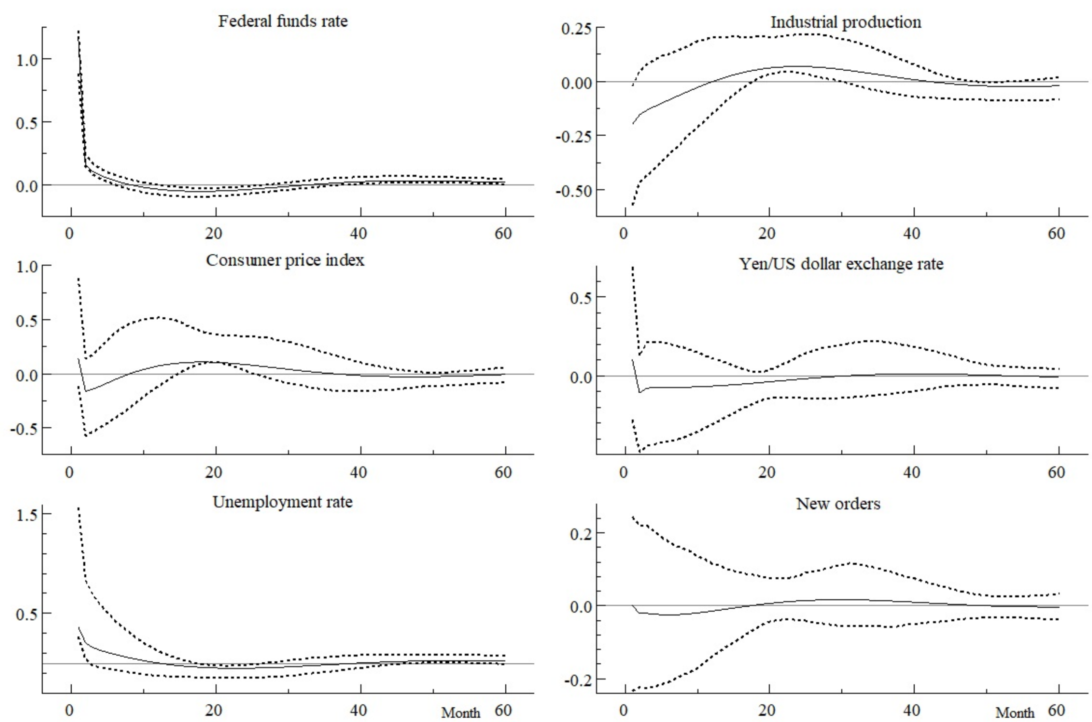

Note: Impulse responses from the FAQVAR model with eight factors, with 95 percent confidence intervals in dotted lines.

Figure 4.4 shows a comparison between responses to negative monetary policy shocks implied by the FAVARMA and FAQVAR models. The responses from the FAVAR model are influenced by crash periods during the global financial crisis and the pandemic that distorted the effects on the consumer price index, exchange rate, and new orders, this generates a greater decay during the first months relative to the responses from the FAQVAR model. In comparison to the FAVARMA model, the FAQVAR model effects on new durable goods orders are smoother and more conservative.

As expected from the proposed non-linear model, the responses from the FAQVAR model generate hump shapes which raise the effect on the consumer price index and industrial production as soon as the interest rate reaches negative territory.[30] In particular, the higher hump-shaped reaction that starts at the 9th month might have originated from the quantitative easing policies during the financial crisis and pandemic, which aimed to boost economic activity.

Figure 4.4: Impulses responses from a negative monetary policy shock, FAVARMA and FAQVAR models

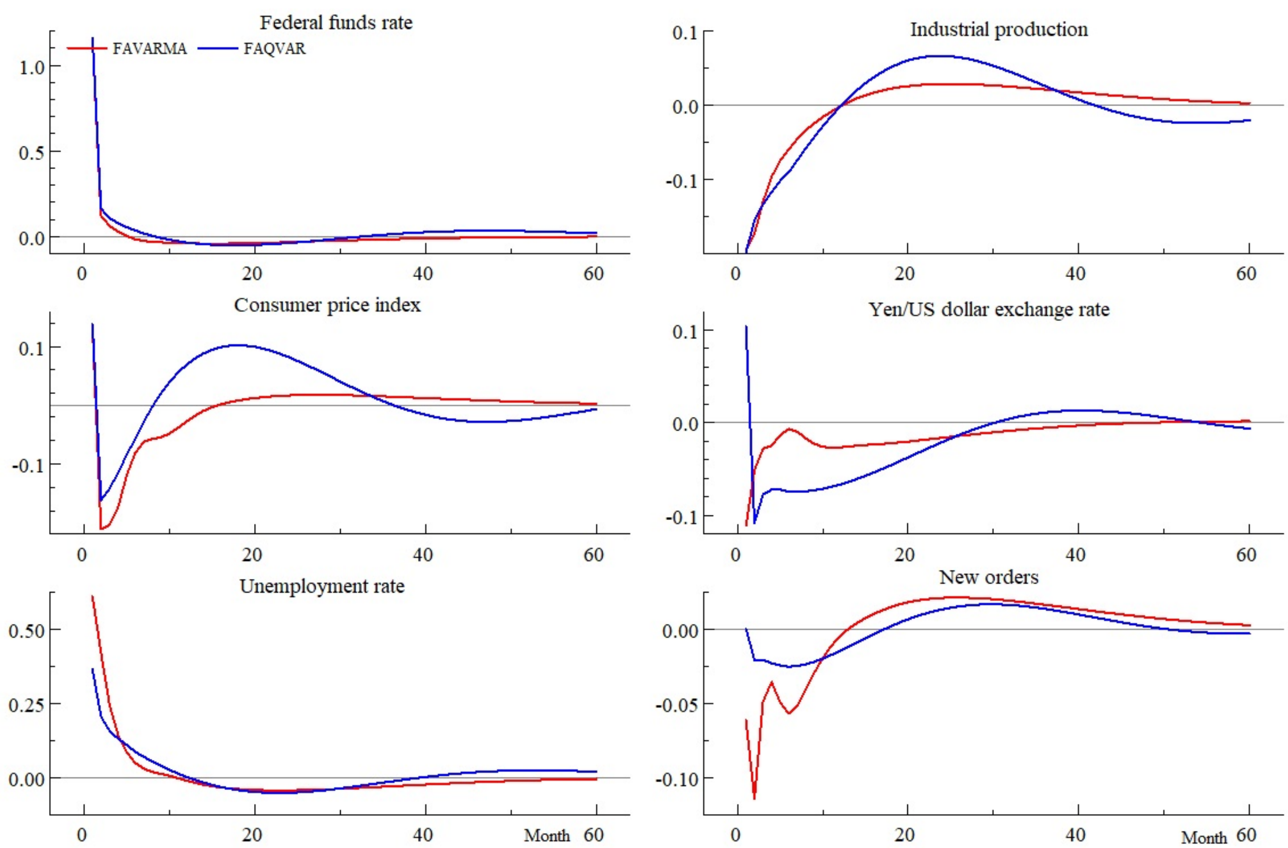

Note: Impulse responses in months from FAVARMA and FAQVAR models with eight factors.

Further, the FAQVAR model captures the turbulent episodes as atypical since it is modelled with a heavy tail distribution. The impulse responses follow the expected pattern when a negative monetary shock occurs: a decrease in industrial production, a decline in prices, a rise in the

[30]This pattern is also observed by Guerron-Quintana et al. (2021) in their non-linear dynamic factor model

unemployment rate, a reduction in the number of orders, and an increase in the Yen/Dollar exchange rate. The FAVAR model estimates of Bernanke et al. (2005) and the FAVARMA model of Defour and Stevanović (2013) find similar patterns for a sample that extends until 2005 which did not include last turbulent episodes.

4.5 Alternative Specifications

In this section I estimate additional models with different numbers of factors to verify the robustness of the estimates in the FAQVAR model, and also I estimate the model using a subsample that does not include the pandemic period. Figure 4.5 shows the impulse responses functions from models that consider two, four and six augmented factors.

Figure 4.5: Impulses responses from a negative monetary policy shock and different number of factors

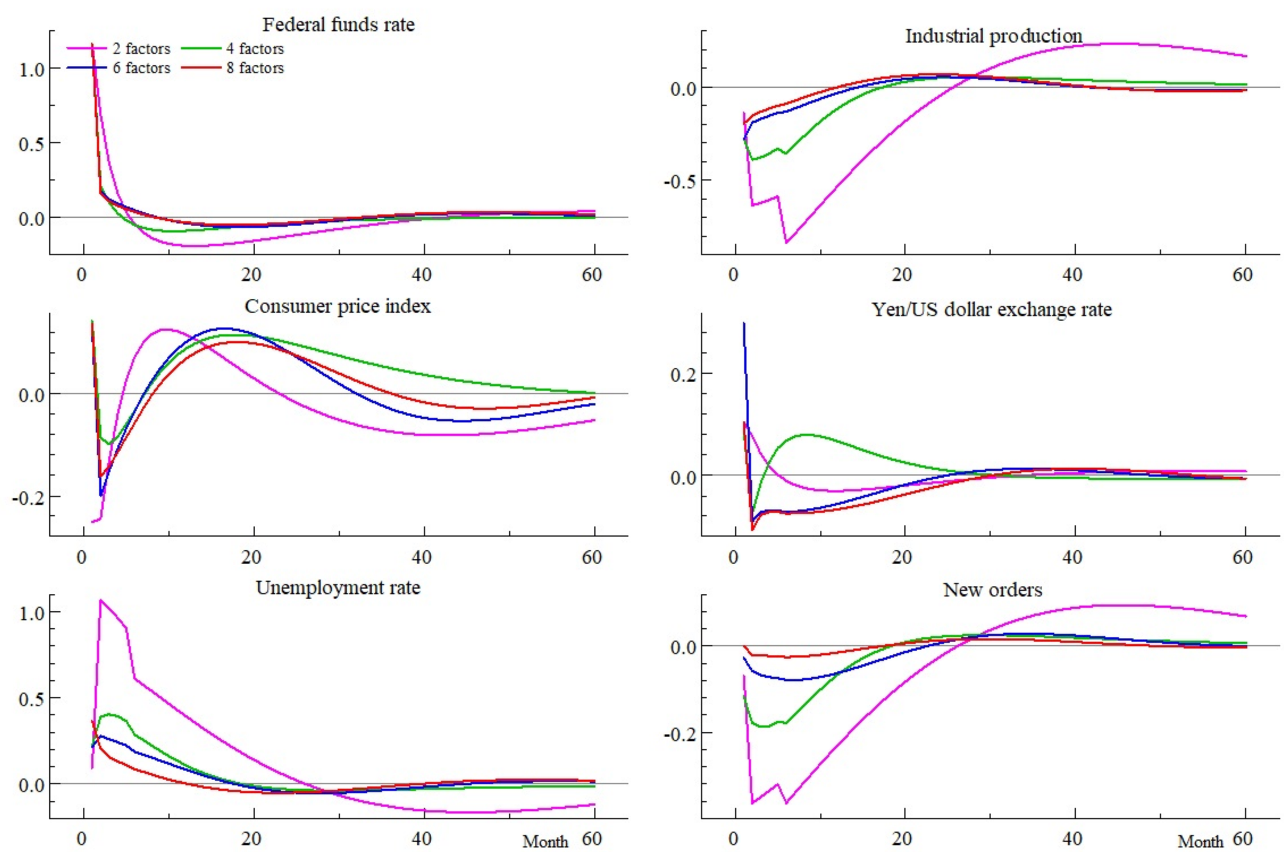

We can observe that the impacts derived from a model that only considers two factors are bigger and exhibit some breaks in industrial production, unemployment rate and new orders. As the dimension increases the responses are smoother in general. The paths of the shocks are similar in all scenarios except for the reaction of the exchange rate when four factors are used. However, as the model incorporates more information from the components the responses become quite similar, for instance, when we compare the figures for six and eight factors. This may suggest informational sufficiency from the informational variables (Forni and Gambetti, 2014).

4.6 Pre and Post COVID-19

I provide an additional robustness check by comparing the subsample up to the end of 2019 before the declaration of the COVID-19 pandemic and the full sample that takes the pandemic into account. As a benchmark exercise, Table 4.4 shows the estimates from the Gaussian FAVARMA model for both samples. We can see the effect of the pandemic on the estimates of the FAVARMA linear model, mainly affecting the estimates associated with the first factor. This means that a Gaussian assumption in times of high uncertainty can have severe effects on the linear model and policy assessment since the model does not accommodate extreme observations in comparison to a heavy tail distribution.

Table 4.4: FAVARMA and FAQVAR models estimates

Parameter	FAVARMA 2019									FAVARMA 2021								
	$1^{st}F$	$2^{nd}F$	$3^{rd}F$	$4^{th}F$	$5^{th}F$	$6^{th}F$	$7^{th}F$	$8^{th}F$	FFR	$1^{st}F$	$2^{nd}F$	$3^{rd}F$	$4^{th}F$	$5^{th}F$	$6^{th}F$	$7^{th}F$	$8^{th}F$	FFR
c'	0.09^a	0.07^a	-0.05^a	-0.08^a	0.05^a	0.00	0.01^c	0.00	0.04^a	0.09^b	0.06	-0.02	-0.10^a	0.10^a	-0.01	0.04	0.02	0.00
	0.99^a	-0.04^a	0.11^a	-0.19^a	-0.16^a	-0.04^a	0.07^a	0.07^a	-0.03^a	0.76^a	-0.10	-0.02	-0.47^a	-0.13	0.13	-0.06	-0.09	-0.02
	0.34^a	0.44^a	-0.33^a	0.12^a	0.11^a	-0.11^a	-0.04^a	-0.07^a	-0.01^a	0.42^a	0.49^a	-0.18^a	-0.04	-0.19^c	-0.18	-0.03	-0.12	-0.02
	0.13^a	-0.28^a	0.66^a	0.23^a	0.28^a	-0.08^a	-0.15^a	-0.01	-0.04^a	-0.07	-0.15^b	0.65^a	0.20^b	0.49^a	-0.23	-0.49^a	-0.16	-0.02
	-0.06^a	-0.20^a	0.00	0.44^a	-0.51^a	0.03^b	-0.12^a	-0.07^a	0.01^a	0.17	-0.45^a	0.04	0.18	-0.81^a	-0.31	-0.20	0.12	0.02
$\hat{\Phi}$	-0.31^a	0.10^a	0.10^a	-0.59^a	0.51^a	-0.11^a	-0.36^a	0.11^a	0.03^a	0.02	-0.12	0.14^b	-0.35^a	0.66^a	-0.97^b	-0.67^b	0.80^b	0.04
	0.00	0.10^a	0.09^a	0.04^a	0.03^a	0.75^a	-0.18^a	-0.02^c	0.02^a	0.16^b	0.06	0.11^a	0.21^a	0.06	0.66^a	-0.12	0.10	0.00
	0.07^a	-0.02^c	-0.04^a	0.08^a	0.08^a	-0.01	0.96^a	0.02^c	-0.03^a	0.00	-0.05	-0.06^c	-0.14^a	-0.03	-0.04	0.78^a	-0.08	-0.03^a
	0.10^a	-0.03^b	0.02^b	0.04^a	-0.02^c	-0.06^a	-0.03^a	0.88^a	-0.01^a	0.19^a	-0.02	0.05	0.08	-0.10	0.10	0.17	0.70^a	-0.03
	0.44^a	-0.28^a	0.95^a	-1.95^a	-1.87^a	-0.31^a	-0.04^a	-0.02^b	0.51^a	1.33^a	-0.69^b	0.79^a	-1.40^a	-2.15^a	-0.16	0.60	0.09	0.56^a
	-0.21^a	0.00	0.00	0.00	0.00	0.00	0.00	0.00	0.00	-0.30^a	0.00	0.00	0.00	0.00	0.00	0.00	0.00	0.00
	0.04^a	-0.17^a	0.00	0.00	0.00	0.00	0.00	0.00	0.00	0.07^a	-0.17^a	0.00	0.00	0.00	0.00	0.00	0.00	0.00
	-0.01^b	-0.13^a	-0.09^a	0.00	0.00	0.00	0.00	0.00	0.00	-0.03^a	-0.13^a	-0.09^a	0.00	0.00	0.00	0.00	0.00	0.00
	-0.02^a	-0.02^a	0.05^a	-0.14^a	0.00	0.00	0.00	0.00	0.00	-0.01	-0.02^a	0.05^a	-0.14^a	0.00	0.00	0.00	0.00	0.00
$\hat{\Omega}^{-1}$	0.01^b	0.02^a	0.04^a	-0.08^a	-0.09^a	0.00	0.00	0.00	0.00	0.05^a	0.02^a	0.05^a	-0.08^a	-0.10^a	0.00	0.00	0.00	0.00
	-0.01^b	0.01^c	0.04^a	0.02^a	0.02^a	-0.12^a	0.00	0.00	0.00	0.01	0.00	0.05^a	0.02^a	0.02^a	-0.13^a	0.00	0.00	0.00
	0.00	-0.01^b	0.02^b	-0.04^a	0.05^a	-0.06^a	-0.09^a	0.00	0.00	-0.01^a	-0.01^b	0.02^a	-0.04^a	0.06^a	-0.06^a	-0.09^a	0.00	0.00
	0.03^a	-0.01^b	0.02^a	-0.01^b	0.01^b	0.03^a	0.00^c	-0.13^a	0.00	0.00	-0.01^b	0.01^c	-0.02^a	0.02^a	0.03^a	0.00	-0.14^a	0.00
	-0.05^b	0.12^a	-0.19^a	-0.05^b	0.19^a	-0.09^a	0.21^a	-0.08^a	0.83^a	-0.07^b	0.13^a	-0.17^a	-0.05^c	0.14^a	-0.09^a	0.17^a	-0.06^b	0.76^a
	0.39^a	0.11^a	-0.10^a	-0.50^a	0.67^a	-0.29^a	0.12^a	-0.01	0.04^a	0.43^a	0.23^a	-0.22^a	-0.47^a	0.56^a	-0.19^a	-0.11^b	0.00	0.03^a
	0.04^a	-0.03^a	-0.51^a	0.16^a	-0.20^a	0.14^a	0.00	0.06^a	0.00	0.06^a	-0.07^b	-0.39^a	0.14^a	-0.08^c	0.09^b	0.14^a	0.10^a	0.01
	-0.05^a	-0.49^a	0.20^a	0.12^a	0.30^a	0.20^a	0.04^a	0.08^a	-0.05^a	-0.01	-0.40^a	0.12^a	0.13^a	0.29^a	0.16^a	0.04	0.12^a	-0.04^a
	-0.03^a	-0.08^a	-0.06^a	0.43^a	-0.09^a	0.12^a	-0.19^a	-0.04^a	0.05^a	0.05^b	0.06^c	-0.14^a	0.38^a	-0.08^b	0.15^a	-0.25^a	-0.01	0.05^a
Ψ	0.13^a	0.15^a	-0.01	-0.24^a	0.39^a	-0.17^a	0.21^a	0.02^b	-0.02^a	0.14^a	0.23^a	-0.04	-0.21^a	0.38^a	-0.14^a	0.13^a	0.01	-0.01^b
	0.03^a	-0.05^a	0.22^a	0.17^a	-0.12^a	0.02^c	-0.06^a	0.03^a	0.00	-0.02	-0.09^a	0.30^a	0.03	0.05	0.06^b	0.02	-0.03	0.00
	-0.11^a	-0.12^a	0.17^a	0.08^a	0.17^a	0.09^a	0.08^a	0.03^a	0.00^c	-0.03^b	-0.02	0.08^a	-0.03	0.24^a	0.06^b	0.11^a	0.05^b	0.01^c
	-0.06^a	0.03^a	0.11^a	0.15^a	-0.04^a	0.11^a	-0.03^a	-0.01	-0.01^a	-0.08^a	0.01	0.16^a	0.18^a	-0.13^a	0.12^a	0.01	0.02	-0.01^b
	1.09^a	-0.70^a	1.73^a	0.18^a	4.55^a	-0.31^a	0.00	-0.07^a	0.43^a	0.52^a	-0.70^a	1.23^a	-0.18	2.54^a	0.09	-0.27^b	-0.44^a	0.32^a
ν					∞									∞				

Notes: ^{a}, ^{b}, and ^{c} denote residual bootstrapping significance at 1%, 5%, and 10%, respectively. The model is $y_t = c + \mu_t + \varepsilon_t$, where $\mu_t = \Phi\mu_{t-1} + \Psi u_{t-1}$ and $\varepsilon_t \sim t_\nu(0, \Omega^{-1}\Omega^{-1\prime})$. F and FFR denote factor and federal funds rate, respectively.

In contrast, the estimates and impulse responses from the FAQVAR model with a Student t distribution are almost identical for both samples. Figure 4.6 exhibits the impulse responses from factors and monetary shocks to their same variables. The responses are identical for the subsample until December 2019 and the full sample until May 2021. There are a couple of points to highlight; first that the estimates of the FAQVAR model are robust to unprecedented behaviour of variables during the pandemic, and second, that the estimates are stable given that the trajectory of the responses are almost the same.

Figure 4.6: Impulses responses from factors and monetary policy shocks

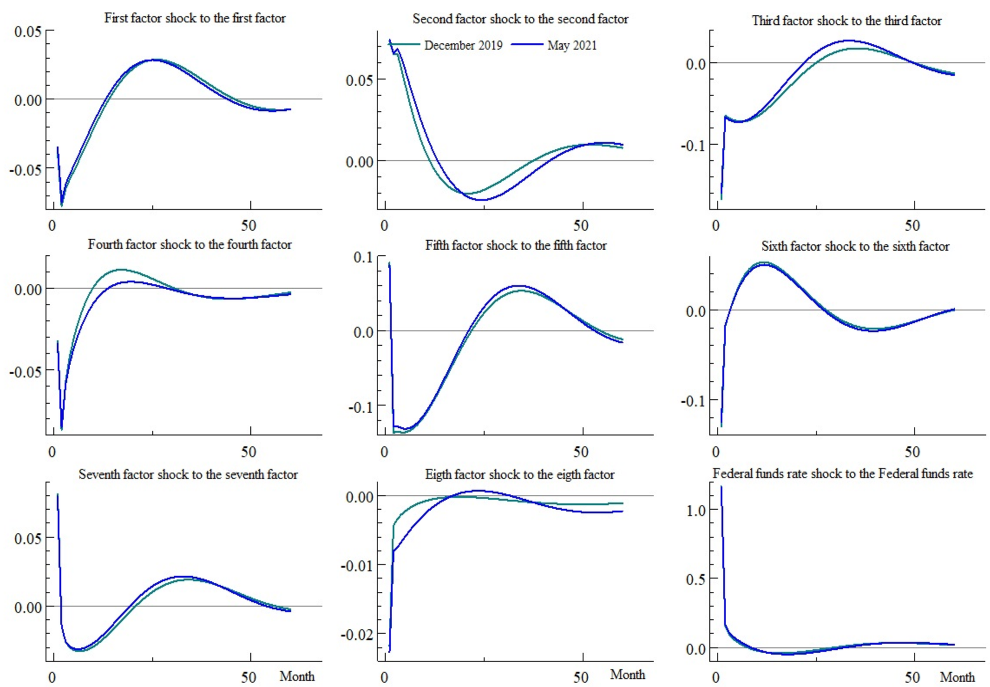

In Table 4.5, I report the bootstrap mean estimates from the FAQVAR models using the subsample until December 2019, and the full sample. In line with the findings of Bobeica and Hartwig (2022), the average of the degrees of freedom estimates supports the model with heavy tails before and after COVID-19 with a slightly lower average when considering the pandemic period.[31] Further, the intercept, persistence and updating matrices display similar entries across both samples.

[31] Also, the median of the bootstrap replications for the degrees of freedom display a decrease from 5.81 before the pandemic to 5.38 for the fill sample.

Table 4.5: FAQVAR models mean bootstrap estimates

Parameter	December 2019									May 2021								
	$1^{st}F$	$2^{nd}F$	$3^{rd}F$	$4^{th}F$	$5^{th}F$	$6^{th}F$	$7^{th}F$	$8^{th}F$	FFR	$1^{st}F$	$2^{nd}F$	$3^{rd}F$	$4^{th}F$	$5^{th}F$	$6^{th}F$	$7^{th}F$	$8^{th}F$	FFR
c'	0.07	0.04	0.01	-0.13	0.14	-0.01	0.06	0.00	-0.10	0.07	0.04	0.01	-0.13	0.14	-0.01	0.04	0.00	-0.08
	1.07	-0.11	0.14	-0.31	-0.32	-0.14	0.02	0.02	-0.02	1.04	-0.09	0.14	-0.29	-0.31	-0.13	0.03	0.07	-0.02
	0.12	0.66	-0.28	0.08	0.19	-0.04	-0.09	0.03	0.01	0.11	0.64	-0.29	0.07	0.18	-0.06	-0.09	0.07	0.01
	0.07	-0.18	0.73	0.23	0.26	0.03	-0.04	-0.03	-0.04	0.08	-0.20	0.71	0.22	0.26	0.04	-0.05	-0.04	-0.04
	-0.04	-0.07	0.05	0.59	-0.31	0.08	-0.01	-0.01	-0.01	-0.04	-0.09	0.03	0.58	-0.33	0.06	-0.03	-0.02	-0.01
$\hat{\Phi}$	0.02	0.03	0.11	-0.16	0.80	-0.03	0.00	0.00	-0.04	0.02	0.04	0.11	-0.15	0.81	-0.03	0.00	0.01	-0.04
	0.03	0.10	0.15	0.07	0.01	0.77	-0.04	-0.01	0.02	0.02	0.09	0.14	0.05	0.01	0.77	-0.05	-0.01	0.02
	0.00	0.03	0.00	-0.01	-0.01	0.03	0.96	0.02	-0.03	0.00	0.02	-0.01	0.00	0.00	0.04	0.97	0.02	-0.02
	0.05	0.00	0.00	0.01	-0.01	0.04	-0.02	0.83	-0.01	0.05	0.01	0.01	0.01	-0.02	0.05	0.01	0.87	-0.02
	0.36	-0.22	0.93	-1.94	-1.98	-0.33	-0.05	-0.01	0.80	0.37	-0.22	0.93	-1.92	-1.97	-0.32	-0.07	-0.02	0.76
	-0.17	0.00	0.00	0.00	0.00	0.00	0.00	0.00	0.00	-0.19	0.00	0.00	0.00	0.00	0.00	0.00	0.00	0.00
	0.02	-0.15	0.00	0.00	0.00	0.00	0.00	0.00	0.00	0.01	-0.15	0.00	0.00	0.00	0.00	0.00	0.00	0.00
	-0.01	-0.07	-0.10	0.00	0.00	0.00	0.00	0.00	0.00	0.00	-0.03	-0.12	0.00	0.00	0.00	0.00	0.00	0.00
	-0.01	-0.01	0.01	-0.12	0.00	0.00	0.00	0.00	0.00	0.00	0.00	0.01	-0.12	0.00	0.00	0.00	0.00	0.00
$\hat{\Omega}^{-1}$	0.01	0.01	0.02	-0.03	-0.09	0.00	0.00	0.00	0.00	0.00	0.00	0.01	-0.01	-0.10	0.00	0.00	0.00	0.00
	0.00	0.01	0.03	0.01	0.01	-0.11	0.00	0.00	0.00	0.00	0.00	0.01	0.00	0.00	-0.12	0.00	0.00	0.00
	0.00	0.00	0.01	-0.02	0.03	-0.02	-0.09	0.00	0.00	0.00	0.00	0.00	-0.01	0.01	-0.01	-0.10	0.00	0.00
	0.01	-0.01	0.01	-0.01	0.01	0.02	0.01	-0.12	0.00	0.00	0.00	0.00	0.00	0.00	0.01	0.00	-0.12	0.00
	-0.02	0.04	-0.09	-0.01	0.05	-0.07	0.04	-0.01	0.63	-0.01	0.03	-0.04	0.00	0.02	-0.03	0.02	0.00	0.64
	0.76	0.42	-0.29	-0.39	0.69	-0.63	0.01	0.00	0.05	0.71	0.37	-0.27	-0.38	0.67	-0.60	0.01	0.01	0.05
	0.28	-0.12	-0.91	-0.12	-0.29	0.03	0.10	0.02	0.02	0.28	-0.13	-0.85	-0.12	-0.29	0.03	0.12	0.07	0.01
	-0.05	-0.83	0.28	0.23	0.41	0.17	-0.09	-0.02	-0.09	-0.04	-0.77	0.24	0.24	0.38	0.14	-0.06	-0.01	-0.08
	-0.03	-0.18	-0.10	0.74	-0.37	0.19	-0.41	-0.01	0.11	-0.02	-0.17	-0.11	0.69	-0.36	0.19	-0.40	0.00	0.09
Ψ	0.24	0.38	-0.09	-0.09	0.56	-0.22	0.04	0.00	-0.02	0.24	0.35	-0.06	-0.07	0.55	-0.21	0.04	-0.01	-0.02
	0.12	0.11	0.18	0.29	-0.25	0.19	-0.15	-0.02	0.03	0.13	0.11	0.18	0.26	-0.24	0.17	-0.13	-0.02	0.03
	-0.17	0.05	0.02	0.03	0.24	0.05	0.09	0.01	0.02	-0.16	0.03	0.03	0.03	0.22	0.05	0.08	0.02	0.02
	0.01	0.02	0.03	0.02	0.02	0.01	0.00	0.11	0.00	0.00	0.05	0.07	0.06	0.07	0.03	0.00	0.03	0.00
	1.38	-0.83	1.74	0.43	4.89	-0.39	0.06	-0.01	0.90	1.37	-0.82	1.74	0.43	4.88	-0.40	0.06	-0.01	0.91
ν					5.60									5.38				

Note: The model is $y_t = c + \mu_t + \varepsilon_t$, where $\mu_t = \Phi\mu_{t-1} + \Psi u_{t-1}$ and $\varepsilon_t \sim t_\nu(0, \Omega^{-1}\Omega^{-1\prime})$. F and FFR denote factor and federal funds rate, respectively.

4.6.1 Zero Lower Bound

The sample considered also covers periods of zero lower bound (ZLB) in the Federal funds rate, which may influence the impulse responses from the monetary policy shock if it occurs at the ZLB. There are recent developments in the literature to deal with lower bounded policy rate, for instance we may extend the FAQVAR model with the interactive VAR model of Caggiano, Castelnuovo, and Pellegrino (2017), but this is extension is beyond the scope of this essay. I instead employ the shadow rate series proposed by Wu and Xia (2016) replacing the effective Federal funds rate observations during ZLB episodes: the first episode started in December 2008 and lasted until December 2015, and the second one started in March 2020 as a quick response from the pandemic threat. I re-estimate the model with the shadow rate and I show in Figure 4.7 the impulse responses from the Federal funds rate and the shadow rate shocks.

Figure 4.7: Impulses responses from Federal funds rate and shadow rate shocks

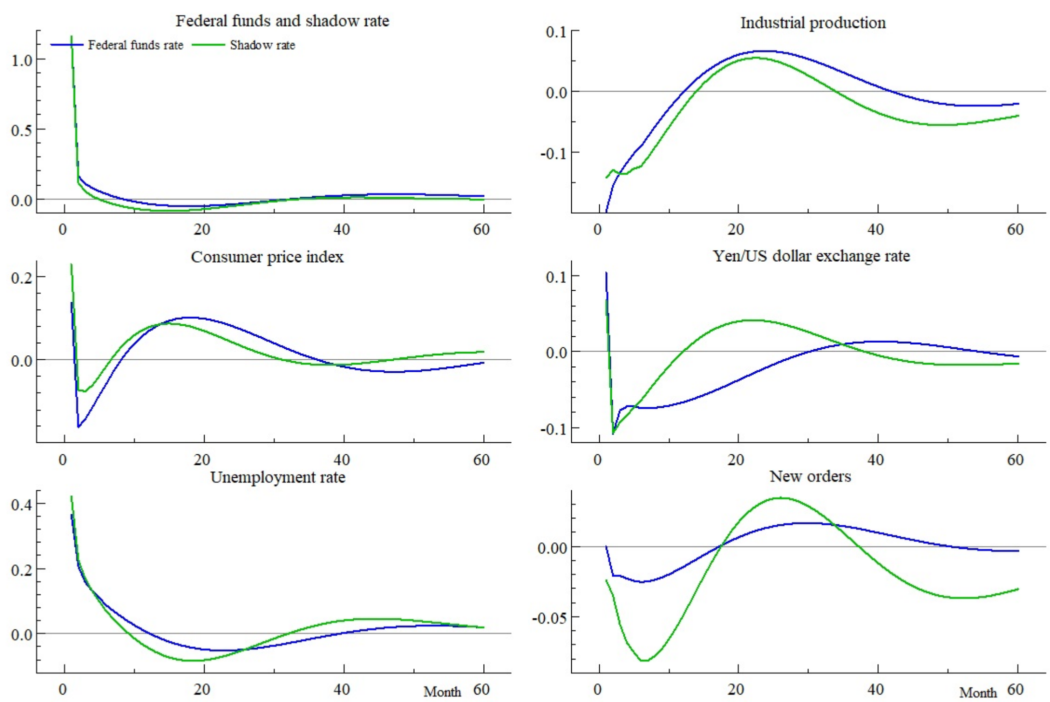

Overall, the impulse responses are similar between the effective and shadow rates exhibiting hump-shaped reactions from the score-driven FAQVAR model. As we can see on the top left response, the shadow rate is even further negative in comparison to the FFR, as a result the initial impact for industrial production is relatively moderate. The prices still show a prize puzzle in the first month, for then generate a disinflationary effect, and a lower increase in the medium term when considering the shadow rate. Also, the unemployment rate and new orders generate slightly bigger reactions from the shadow rate shock, and there is a more pronounced hump-shaped reaction in the exchange rate response.

4.7 Conclusions

This work studies a factor-augmented quasi-vector autoregression model. The benefit of this approach is its flexibility as a non-linear model and its robustness to critical episodes such as the US. financial crisis and the pandemic. Unlike traditional FAVARMA models, FAQVAR models assume a Student t distribution model for their multivariate errors, and they are observation and score-driven. The addition of these features generate stable estimates through turbulent episodes.

With respect to the base FAVARMA model, the FAQVAR model generates better in-sample fit and the generated impulse responses are hump-shaped. An assessment of monetary policy in the USA unveils that the characterised Student t errors provide a significant improvement to macro-modelling relative to FAVARMA models and the impulse responses from factor and monetary shocks are robust. Further, the impulse responses to a group of informational variables are in line with economic theory.

The proposed model allows several extensions, for instance, the modelling of heteroskedastic errors, time-varying parameters for the multivariate location model, specific modelling at or around the lower bound with interactive or Markov-switching models, and additional identification for structural shocks.

4.8 Appendix

I group the data using Bernanke et al. (2005) categories from FRED-MD as of May 2021. The associated index for the transformation of variables are: 1 if no transformation, 2 if first-differenced, 3 if two-times differenced, 4 if the variable is in logarithm, 5 when the variables are first differenced after taking logarithms, 6 if twice differenced after taking logarithm, 7 when growth is differenced.

Real output and income

	Variable	Index	Description	Sample
1	RPI	5	Real Personal Income	1959:01-2021:05
2	W875RX1	5	Real personal income ex transfer receipts	1959:01-2021:05
3	INDPRO	5	IP Index	1959:01-2021:05
4	IPFPNSS	5	IP: Final Products and Nonindustrial Supplies	1959:01-2021:05
5	IPFINAL	5	IP: Final Products (Market Group)	1959:01-2021:05
6	IPCONGD	5	IP: Consumer Goods	1959:01-2021:05
7	IPDCONGD	5	IP: Durable Consumer Goods	1959:01-2021:05
8	IPNCONGD	5	IP: Nondurable Consumer Goods	1959:01-2021:05
9	IPBUSEQ	5	IP: Business Equipment	1959:01-2021:05
10	IPMAT	5	IP: Materials	1959:01-2021:05
11	IPDMAT	5	IP: Durable Materials	1959:01-2021:05
12	IPNMAT	5	IP: Nondurable Materials	1959:01-2021:05
13	IPMANSICS	5	IP: Manufacturing (SIC)	1959:01-2021:05
14	IPB51222s	5	IP: Residential Utilities	1959:01-2021:05
15	IPFUELS	5	IP: Fuels	1959:01-2021:05
16	CUMFNS	2	Capacity Utilization: Manufacturing	1959:01-2021:05

Labor

	Variable	Index	Description	Sample
17	HWI	2	Help-Wanted Index for United States	1959:01-2021:04
18	HWIURATIO	2	Ratio of Help Wanted/No. Unemployed	1959:01-2021:04
19	CLF16OV	5	Civilian Labor Force	1959:01-2021:05
20	CE16OV	5	Civilian Employment	1959:01-2021:05
21	UNRATE	2	Civilian Unemployment Rate	1959:01-2021:05
22	UEMPMEAN	2	Average Duration of Unemployment (Weeks)	1959:01-2021:05
23	UEMPLT5	5	Civilians Unemployed - Less Than 5 Weeks	1959:01-2021:05
24	UEMP5TO14	5	Civilians Unemployed for 5-14 Weeks	1959:01-2021:05
25	UEMP15OV	5	Civilians Unemployed - 15 Weeks & Over	1959:01-2021:05
26	UEMP15T26	5	Civilians Unemployed for 15-26 Weeks	1959:01-2021:05
27	UEMP27OV	5	Civilians Unemployed for 27 Weeks and Over	1959:01-2021:05
28	CLAIMSx	5	Initial Claims	1959:01-2021:05
29	PAYEMS	5	All Employees: Total nonfarm	1959:01-2021:05
30	USGOOD	5	All Employees: Goods-Producing Industries	1959:01-2021:05
31	CES1021000001	5	All Employees: Mining and Logging: Mining	1959:01-2021:05
32	USCONS	5	All Employees: Construction	1959:01-2021:05
33	MANEMP	5	All Employees: Manufacturing	1959:01-2021:05
34	DMANEMP	5	All Employees: Durable goods	1959:01-2021:05
35	NDMANEMP	5	All Employees: Nondurable goods	1959:01-2021:05
36	SRVPRD	5	All Employees: Service-Providing Industries	1959:01-2021:05
37	USTPU	5	All Employees: Trade, Transportation & Utilities	1959:01-2021:05
38	USWTRADE	5	All Employees: Wholesale Trade	1959:01-2021:05
39	USTRADE	5	All Employees: Retail Trade	1959:01-2021:05
40	USFIRE	5	All Employees: Financial Activities	1959:01-2021:05
41	USGOVT	5	All Employees: Government	1959:01-2021:05
42	CES0600000007	1	Avg Weekly Hours : Goods-Producing	1959:01-2021:05
43	AWOTMAN	2	Avg Weekly Overtime Hours : Manufacturing	1959:01-2021:05
44	AWHMAN	1	Avg Weekly Hours : Manufacturing	1959:01-2021:05

Consumption

	Variable	Index	Description	Sample
45	DPCERA3M086SBEA	5	Real personal consumption expenditures	1959:01-2021:05
46	PCEPI	6	Personal Cons. Expend.: Chain Index	1959:01-2021:05
47	DDURRG3M086SBEA	6	Personal Cons. Exp: Durable goods	1959:01-2021:05
48	DNDGRG3M086SBEA	6	Personal Cons. Exp: Nondurable goods	1959:01-2021:05
49	DSERRG3M086SBEA	6	Personal Cons. Exp: Services	1959:01-2021:05

Housing starts and sales

	Variable	Index	Description	Sample
50	HOUST	4	Housing Starts: Total New Privately Owned	1959:01-2021:05
51	HOUSTNE	4	Housing Starts, Northeast	1959:01-2021:05
52	HOUSTMW	4	Housing Starts, Midwest	1959:01-2021:05
53	HOUSTS	4	Housing Starts, South	1959:01-2021:05
54	HOUSTW	4	Housing Starts, West	1959:01-2021:05
55	PERMIT	4	New Private Housing Permits (SAAR)	1960:01-2021:05
56	PERMITNE	4	New Private Housing Permits, Northeast (SAAR)	1960:01-2021:05
57	PERMITMW	4	New Private Housing Permits, Midwest (SAAR)	1960:01-2021:05
58	PERMITS	4	New Private Housing Permits, South (SAAR)	1960:01-2021:05
59	PERMITW	4	New Private Housing Permits, West (SAAR)	1960:01-2021:05

Inventories and orders

	Variable	Index	Description	Sample
60	CMRMTSPLx	5	Real Manu. and Trade Industries Sales	1959:01-2021:04
61	RETAILx	5	Retail and Food Services Sales	1959:01-2021:05
62	ACOGNO	5	New Orders for Consumer Goods	1992:02-2021:04
63	AMDMNOx	5	New Orders for Durable Goods	1959:01-2021:05
64	ANDENOx	5	New Orders for Nondefense Capital Goods	1968:02-2021:05
65	AMDMUOx	5	Unfilled Orders for Durable Goods	1959:01-2021:05
66	BUSINVx	5	Total Business Inventories	1959:01-2021:04
67	ISRATIOx	2	Total Business: Inventories to Sales Ratio	1959:01-2021:04

Stock market

	Variable	Index	Description	Sample
68	S&P 500	5	S&P's Common Stock Price Index: Composite	1959:01-2021:05
69	S&P: indust	5	S&P's Common Stock Price Index: Industrials	1959:01-2021:05
70	S&P div yield	2	S&P's Composite Common Stock: Dividend Yield	1959:01-2021:03
71	S&P PE ratio	5	S&P's Composite Common Stock: Price-Earnings Ratio	1959:01-2021:04
72	VXOCLSx	1	VXO	1962:07-2021:05

Exchange rates

	Variable	Index	Description	Sample
73	TWEXAFEGSMTHx	5	Trade Weighted U.S. Dollar Index: Major Currencies	1973:01-2021:05
74	EXSZUSx	5	Switzerland / U.S. Foreign Exchange Rate	1959:01-2021:05
75	EXJPUSx	5	Japan / U.S. Foreign Exchange Rate	1959:01-2021:05
76	EXUSUKx	5	U.S. / U.K. Foreign Exchange Rate	1959:01-2021:05
77	EXCAUSx	5	Canada / U.S. Foreign Exchange Rate	1959:01-2021:05

Interest rates

	Variable	Index	Description	Sample
78	FEDFUNDS	2	Effective Federal Funds Rate	1959:01-2021:05
79	CP3Mx	2	3-Month AA Financial Commercial Paper Rate	1959:01-2020:03
79	CP3Mx	2	3-Month AA Financial Commercial Paper Rate	2020:05-2021:05
80	TB3MS	2	3-Month Treasury Bill	1959:01-2021:05
81	TB6MS	2	6-Month Treasury Bill	1959:01-2021:05
82	GS1	2	1-Year Treasury Rate	1959:01-2021:05
83	GS5	2	5-Year Treasury Rate	1959:01-2021:05
84	GS10	2	10-Year Treasury Rate	1959:01-2021:05
85	AAA	2	Moody's Seasoned Aaa Corporate Bond Yield	1959:01-2021:05
86	BAA	2	Moody's Seasoned Baa Corporate Bond Yield	1959:01-2021:05
87	COMPAPFFx	1	3-Month Commercial Paper Minus FEDFUNDS	1959:01-2020:03
87	COMPAPFFx	1	3-Month Commercial Paper Minus FEDFUNDS	2020:05-2021:05
88	TB3SMFFM	1	3-Month Treasury C Minus FEDFUNDS	1959:01-2021:05
89	TB6SMFFM	1	6-Month Treasury C Minus FEDFUNDS	1959:01-2021:05
90	T1YFFM	1	1-Year Treasury C Minus FEDFUNDS	1959:01-2021:05
91	T5YFFM	1	5-Year Treasury C Minus FEDFUNDS	1959:01-2021:05
92	T10YFFM	1	10-Year Treasury C Minus FEDFUNDS	1959:01-2021:05
93	AAAFFM	1	Moody's Aaa Corporate Bond Minus FEDFUNDS	1959:01-2021:05
94	BAAFFM	1	Moody's Baa Corporate Bond Minus FEDFUNDS	1959:01-2021:05

Money and credit

	Variable	Index	Description	Sample
95	M1SL	6	M1 Money Stock	1959:01-2021:05
96	M2SL	6	M2 Money Stock	1959:01-2021:05
97	M2REAL	5	Real M2 Money Stock	1959:01-2021:05
98	BOGMBASE	6	St. Louis Adjusted Monetary Base	1959:01-2021:05
99	TOTRESNS	6	Total Reserves of Depository Institutions	1959:01-2021:05
100	NONBORRES	7	Reserves Of Depository Institutions	1959:01-2021:05
101	BUSLOANS	6	Commercial and Industrial Loans	1959:01-2021:05
102	REALLN	6	Real Estate Loans at All Commercial Banks	1959:01-2021:05
103	NONREVSL	6	Total Nonrevolving Credit	1959:01-2021:04
104	CONSPI	2	Nonrevolving consumer credit to Personal Income	1959:01-2021:04
105	MZMSL	6	MZM Money Stock	1959:01-2021:01
106	DTCOLNVHFNM	6	Consumer Motor Vehicle Loans Outstanding	1959:01-2021:04
107	DTCTHFNM	6	Total Consumer Loans and Leases Outstanding	1959:01-2021:04
108	INVEST	6	Securities in Bank Credit at All Commercial Banks	1959:01-2021:05

Prices

	Variable	Index	Description	Sample
109	WPSFD49207	6	PPI: Finished Goods	1959:01-2021:05
110	WPSFD49502	6	PPI: Finished Consumer Goods	1959:01-2021:05
111	WPSID61	6	PPI: Intermediate Materials	1959:01-2021:05
112	WPSID62	6	PPI: Crude Materials	1959:01-2021:05
113	OILPRICEx	6	Crude Oil, spliced WTI and Cushing	1959:01-2021:05
114	PPICMM	6	PPI: Metals and metal products:	1959:01-2021:05
115	CPIAUCSL	6	CPI : All Items	1959:01-2021:05
116	CPIAPPSL	6	CPI : Apparel	1959:01-2021:05
117	CPITRNSL	6	CPI : Transportation	1959:01-2021:05
118	CPIMEDSL	6	CPI : Medical Care	1959:01-2021:05
119	CUSR0000SAC	6	CPI : Commodities	1959:01-2021:05
120	CUSR0000SAD	6	CPI : Durables	1959:01-2021:05
121	CUSR0000SAS	6	CPI : Services	1959:01-2021:05
122	CPIULFSL	6	CPI : All Items Less Food	1959:01-2021:05
123	CUSR0000SA0L2	6	CPI : All items less shelter	1959:01-2021:05
124	CUSR0000SA0L5	6	CPI : All items less medical care	1959:01-2021:05

Average hourly earnings and consumer sentiment index

	Variable	Index	Description	Sample
125	CES0600000008	6	Avg Hourly Earnings : Goods-Producing	1959:01-2021:05
126	CES2000000008	6	Avg Hourly Earnings : Construction	1959:01-2021:05
127	CES3000000008	6	Avg Hourly Earnings : Manufacturing	1959:01-2021:05
128	UMCSENTx	2	Consumer Sentiment Index	1959:01-2021:05

5 Conclusions and recommendations

5.1 Summary of thesis

In this dissertation I propose new dynamic conditional score models for analysing the scale or volatility in emerging markets in the Americas. I also develop factor DCS models of the location or mean for the study of monetary policy shocks in the U.S. The DCS framework is able to handle atypical observations and big shocks given its flexibility for the modelling of time-varying scale or location processes in a model. Multiple atypical shocks have arisen in the recent decades. Just to name a few, we have the Asian crisis in 1998, the global financial crisis in 2008, the pandemic in 2020, and the world may soon experience a war shock.

Being able to develop models to capture these episodes, and not just omit them from the sample, is relevant these days. Even more, the DCS approach is observation-driven since the model is fully conditioned through a term proportional to the score of each model. This allows estimation with traditional methods like maximum likelihood for example, which brings practitioners another alternative to the estimation of models using Bayesian techniques.

My first essay proposes an alternative approach to deal with series of high persistence. I develop a dynamic conditional score model for modelling time-varying volatilities with random shifts. I show that this model explains much of the dynamics of volatility in emerging stock markets. The study of South American equity markets reveals that they follow a pattern associated with a model with short-memory and random shifts, rather than a long-memory model.

I apply the RS-Beta-t-EGARCH model and I find that multiple regime shifts in these stock markets are related to events such as the U.S. financial crisis in 2007 and the current pandemic. The addition of random shifts in the model reduces the impact of a volatility shock. A comparison between the RS-Beta-t-EGARCH model with respect to the base Beta-t-EGARCH model shows gains in terms of fit to the data and out-sample density forecasts.

I study score-driven copula models with components in my second essay. This work explores the benefits of specifying both a long and short component, when modelling persistence in the dependence parameter of score-driven copula models. In addition, the two components allow for a shorter persistence dynamic that captures transitory shocks and leaves the long-component for more persistent shocks. I analyse three copula specifications: score-driven Clayton, score-driven rotated Gumbel copula, and the score-driven t-copula models to bivariate equity markets in the American continent. When I add the two-components to their structure they exhibit better in-sample fit according to likelihood ratio tests in comparison to the single-component specification. Also, the model with two components outperforms the unique component model in terms of out-of-sample density forecasts.

In particular, the two-component score-driven t-copula model, which is a symmetric model capturing positive and negative shocks, outperforms all the other models. The application of the two components model shows that the time-varying dependencies are high in turmoil times associated with the Asian crisis, the global financial crisis in 2008 and the COVID-19 pandemic, as a result of external shocks. Then, I demonstrate the high persistence of the long-term component plotting autocorrelation functions that display an hyperbolic decay behaviour. The short-term component instead exhibits a shape similar to a white noise process. Further, the symmetric two-component score-driven t-copula specification is robust to the COVID-19 crisis.

My third essay establishes a new factor-augmented quasi-vector autoregression model with heavy tails. This FAQVAR model is driven by its score and it is able to accommodate critical episodes in the sample of study for the U.S., which includes the last COVID-19 crisis. In comparison to the standard Gaussian FAVARMA models, my model assumes a Student t distribution model for its multivariate errors. These features generate stable estimates through turbulent episodes. Even before the COVID-19 crisis, the proposed model supports a heavy tail specification with a small estimate for the degrees of freedom.

Further, the FAQVAR model has a superior performance with a better in-sample fit than the FAVARMA specifications. The generated impulse responses from the analysis of monetary policy in the USA are hump-shaped, and their responses are in line with the economic theory. A negative monetary shock contracts industrial production, the demand for new orders for durable goods, and a rise in the unemployment rate. All impulses responses from the aggregate variables could be generated because of the factor-augmented structure.

The study considers episodes of zero lower bound for the monetary policy instrument. The first is a policy measure against the global financial crisis which started at the end of 2008 and lasted until

December 2015. More recently, the Federal Reserve Board has set its funds rate at the zero lower bound since March 2021 as a result of the pandemic. I replace these zero lower bound episodes with a shadow rate, and the responses are fairly stable relative to the constrained Federal funds rate.

5.2 Recommendations for further research

Dynamic conditional score models constitutes a relatively new approach to deal with time-varying parameters such as the volatility, or the scale, and the location, or mean, as well as breaks and regime changes, and other applications in the literature. The flexibility of this framework in the modelling of heavy tails permits to capture outliers and atypical events. There are more frequent uncertain events that suddenly may disrupt the world economy. Only considering the recent events we can count the pandemic and the war conflict in Europe, which could trigger a large-scale shock in the near future. The DCS framework brings a flexible solution for modelling these and other shocks in a unique framework. Even more, given its flexibility it is feasible to estimate with frequentist estimation methods.

My dissertation allows several avenues for research. Additional extensions may include the estimation of common regimes of volatility in multivariate DCS models. The estimation of volatility regimes in South American emerging markets suggest that these regimes may coincide across countries as a result of common regional or global shocks. There is a significant dependence of these economies to big markets in the U.S. and China, for instance. Moreover, Latin American economies relied historically on the U.S. dollar after hyperinflation episodes in the region during the 1980s and 1990s. This dollarization might mean another source of shocks from speculative flows of capitals in times of high uncertainty. In addition, stock returns show a marked skewness, so we may consider a more general distribution like the skewed generalized Student t distribution.

Fry, Martin and Tang (2010) highlight the importance of skewness during financial crises since this asymmetry measure tends to switch from negative to positive with proper dynamics. Hence, it would be relevant to model the co-skewness features in univariate and multivariate dynamic conditional score models. In addition, researchers may explore common regimes of volatility in other emerging equity markets in Africa, South-East Asia, Eastern Mediterranean or Western Pacific that share some similarities to countries in the Americas since they are susceptible to multiple shocks and also are dependent on bigger economies.

The modelling of a set of variables and their measures of association within the DCS framework could include multivariate copula models. These copulas utilise the residuals from the marginal model of individual series. In this dissertation, I employ an asymmetric GARCH model for stock returns, but further extensions such as fractional integration GARCH specifications or score-driven dynamics for volatility could be explored. Moreover, if a score-driven marginal model is added into two-component score-driven copulas, we could investigate gains in the efficiency of estimates as suggested by Joe (2005) for the GARCH approach.

With respect to score-driven copulas, the addition of more components for the time-varying dependence parameter could contribute to a better understanding in the dynamic of shocks. Three components may model short-term, medium-term and long-term shocks, for example. I analysed the benefits of modelling long-term and short components in bivariate settings, but richer dynamics could be explored if we consider a panel of more than two countries and analyse common shocks to their volatility dependence using the score-driven framework.

In addition, I considered three types of symmetric and asymmetric copulas, but there are further copulas for modelling negative and positive shocks, and a variety of associations between variables in the literature. For instance, more general Archimedean copulas (Genest and MacKay, 1986) or a mix of copulas (Manguzvane and Muteba, 2020). In this dissertation, I focus on dependencies in volatility; nonetheless, topics such as financial contagion and spillovers (Forbes and Rigobon, 2002) could explain the origin and sources of propagation shocks that escalate to and from more developing and developed countries. The appropriate model of these shocks either with univariate or multivariate models could serve as an input to value at risk (VaR) analysis for assessment of credit risks of commercial financial institutions and central banks (Caballero, Lucas, Schwaab and Zhang, 2020).

As in the work of Ayala et al. (2022) where they assess the Russian rouble exchange rate using a two-component model, financial analysts could explore the multivariate dynamics of exchanges rates in emerging markets using copula models with components. In times of distress or a rise in the Federal funds rate in the USA could trigger a common big exchange rate shock in countries highly dollarized. Recently, articles in the components literature by Linton and Wu (2020) and Opschoor and Lucas (2021) adopt a specific dynamic for daytime and overnight volatility in stock markets. Thus, it would be interesting to shed light on the measures of association with copulas of these types of volatility across different indices in a regional and a global scale.

Most applications using DCS models are in finance since this approach can handle large shocks, but scarce work has been undertaken in the macroeconomic field. In this dissertation, I contribute to this literature with a factor-augmented quasi VAR model that models directly atypical observations through the assumed multivariate Student t distribution. In particular, I focus on monetary policy shocks in the USA. A further analysis could be implemented for an empirical application in the Euro area and other economies that faced similar large shocks as in the U.S. In addition, the model could be extended to include commodity prices, unemployment, and other macroeconomic variables to the main system. Doing so, we could explore additional responses from a variety of shocks in the economy.

Adding more variables into the main system might require further restrictions (e.g. sign restrictions) for the identification of the model beyond the recursive identification from the standard Cholesky decomposition. Another avenue for research is the modelling of heteroskedastic errors, which will allow for more interactions between variables. Along with these developments, a researcher may consider time-varying parameters for the assumed fixed matrices of the FAQVAR model. Finally, one might add more lags to the vector autoregressive component of this model in case the impulse responses exhibit high persistence.

References

[1] Abbate, A., S. Eickmeier, W. Lemke, and M. Marcellino (2016), "The Changing International Transmission of Financial Shocks: Evidence from a Classical Time-Varying FAVAR," *Journal of Money, Credit and Banking* **48(4)**, 573-601.

[2] Akaike, H. (1974), "A new look at the statistical model identification," *IEEE Transactions on Automatic Control* **19(6)**, 716-723.

[3] Alanya-Beltran, Willy (2022a), "Modelling Stock Returns Volatility with Dynamic Conditional Score Models and Random Shifts," *Finance Research Letters* **45**, 102121.

[4] Alanya-Beltran, Willy (2022b), "Modelling Volatility Dependence with Score Copula Models," Mimeo.

[5] Alanya-Beltran, Willy (2022c), "Factor-Augmented QVAR Models: An Observation-Driven Approach," Mimeo.

[6] Alizadeh, S., M. Brandt, and F. Diebold (2002), "Range-based estimation of stochastic volatility models," *Journal of Finance* **57**, 1047-1091.

[7] Amisano, G., and R. Giacomini (2007), "Comparing density forecasts via weighted likelihood ratio tests," *Journal of Business & Economic Statistics* **25(2)**, 177-190.

[8] Angelini, G. and P. Gorgi (2018), "DSGE models with observation-driven time-varying volatility," *Economics Letters* **171**, 169-171.

[9] Antolín-Díaz, J., T. Drechsel, and I. Petrella (2021), "Advances in Nowcasting Economic Activity," Mimeo.

[10] Ayala, A., and S. Blazsek (2018), "Score-driven copula models for portfolios of two risky assets," *The European Journal of Finance* **24(18)**, 1861-1884.

[11] Ayala, A., S. Blazsek, and A. Licht (2022), "Score-driven stochastic seasonality of the Russian rouble: an application case study for the period of 1999 to 2020," *Empirical Economics* **62**, 2179–2203.

[12] Bai, J., and S. Ng (2002), "Determining the number of factors in approximate factor models," *Econometrica* **70(1)**, 191-221.

[13] Bai, J., and P. Perron (2003), "Computation and analysis of multiple structural change models," *Journal of Applied Econometrics* **18(1)**, 1-22.

[14] Bazzi, M., F. Blasques, S. J. Koopman, and A. Lucas (2017), "Time Varying Transition Probabilities for Markov Regime Switching Models," *Journal of Time Series Analysis* **38**, 458-478.

[15] Bernanke, B. S., J. Boivin, and P. Eliasz (2005), "Measuring the Effects of Monetary Policy: A Factor-Augmented Vector Autoregressive (FAVAR) Approach," *The Quarterly Journal of Economics* **120(1)**, 387-422.

[16] Bernardi, M., and L. Catania (2019), "Switching generalized autoregressive score copula models with application to systemic risk," *Journal of Applied Econometrics* **34(1)**, 43-65.

[17] Blasques, F., P. Gorgi, S. J. Koopman, and O. Wintenberger (2018), "Feasible Invertibility Conditions and Maximum Likelihood Estimation for Observation-Driven Models," *Electronic Journal of Statistics* **12**, 1019-1052.

[18] Blazsek, S., A. Escribano, and A. Licht (2017), "Score-Driven Nonlinear Multivariate Dynamic Location Models," Working Paper 17-14, Universidad Carlos III de Madrid, Department of Economics.

[19] Blazsek, S., A. Escribano, and A. Licht (2020), "Dynamic stochastic general equilibrium inference using a score-driven approach," Working Paper 20-05, Universidad Carlos III de Madrid, Department of Economics.

[20] Blazsek, S., and A. Licht (2020), "Dynamic conditional score models: a review of their applications," *Applied Economics* **52(11)**, 1181-1199.

[21] Blazsek, S., A. Escribano, and A. Licht (2022), "Score-driven location plus scale models: asymptotic theory and an application to forecasting Dow Jones volatility," forthcoming *Studies in Nonlinear Dynamics & Econometrics.*

[22] Blomqvist, N. (1950), "On a measure of dependence between two random variables," *Annals of Mathematical Statistics* **21**, 593–600.

[23] Bobeica, E., and B. Hartwig (2022), "The COVID-19 shock and challenges for inflation modelling," forthcoming *International Journal of Forecasting.*

[24] Bollerslev, T. (1986), "Generalized autoregressive conditional heteroskedasticity," *Journal of Econometrics* **31**, 307-327.

[25] Caballero, D., A. Lucas, B. Schwaab, and X. Zhang (2020), "Risk endogeneity at the lender/investor-of-last-resort," *Journal of Monetary Economics* **116**, 283-297.

[26] Caggiano, G., E. Castelnuovo., and G. Pellegrino (2017), "Estimating the real effects of uncertainty shocks at the Zero Lower Bound," *European Economic Review* **100**, 257-272.

[27] Carriero, A., T. E. Clark, M. Marcellino., and E. Mertens (2021), "Addressing COVID-19 Outliers in BVARs with Stochastic Volatility," Working Paper 21-02, Federal Reserve Bank of Cleveland.

[28] Creal, D., S. J. Koopman, and A. Lucas (2011), "A Dynamic Multivariate Heavy-Tailed Model for Time-Varying Volatilities and Correlations," *Journal of Business & Economic Statistics* **29**, 552-63.

[29] Creal, D., S. J. Koopman, and A. Lucas (2013), "Generalized autoregressive score models with applications," *Journal of Applied Econometrics* **28**, 777-795.

[30] Diebold, F. X., and R. S. Mariano (1995), "Comparing predictive accuracy," *Journal of Business & Economic Statistics* **13**, 253-263.

[31] Dufour, J., and D. Stevanović (2013), "Factor-Augmented VARMA Models With Macroeconomic Applications," *Journal of Business and Economic Statistics* **31(4)**, 491-506.

[32] Dungey, M., R. Fry, B. González-Hermosillo, and V. Martin (2011), "Transmission of financial crises and contagion: A latent factor approach," U.K: Oxford University Press publishers.

[33] Engle, R. (2002), "Dynamic conditional correlation: a simple class of multivariate generalized autoregressive conditional heteroskedasticity models," *Journal of Business & Economic Statistics* **20(3)**, 339-350.

[34] Engle, R., and G. Lee (1999), A long-run and short-run component model of stock return volatility. In R. Engle and H. White (eds.), *Cointegration, Causality, and Forecasting: A Festschrift in Honour of Clive WJ Granger*, 475-497. Oxford University Press.

[35] Engle, R., and J. Rangel (2008), "The spline-GARCH model for low-frequency volatility and its global macroeconomic causes," *Review of Financial Studies* **21**, 1187-1222.

[36] Engle, R., E. Ghysels, and B. Sohn (2013), "Stock market volatility and macroeconomic fundamentals," *Review of Economics and Statistics* **95(3)**, 776-797.

[37] Genest, C., and R. J. MacKay (1986), "Copules archimédiennes et familles de lois bidimensionnelles dont les marges sont données," *The Canadian Journal of Statistics* **14**, 145-159.

[38] Geweke, J., and S. Porter-Hudak (1983), "The estimation and application of long memory time series models," *Journal of Time Series Analysis* **4**, 221-238.

[39] Giacomini, R., and H. White (2006), "Tests of conditional predictive ability," *Econometrica* **74**, 1545-1578.

[40] Glosten, L. R., R. Jagannathan, and D. E. Runkle (1993), "On the relation between the expected value and the volatility of the nominal excess return on stocks," *Journal of Finance* **48(5)**, 1779–1801.

[41] Guarín, A., J. F. Moreno, and H. Vargas (2014), "Un análisis empírico de la relación entre las tasas de interés de los bonos soberanos de largo plazo de Estados Unidos y Colombia," *Ensayos sobre Política Económica* **32**, 68-86.

[42] Guerron-Quintana, P. A., A. Khazanov, and M. Zhong (2021), "Nonlinear Dynamic Factor Models," Unpublished manuscript.

[43] Forbes, K. J., and R. Rigobon (2002), "No contagion, only interdependence: measuring equity market comovements," *Journal of Finance* **57**, 2223–2261.

[44] Forni, M. and L. Gambetti (2014), "Sufficient information in structural VARs," *Journal of Monetary Economics* **66**, 124-136.

[45] Fry, R. A., V. L. Martin, and C. Tang (2010), "A New Class of Tests of Contagion With Applications," *Journal of Business & Economic Statistics* **28(3)**, 423-437.

[46] Fry-McKibbin, R., C. Y.-L. Hsiao, and C. Tang (2014), "Contagion and Global Financial Crises: Lessons from Nine Crisis Episodes," *Open Economies Review* **25**, 521-570.

[47] Fry-McKibbin, R., M. Greenwood-Nimmo, C. Y.-L. Hsiao, and L. Qi (2022), "Higher-order comoment contagion among G20 equity markets during the COVID-19 pandemic," *Finance Research Letters* **45**, 102150.

[48] Hannan, E. J., and B. G. Quinn (1979), "The Determination of the order of an autoregression," *Journal of the Royal Statistical Society Series B* **41**, 190-195.

[49] Hansen, P. R. (1994), "Autoregressive conditional density estimation," *International Economic Review* **35(3)**, 705-730.

[50] Harding, A., and A. Pagan (2002), "Dissecting the cycle: a methodological investigation," *Journal of Monetary Economics* **49**, 365-381.

[51] Hartwig, B. (2021), "Bayesian VARs and prior calibration in times of COVID-19," Working Paper SSRN 3792070.

[52] Harvey, A. C., and T. Chakravarty (2008), "Beta-t-(E)GARCH," Cambridge Working Papers in Economics (CWPE0840), University of Cambridge.

[53] Harvey, A. C. (2013), "Dynamic Models for Volatility and Heavy Tails: with Applications to Financial and Economic Time Series," Econometric Society Monograph, Cambridge University Press.

[54] Harvey, A. C., and G. Sucarrat (2014), "EGARCH models with fat tails, skewness and leverage," *Computational Statistics & Data Analysis* **76**, 320-338.

[55] Harvey, A. C., and R. Lange (2018), "EGARCH models with fat tails, skewness and leverage," *Journal of Time Series Analysis* **39**, 909-919.

[56] Harvey, A. C., and R. Ito (2020), "Modeling time series when some observations are zero," *Journal of Econometrics* **214(1)**, 33-45.

[57] Harvey, A. C., and D. Palumbo (2019), "Score-Driven Models for Realized Volatility," Cambridge Working Papers in Economics (CWPE1950), University of Cambridge.

[58] Harvey, A. C., and Y. Liao (2019), "Dynamic Tobit models," Cambridge Working Papers in Economics (CWPE1913), University of Cambridge.

[59] Huber, P. J. (1967), "The Behavior of Maximum Likelihood Estimates under Nonstandard Conditions," in Proceedings of the Fifth Berkeley Symposium on Mathematical Statistics and Probability, vol. I, 221-233.

[60] Ito, R. C. (2016), "Spline-DCS for Forecasting Trade Volume in High-Frequency Finance," Cambridge Working Papers in Economics (CWPE1606), University of Cambridge.

[61] Jaquier, E., N. Polson, and P. Rossi (1994), "Bayesian Analysis of Stochastic Volatility Models," *Journal of Business & Economic Statistics* **12**, 371-389.

[62] Joe, H. (2015), "Dependence modelling with copulas," CRC Press, Taylor & Francis Group: Boca Raton, FL.

[63] Klaassen, F (2002). "Improving GARCH volatility forecasts with regime-switching GARCH," *Empirical Economics* **27**, 363-394.

[64] Laine, O. J. (2020), "The effect of the ECB's conventional monetary policy on the real economy: FAVAR-approach," *Empirical Economics* **59**, 2899–2924.

[65] Lenza, M., and G. Primiceri (2021), "How to Estimate a VAR after March 2020," forthcoming *Journal of Applied Econometrics*.

[66] Linton, O., and J. Wu (2020), "A coupled component DCS-EGARCH model for intraday and overnight volatility," *Journal of Econometrics* **217**, 176-201.

[67] Lucas, A., and A. Opschoor (2019), "Fractional integration and fat tails for realized covariance kernels and returns," *Journal of Financial Econometrics* **17(1)**, 66-90.

[68] Manguzvane, M. M., and J. W. Muteba (2020), "GAS-Copula Models on who's systemically important in South Africa: Banks or Insurers," *Empirical Economics* **20**, 87-109.

[69] McCracken, M. W., and S. Ng (2016), "FRED-MD: A Monthly Database for Macroeconomic Research," *Journal of Business Economics & Statistics* **34(4)**, 574–589.

[70] Mejía-Posada, F., D. C. Restrepo-Ochoa, and J. E. Isaza (2022), "Do Investors React to Terrorism and Peace in Colombia?," *Emerging Markets Finance and Trade* **58(6)**, 1550-1565.

[71] Nelson, D. B. (1991), "Conditional heteroscedasticity in asset returns: a new approach," *Econometrica* **59(2)**, 347-370.

[72] Newey, W. K., and K. D. West (1987), "A Simple, Positive Semi-definite, Heteroskedasticity and Autocorrelation Consistent Covariance Matrix," *Econometrica* **55(3)**, 703–708.

[73] Nitçi, M., and M. M. Pochea (2020), "Time-varying dependence in European equity markets: A contagion and investor sentiment driven analysis," *Economic Modelling* **86**, 133-147.

[74] Oh, D., H. and A. J. Patton (2018), "Time-Varying Systemic Risk: Evidence From a Dynamic Copula Model of CDS Spreads," *Journal of Business & Economic Statistics* **36(2)**, 275-290.

[75] Opschoor, A., and A. Lucas (2021), "Observation-driven models for realized variances and overnight returns applied to Value-at-Risk and Expected Shortfall forecasting," *International Journal of Forecasting* **37**, 622-633.

[76] Opschoor, A., A. Lucas, I. Barra, and D. van Dijk (2021), "Closed-Form Multi-Factor Copula Models With Observation-Driven Dynamic Factor Loadings," *Journal of Business & Economic Statistics* **39(4)**, 1066-1079.

[77] Patton, A. J. (2006), "Modelling asymmetric exchange rate dependence," *International Economic Review* **47**, 527-556.

[78] Patton, A. J. (2013), "Copula Methods for Forecasting Multivariate Time Series," in *Handbook of Economic Forecasting* (Vol. 2), eds. G. Elliott and A. Timmermann, Oxford: Elsevier, 899-960.

[79] Perron, P., and Z. Qu (2010), "Long-memory and level shifts in the volatility of stock market return indices," *The Econometrics Journal* **16(3)**, 309-339.

[80] Politis, D. N., and J. P. Romano (1994), "The Stationary Bootstrap," *Journal of the American Statistical Association* **89**, 1303-1313.

[81] Pong, S., M. B. Shackleton, and S. J. Taylor (2008), "Distinguishing short and long memory volatility specifications," *The Econometrics Journal* **11**, 617-637.

[82] Qu, Z., & P. Perron (2013), "A stochastic volatility model with random level shifts and its applications to S&P 500 and NASDAQ return indices," *The Econometrics Journal* **16(3)**, 309-339.

[83] Santa-Cruz, A. (2012), "Canada–Mexico Relations: Interdependence, Shared Values and the Limits of Cooperation," *American Review of Canadian Studies* **42(3)**, 401-417.

[84] Schorfheide, F. and D. Song (2021), "Real-time forecasting with a (standard) mixed-frequency VAR during a pandemic," Technical report, National Bureau of Economic Research.

[85] Schwarz, G. E. (1978), "Estimating the dimension of a model," *Annals of Statistics* **6(2)**, 461-464.

[86] Sims, C. A. (1980), "Macroeconomics and Reality," *Econometrica* **48**, 1-48.

[87] Sklar, A. (1959), "Fonctions de répartition à n dimensions et leurs marges," *Publications de l'Institut Statistique de l'Université de Paris* **8**, 229–31.

[88] Sosa, M., E. Ortiz, and A. Cabello (2017), "Crisis financiera global y su impacto en la dinámica bursátil europea y americana," *Revista Mexicana de Economía y Finanzas* **12(3)**, 1-27.

[89] Stock, J., and M. Watson (2002), "Macroeconomic Forecasting Using Diffusion Indexes," *Journal of Business Economics and Statistics* **32**, 147–162.

[90] Stock, J., and M. Watson (2016), "Core inflation and trend inflation," *The Review of Economics and Statistics* **98**, 770–784.

[91] Wu, J. C., and F. D. Xia (2016), "Measuring the Macroeconomic Impact of Monetary Policy at the Zero Lower Bound," *Journal of Money, Credit and Banking* **48(2)**, 253-291.

[92] Yamamoto, Y. (2019), "Bootstrap inference for impulse response functions in factor-augmented vector autoregressions," *Journal of Applied Econometrics* **34**, 247-267.